UNIVERSITY OF CANTERBURY

MASTER'S THESIS

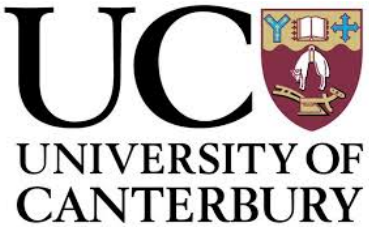

Optimising the Use of an EPID-Based In-Vivo Dose Verification System for 3DCRT Breast Treatments

Author:

Abinaya RAJASEKAR

Supervisors:

Dr. Alicia MOGGRE

Dr. Andrew COUSINS

Dr. Steven MARSH

A thesis submitted in fulfilment of the requirements

for the degree of Master of Science

in the

Department of Physical and Chemical Sciences

April 2019

Abstract

Purpose

Christchurch Hospital has implemented EPIgray, an EPID based in-vivo dosimetry (IVD) system for dosimetric verification of treatment. The current EPIgray clinical tolerance of $\pm 5\%$ has been set for all sites treated using 3D conformal radiation therapy (3DCRT). This project aims to optimise the use of EPIgray for treatment verification of 3DCRT breast treatments, by establishing a site specific clinical tolerance, reducing false positive results and investigating causes of error.

Methods

A retrospective study was performed in which 30 previously treated 3DCRT breast patients were re-analysed within EPIgray with the current tolerance. EPID based IVD systems are susceptible to setup errors on treatment. Positional corrections in EPIgray were performed to identify groups of patients at increased risk of having setup errors on treatment, and the impact of these on the EPIgray result. For controlled tests to validate the findings of the retrospective study, a phantom representing breast and lung tissue was designed. The phantom was positioned for treatment with setup errors of known magnitude in all orthogonal planes to compare EPIgray reconstructed doses against other routinely used dosimeters. An uncertainties investigation was also conducted in which the uncertainties associated with the EPIgray reconstructed doses were determined specifically for the treatment parameters used for 3DCRT breast treatments.

Results

The retrospective study has revealed that right breast patients and large breast patients were more prone to setup errors than left breast patients and small breast patients. The phantom study revealed that EPIgray reported doses are in agreement with the delivered dose. Whilst the accuracy of EPIgray was determined to be systematically offset from other dosimeters, the results have indicated that EPIgray can be reliably used with appropriate tolerances. The results of the uncertainties investigation have shown that the intervention clinical tolerance for 3DCRT breast treatments can be reduced to $\pm 3.5\%$ with the aim of detecting potential treatment errors whilst still accounting for inherent uncertainties associated with EPIgray and the uncertainties associated with the variations in treatment.

Conclusions

This project has clinically validated the use of EPIgray for treatment verification of 3DCRT breast treatments. A new intervention tolerance of $\pm 3.5\%$ was recommended for all 3DCRT breast patients. This tolerance is smaller than the current intervention tolerance of $\pm 5.0\%$ and would aid in the reduction of false results.

Acknowledgements

The completion of this thesis would not have been possible without considerable contributions from incredible people. I would like to express my gratitude to the following individuals:

- Dr. Alicia Moggre for her continued guidance, encouragement and support. It was a true honour to have had her as my thesis supervisor. Without the depth of her scientific knowledge and constructive input, this thesis would not have reached its present form. Thank you Alicia for being an incredible, proactive supervisor but also reminding me that it is alright to take a break.
- Dr. Andrew Cousins, for his scientific advice and on-going support. Dr. Andrew Cousins' feedback has been invaluable as are his dad jokes. I would also like to thank Dr. Steven Marsh, for his support, valuable suggestions and input towards this project.
- Dr. Anna Arns, for her support in the final few months of this project. Her enthusiasm and keen eye for detail have been inspirational. I'd like to thank Anna for her kindness and moral support during all the late nights at the office.
- Victoria Beenstock, my training supervisor for allowing me to juggle between my training and thesis time and for her scientific input and general advice in approaching problems and roadblocks.
- David Little, Ben Wilder, Beat Billson, Dr. Paul Ronaldson, Grace Healy, Christine Reed and my fellow registrars for their continued support. Thank you for all the banter and laughs. But also, I thank you all for taking the time to have valuable discussions and for your willingness to participate in this project.
- The Medical Physics and Bioengineering team for their assistance in manufacturing the phantom used in this study.
- The radiation therapists at Christchurch Hospital for all their help, suggestions and input regarding patient treatment and setup. Special thank you to the radiation therapists at the CT for allowing me to squeeze in-between patients to use the CT.
- Lastly, I would like to thank Revan Ram and my parents, Ami and Sekar for their unbelievable patience and kindness. Thank you for being my pillars of support.

Contents

List of Figures

List of Tables

List of Abbreviations

%DD	Percentage Dose Difference
%DD$_{DRP}$	Percentage Dose Difference at the Dosimetric Reference Point
%DD$_{vol}$	Percentage Dose Difference of the EPIgray Volume
2D	2-Dimensional
3D	3-Dimensional
3DCRT	3D Conformal Radiation Therapy
aSi	Amorphous Silicon
BIPM	International Bureau of Weights and Measures
CT	Computed Tomography
DICOM	Digital Imaging and Communications in Medicine
DNA	Deoxyribonucleic Acid
DRR	Digitally Reconstructed Radiograph
DRP	Dose Reference Point
EBRT	External Beam Radiation Therapy
EPID	Electronic Portal Imaging Device
EQS	Equivalent Square Field
FF	False Fail
FP	False Pass
FPR	False Positive Rate
IC	Ionisation Chamber(s)
IAEA	International Atomic Energy Agency
ICRP	International Commission on Radiological Protection
ICRU	International Commission on Radiation Units and Measurements
IMRT	Intensity Modulated Radiation Therapy
ISF	Inverse Square Factor
ISL	Inverse Square Law
IVD	In-Vivo Dosimetry
Linac	Linear Accelerator
MLC	Multi-Leaf Collimator
MoHNZ	Ministry of Health New Zealand
MU	Monitor Unit(s)
OAR	Organ At Risk
PDD	Percentage Depth Dose
PMT	Photomultiplier Tube
QA	Quality Assurance
SCD	Source to Chamber Distance
SDD	Source to Detector Distance
SSD	Source to Surface Distance
TF	True Fail
TP	True Pass
TPR	True Positive Rate
TPS	Treatment Planning System
WCRF	World Cancer Research Fund
WHO	World Health Organisation

1 Introduction

1.1 Breast Cancer Overview

Cancer is the uncontrolled growth and spread of abnormal cells [1]. Ordinarily, normal cell behaviour such as cell division, specialisation and death are under the control of signals from the homeostatic system. Abnormal cancer cells however do not obey these signals. Cancer cells therefore increase in size and number, persisting at the expense of the organism without any given benefits. The presence of cancer cells interferes with normal cell function ultimately leading to illness and death.

Recent data published by the World Health Organisation (WHO) has shown breast cancer to be the most common form of cancer in women in New Zealand (Figure 1.1) and worldwide (Figure 1.2). Figures 1.1 and 1.2 also identify breast cancer to be one of the leading causes of cancer-related death in women. Cancer trends published by the Ministry of Health New Zealand (MoHNZ) reveal that more people in New Zealand are now developing cancer, largely as a result of an ageing population [2]. WHO predicts that by 2040, the incidence of breast cancer in New Zealand will increase by 30% from the 2018 incidence rates [3]. However, whilst the prevalence of breast cancer is considered to be high, the burden of cancer can be dramatically reduced through early detection and appropriate treatment.

Surgery, chemotherapy and radiation therapy are the most common treatments for breast cancer. Each treatment option has associated advantages and disadvantages that are extensively discussed in literature [4]. It is reported that over 50% of all cancer patients may benefit from radiation therapy in the management of cancer [5]. While lumpectomy and mastectomy are effective surgical procedures for treatment of breast cancer where the tumour or the entire breast is respectively removed, an abundance of research reveals that the local recurrence of breast cancer can be dramatically decreased with adjuvant radiotherapy [6], [7].

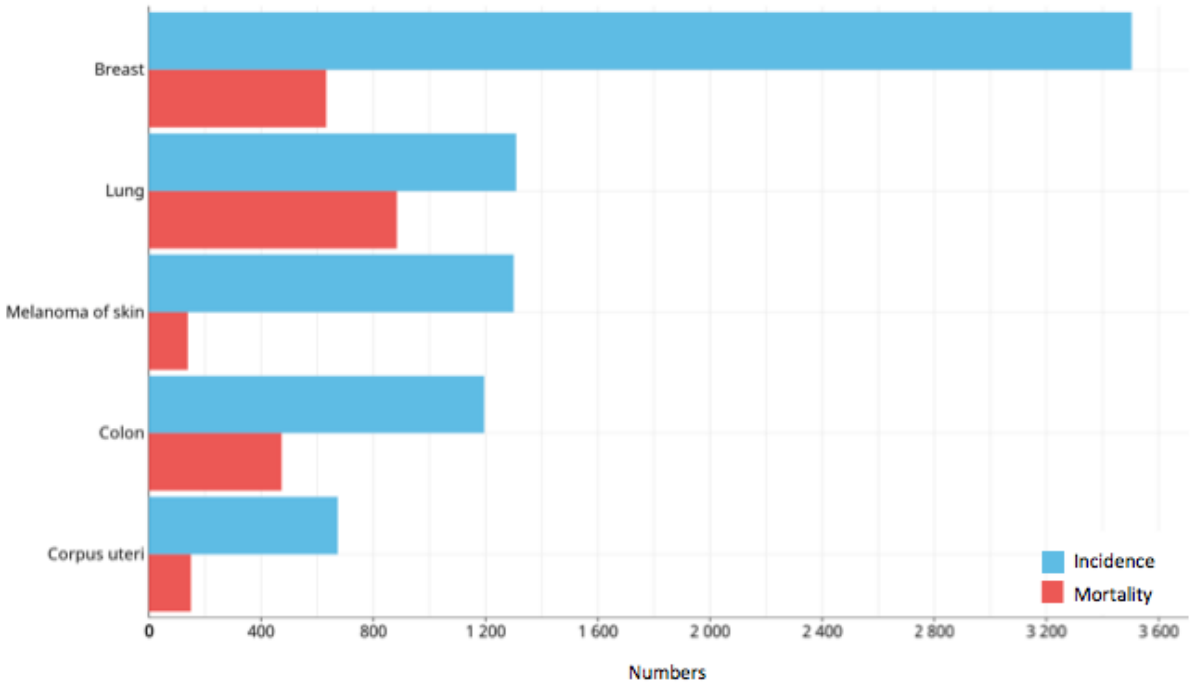

FIGURE 1.1: Estimated number of incident cases and deaths in women in New Zealand [3]

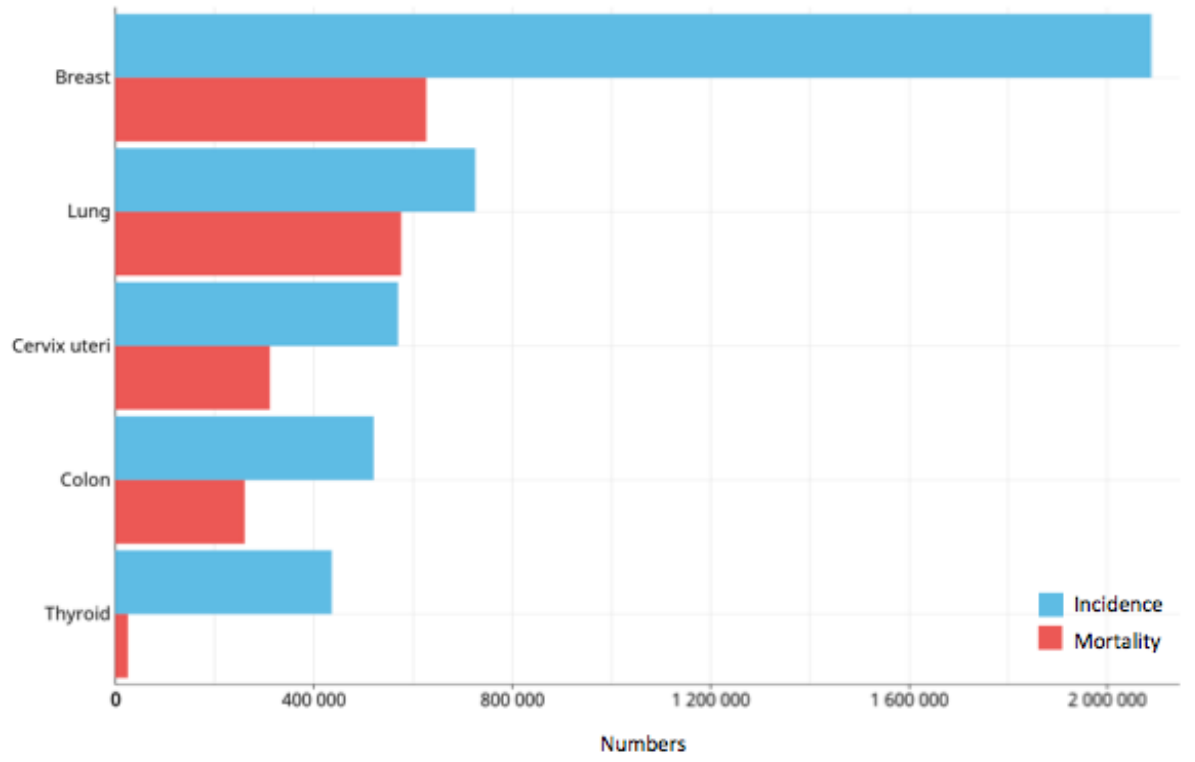

FIGURE 1.2: Estimated number of incident cases and deaths in women worldwide [3]

1.2 Radiotherapy for Treatment of Breast Cancer

Radiation therapy for cancer treatments involves the use of radiation to kill cancer cells. The foundation of radiotherapy relies on the interaction between high energy ionising radiation and the molecules that make up the deoxyribonucleic acid (DNA) of a cell [8]. Cell DNA contains information associated with the cell division, growth and development. Therefore the interactions that occur between the ionising radiation and the cell DNA causes disruption to the cell function, ultimately leading to cell death [9].

Numerous radiotherapy techniques such as brachytherapy, intra-operative radiotherapy and external beam radiation therapy (EBRT) are employed for the treatment of breast cancer [10]. EBRT is the most common form of radiotherapy treatment for breast cancer. In EBRT, the radiation is externally produced and is focused on the tumour as opposed to placing a radioactive source within the tumour [11]. The radiation for modern EBRT techniques are typically generated by a linear accelerator (linac), shown in Figure 1.3.

FIGURE 1.3: Linear accelerator at Christchurch Hospital

The radiation produced for EBRT treatments must travel from an external source to the treatment site. Radiation does not selectively affect cancer cells and therefore radiation interactions with healthy cells will also result in the damage or death of normal cells which may lead to detrimental consequences for the patient [12]. The ultimate aim of radiotherapy is to accurately deliver the prescribed dose to the tumour volume whilst minimising the dose to the surrounding healthy tissue.

Radiotherapy treatments are administered by prescribing a radiation dose to a specific treatment volume. The absorbed radiation dose is defined as the mean energy imparted by ionising radiation per unit mass. The absorbed dose has units of Gray (Gy), where 1 Gy is equivalent to 1 J kg^{-1}. Complete avoidance of healthy tissue irradiation cannot always be achieved. As such, fractionation of radiotherapy treatments was introduced to increase eradication of cancer cells whilst sparing normal tissue through repair of sublethal damage. Fractionation of the total prescribed dose refers to a treatment scheme in which the total prescribed dose is delivered in smaller doses over multiple treatment sessions. For example 30 Gy total dose is delivered to the patient in 2 Gy over 15 treatment sessions (fractions). The basis of fractionation is explained by the four Rs of radiotherapy [13]:

1. **Repair**: The time between fractions allows normal cells to repair sublethal damage.
2. **Repopulation**: The time between fractions allows for repopulation of normal cells.
3. **Redistribution**: The time between fractions redistributes the cancer cells to radiosensitive cell cycle phase to increase cell killing when exposed to radiation.
4. **Reoxygenation**: The time between fractions allows reoxygenation of the tumour volume, which subsequently increases the radiosensitivity of the cell [14].

During breast cancer EBRT treatments other normal cells and organs at risk (OAR) such as the heart and lungs may receive an unnecessary radiation dose. Consequently, measures are taken in the planning and execution stages of the radiotherapy treatment to decrease the dose to the normal cells and organs at risk.

1.2.1 EBRT Radiotherapy Treatment Process

The steps of the radiotherapy treatment process are schematically shown in Figure 1.4. Following diagnosis and decision to treat, the patient will have a consultation appointment with the radiation oncologist to receive information regarding their radiotherapy treatment. Following patient consent, the patient will undergo a series of preparative processes to be able to deliver the radiation treatment accurately [15].

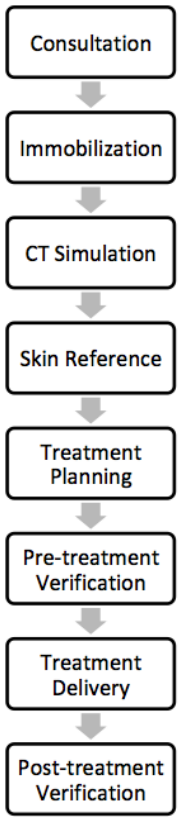

FIGURE 1.4: Flow diagram of the radiotherapy treatment process

Firstly, the computed tomography (CT) simulation takes place, in which CT images are acquired of the patient in their expected treatment position. The patient is set up using a range of immobilisation devices customised to their body for two reasons. The first is to ensure that the patient is in a reproducible treatment position for all fractions of their treatment. Slight differences in patient positioning from intended position could lead to a full or partial geometric miss of the tumour volume giving rise to a lack of local tumour control and additional increase in the risk of normal tissue complications. Secondly, immobilisation devices are also employed to allow better access to the treatment site, whilst providing a comfortable position for the patient. For example, immobilisation devices are used to support the patient's arms when they are asked to hold their arms above their heads for treatment of breast cancer. By placing arms above their head, the arms will receive comparatively lower dose than if the arms were placed directly adjacent to the breasts.

In addition to customisation of immobilisation devices, the patient will also receive small tattoos (often called skin reference points), where the external lasers in the CT room are incident

upon their skin. On treatment, the patient will be set up in their treatment position using identical immobilisation devices. The external lasers in the treatment bunker and the patient reference tattoos are used to setup the patient in a near identical position to their setup at the CT simulation. It is important to maintain the same patient position from simulation CT through every fraction of the treatment as the simulation CT scans will be used in the treatment planning process.

Images from these CT scans allow the treatments to be specifically tailored to each patient. The simulation CT images that were acquired are imported into the treatment planning system (TPS). The TPS is used to contour the relevant anatomical structures. Delineation of these structures not only allow effective beam placement during treatment planning but also allows for calculation of doses to these structures. The Hounsfield Units associated with the CT images are converted to electron densities within the TPS. The TPS uses a dose calculation algorithm and combines patient anatomical information from the CT with the physical radiation processes that are expected to occur as the radiation interacts with the tissues that it traverses through to provide the dose distribution within the patient.

The treatment plan is then evaluated and approved for treatment. Treatment plans are evaluated with reference to the dose constraints for normal tissue and treatment volume to ensure that there is minimal normal tissue complication whilst maintaining an appropriate level of tumour control. Following evaluation and acceptance of the plan, an independent check is performed on the plan to identify any errors in the treatment planning process and data transfer to the linac console. If necessary, plan-specific quality assurance (QA) is performed to assess the dosimetric accuracy of the plan. QA in radiotherapy is defined as "all procedures that ensure consistency of the medical prescription, and safe fulfilment of that prescription, as regards to the dose to the target volume, together with minimal dose to normal tissue... and adequate patient monitoring aimed at determining the end result of the treatment" [16]. QA in radiotherapy serves to detect errors and prevent the corresponding consequences early in the treatment process. Additionally QA may minimise the uncertainties associated with each stage of the radiotherapy process to better improve the overall accuracy of radiotherapy treatments.

Following evaluation of plan safety and acceptance of the plan, the patient treatment can begin. The reference tattoos and lasers are used to approximately position the patient on treatment to be the same as at CT simulation. Pre-treatment imaging is then performed to verify the position of the treatment volume and OAR before the treatment commences. Pre-treatment imaging involves acquisition of verification images on treatment and comparing these images to the images from CT simulation to ensure that the patient is in the correct treatment position. Further shifts of the patient on treatment are performed as required. Once the patient position on treatment is verified, the treatment is delivered to the patient.

Safety in Radiotherapy

Over time radiotherapy has become a highly complex process as a result of advancing research and improving technology. The professional expertise required to execute such treatments is rapidly on the rise. The complexity of modern radiotherapy is mainly attributed to the numerous steps involved in the planning and delivery processes of these treatments [17]. Increasing complexity of these treatments has led to an increase in the number of errors that could arise which may compromise the treatment intent. Ford *et al.* identified 127 possible failure modes, starting from the decision to treat with radiotherapy to ultimately delivering the dose to the patient [17].

An error in radiotherapy is defined as "a non-conformance where there is an unintended divergence between a radiotherapy treatment delivered or a radiotherapy process followed and that defined as correct by local protocol" [18]. Error in radiotherapy may occur in any one of the steps involved in the treatment process. While the consequences of the errors may vary in severity, precautions must be taken to avoid errors at each and every step to ensure the most accurate treatment possible. Unintended adverse effects following radiotherapy may be indicative of clinically significant error in radiotherapy. The risk of a clinically significant error in radiotherapy was estimated to be 3 per 100,000 courses of treatment [19]. Although the risk is considered to be small, complacency is not an option because the consequences could be fatal.

1.3 Treatment Verification

Modern radiotherapy is continuously evolving in order to more effectively concentrate the dose to the tumour volume. With increasing complexity, the treatment plans become less intuitive and more reliant on the algorithms employed by the TPS. While using the TPS is beneficial in avoiding human errors in dose calculations, the associated decrease in human input into the treatment plan may give rise to other errors. While pre-treatment QA procedures minimise errors and uncertainties with reference to the dose delivery, in more complex treatments, pre-treatment QA procedures are not sufficient at identifying radiotherapy errors. Treatment verification consequently became an important aspect of radiotherapy treatments.

Treatment verification is defined as the "process by which the accuracy of radiotherapy is assessed" [18]. Treatment verification as part of QA is relatively new in comparison to the existence of radiotherapy treatments. However, treatment verification is increasingly being used and is widely recommended by various international bodies including WHO, the International Commission on Radiological Protection (ICRP) and the International Atomic Energy Agency (IAEA) [20]. The doses predicted by the TPS in comparison to the doses delivered to the patient during treatment are subject to minor and major variations. Various factors ranging from minor setup errors to major treatment errors can lead to differences in the dose delivered to the patient.

Although not required by legislation in New Zealand, in-vivo dosimetry (IVD) is now increasingly being recommended by the MoHNZ to ensure treatments are executed as expected [21]. IVD refers to the measurement of the dose delivered to the patient during treatment delivery. IVD is therefore the most direct method of verifying that the correct dose has been delivered to the patient. Because radiotherapy treatments are typically fractionated, performing treatment verification early in the treatment serves as an additional safe guard against major dosimetric errors that may have gone unnoticed until the consequences of incorrect treatment become apparent. IVD entails the use of a radiation dose detector (dosimeter) to provide an indication of the dose delivered to the patient. The dose indicated by the dosimeter is subsequently compared to the dose calculated by the TPS to provide an indication of the accuracy of the

treatment delivered.

1.3.1 In-Vivo Dosimeters

There are many types of IVD dosimeters in clinical use. A summary of the dosimeters used in this study and the corresponding advantages and disadvantages are outlined below.

Ionisation Chambers

Ionisation chambers (IC) are gas filled volumes with polarising electrodes (anode and cathode) as shown in Figure 1.5. Radiation interaction with the gas volume inside the chamber results in the formation of positive and negative ions. The polarity of the electrodes attracts the ions of the opposite charge. The magnitude of the charge collected is subsequently correlated to the number of radiation interactions that have occurred. Consequently, the radiation dose to a particular point can be inferred.

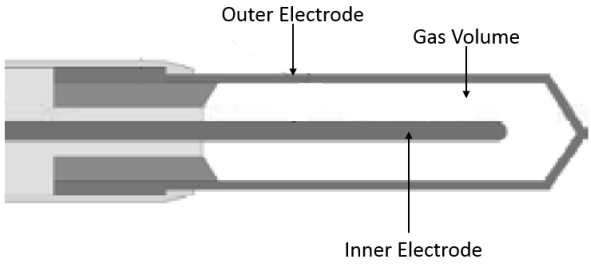

FIGURE 1.5: Simple diagram of a farmer type ionisation chamber [14]

Literature has shown that an IC of an appropriate volume will provide an accurate measurement of dose. As such, IC are clinically used for determination of dose to water which are subsequently used for dose calculations. Other advantages of IC include good long-term stability, reproducibility, linear response to dose, small angular dependence and immediate read-out. IC are also often used in patient specific QA procedures in which the IC is inserted into a phantom (representing the patient) to measure the absolute dose to a point. This measured dose is then compared to the TPS dose to check for consistency between the treatment plan and treatment delivery. While IC has a range of applications in radiation oncology, IC are typically unsuitable for most IVD applications because of the required polarising voltage and difficulty

in positioning the IC at a clinically relevant position. Furthermore the positioning of the IC is also important because any offset will introduce uncertainties to the point dose measurements [22].

Radiochromic Film

Radiochromic film is a widely adopted dosimeter in radiation oncology departments. Radiochromic film have one or two thin radiosensitive layers. The radiosensitive layers consists of microcrystals of a monomer dispersed in a gelatinous binder. The radiosensitive layers undergo polymerisation when irradiated with ionising radiation. The polymerisation causes the radiochromic film to change optical density as a function of dose. The opacity of the film is then correlated to the dose deposited to the film.

Radiochromic film have many features that ensure its use in radiotherapy as a dosimeter. Major advantages of the radiochromic film are the near tissue equivalency of the sensitive layer and decreased sensitivity to light in comparison to radiographic film. Additionally, radiochromic film do not require chemicals to process, and they provide information on the two-dimensional (2D) dose distributions. While radiochromic film have many associated advantages, they are also relatively expensive, require scanning equipment to determine the dose delivered and have strict readout protocols. Additionally dosimetric analysis using radiochromic film is time consuming and cannot be performed in real time [22].

Electronic Portal Imaging Device

Electronic portal imaging devices (EPIDs) were first invented to replace film in radiotherapy and were designed for positional verification of patients on treatment, where the treated area could be reviewed post treatment. EPIDs are typically employed for transit dosimetry in which a patient or a phantom is placed in the beam between the source and the EPID. Figure 1.6a shows an acquisition of a transmission EPID image of a patient using a built-in EPID on a linac. The linac gantry is rotated around the patient to deliver treatment from various gantry angles. The linac gantry and the EPID always oppose each other and therefore EPID images

can be acquired at any gantry angle. The EPID positioned on the other side of the patient registers the x-rays that have been attenuated by the patient as a 2D image [23].

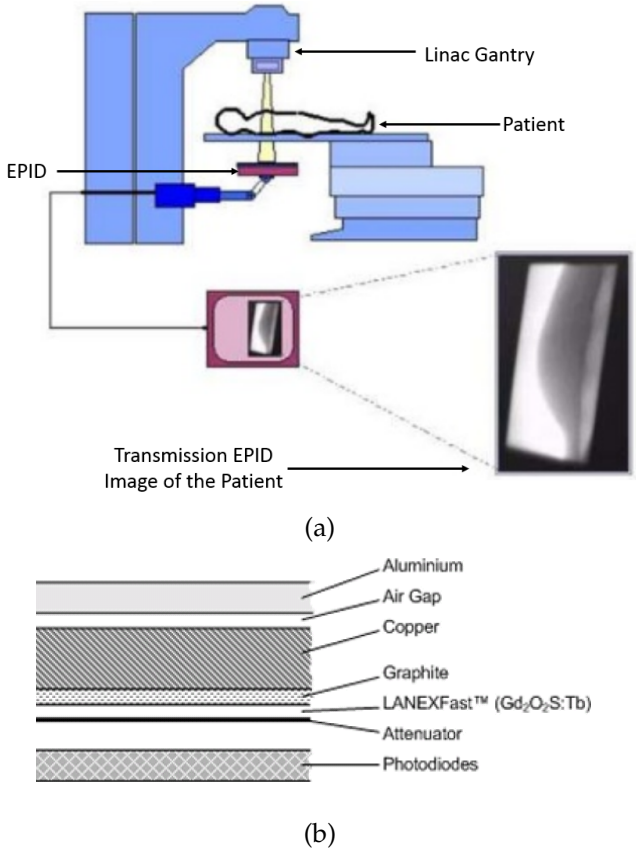

FIGURE 1.6: EPID on a linac (a) Patient transmission EPID image acquisition setup [24] (b) Perkin Elmer aSi EPID [25]

The most commonly used EPIDs are amorphous silicon (aSi) EPIDs. Figure 1.6b shows the construction of the EPID panel used in this study. The major components an aSi EPID are the scintillator plate, aSi photodiode array and electronics for reading out the image formed. The interaction between the radiation and the scintillator material, Gd_2O_2S:Tb results in the conversion of radiation to light. The light produced is then detected by an array of photodiodes that are implanted in the aSi. The photodiodes then integrate the light into charge captures and are registered as values for that pixel. Therefore the signal formed is dependent on the amount of charge captured per unit pixel of the imaging panel. The image captured on the EPID is proportional to the amount of transmission through the patient or the phantom. The values can consequently be used to infer the level of attenuation that has occurred as a result of having an attenuating medium in the path of the beam. The aSi EPID used in this study has a resolution

of 1024 x 1024 16-bit pixel images and an effective detector size of 26 x 26 cm at the isocentre [1]. EPID images are used for positional verification by comparison to the digitally reconstructed radiograph (DRR) simulated by the TPS.

The use of EPIDs in EBRT radiotherapy treatment verification is rapidly increasing because of their many advantages including its ability to provide high resolution images and an instant readout [20]. Additionally EPID images can be saved as a permanent electronic copy for record keeping. Furthermore, the use of EPID in EBRT for positional verification can be achieved without additional radiation dose to the patient because most modern linacs already have a built-in EPID and therefore images can be acquired during the treatment beam. Additionally, the images acquired using an EPID also allows the determination of dose to a point within the patient/phantom, given that the oncology department possesses a dose calculation algorithm for calculating dose using EPID images. Due to its many advantages, EPIDs have been highly researched in order to implement their use for positional and dosimetric verification in radiotherapy treatments [22].

1.3.2 Literature Review: Current Use of EPID-Based IVD

The use of EPIDs for positional verification is common at most radiotherapy centres however EPID based dosimetric verification is still relatively new. Numerous publications have addressed different aspects of EPIDs for use in dosimetry. Boyer *et al.* provided a detailed overview of the historical perspective that lead to the technological development of the EPID [27]. More recently Antonuk [28], and Kirby and Glendinning have also published the technological advancements in EPID technology to the current state [29].

The prospect of using EPID for dosimetric analysis and treatment verification has been under rapid development because the image acquisition using an EPID is efficient, of high resolution and is acquired in a digital format with capability of use in IVD. Consequently, the dosimetric and physical properties of aSi EPID have been studied by several groups [23]. Figure 1.7 shows the rapid increase in interest through journal publications relating to EPID dosimetry.

[1] In radiation oncology, the isocenter is a point in space through which the central rays of the radiation beam pass through [26].

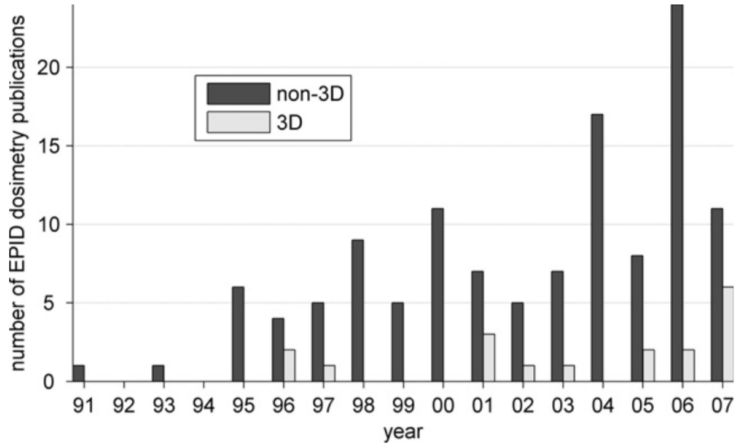

FIGURE 1.7: Number of publications relating to EPID dosimetry [23]

Point-Dose Verification

The ability to determine the dose to a point of interest has historically been shown to be useful in identifying clinically significant, systematic errors that are likely to recur in each successive fraction [30]. The initial motivation for point-dose verification based on EPID transmission images arose to eliminate diodes in IVD. Diode measurements are performed by placing a diode either at the entrance or the exit surface of the patient [31]. The diode would need to be calibrated to measure the dose at a specified point within the patient. However, the use of diodes for IVD entails set up time on treatment as well as additional time associated with the accurate calibration of the device. Additionally diodes also affect the treatment by attenuating the beam. EPIDs can overcome these issues [23].

Comparisons of transmission based point dose measurements have been performed at various positions. These include comparisons of measurements made at the plane of the EPID [32], back projected to a point of interest within the patient (variable in depth) or a generic point within the patient, e.g. 5 cm depth ([33], [34]) or at the isocentre ([35]–[38]). These publications reveal that the accuracy of the reconstructed doses, regardless of the position at which the doses are calculated is strongly dependent upon two factors. The first is the dose reconstruction algorithm, and the second is the treatment site.

Errors Detected Using EPID Dosimetry

Elmpt *et al.* have identified a number of errors that are clinically detectable using EPID dosimetry. These errors were categorised as treatment related or patient related errors. Publications have shown that both systematic and random errors associated with the treatment can be identified using EPID dosimetry. Treatment related errors include unexpected variations in the treatments parameters and linac radiation output. These errors are detectable using EPID due to the differences in the dose distribution measured using an EPID and the dose distribution provided by the TPS. The ability to detect these errors in earlier fractions will prevent major dosimetric errors and consequently will be clinically beneficial [23].

Patient related errors particularly errors that occur as a result of patient positioning on treatment or changes in patient anatomy from the planning stages of the treatment are also identifiable using EPID dosimetry. Regardless of which category these errors fall into, the EPID dosimetry measurements made during the first fraction of the treatment are capable of alerting treatment staff to errors that have the capacity to cause drastic changes to the expected treatment outcome. Therefore EPID treatment images that are acquired during treatment with no added setup time or dose to the patient, serve as an additional check and a record of the accuracy of the treatment [23].

Breast Treatment IVD Using EPID

Numerous publications have addressed the use of point-dose treatment verification for various sites using EPID dosimetry [33]–[38]. Ricketts *et al.* evaluated a transit dosimetry protocol and assessed the issues in the clinical implementation of EPIDs for IVD treatment verification. Ricketts *et al.* studied a number of treatment sites including breast, prostate, tonsil, tongue, and larynx and found that the magnitude of dose difference between the planned and the delivered treatment is dependent on the treatment site. Their study concluded that an optimisation of the dose calculation for different treatment sites and groups of patients would be an advantageous possibility [39].

Celi *et al.* more specifically examined the use of EPIgray. EPIgray (DOSIsoft, France) is a dose reconstruction software for IVD which uses the EPID images acquired on treatment to reconstruct a dose to a point of interest within the patient. Celi *et al.* found that the EPIgray reconstructed doses of breast treatments in comparison to other sites more often showed greater dose deviations from the TPS planned doses. Root cause analysis was subsequently performed across all their patients to study the cause of these deviations. Celi *et al.* have found that the EPIgray dose reconstruction is often performed over an incorrect environment as a consequence of variations in patient and EPID positioning on treatment. Celi *et al.*'s findings regarding the misalignment of the patient and EPID positioning has resulted in DOSIsoft developing algorithms for automatic image repositioning to accurately represent treatment conditions for the dose reconstructions [40]. Literature research has revealed that currently there is a lack of information regarding the optimisation of EPIgray for different treatment sites. Additionally, Celi *et al.* have identified the need for site specific optimisation of the EPIgray software for reliable use. This project aims to optimise the use of EPIgray for 3DCRT breast treatments.

1.4 EPIgray

EPIgray utilises the information contained in the transmission EPID images of the patient in their treatment position to reconstruct a dose to a point of interest within the patient. The intensity values associated with the pixels of the grey scale image is associated with a dose through the use of a calibration factor. The calibration factor is determined during EPID calibrations in which a known dose is delivered to the EPID and the resulting grey scale values of that image are correlated to the dose delivered. Using the transmission EPID image, EPIgray employs a back-projection dose calculation algorithm described by Francois *et al.* to reconstruct the dose a point of interest [41]. Francois *et al.*'s formalism employs a dose reconstruction approach in which the dose at the EPID plane is back-projected to a point of interest within the patient. The steps of the formalism are outlined below.

1. The dose measured on the EPID is converted to dose to water.
2. The dose to water from the previous step is converted to dose to water without an attenuator (patient or phantom) in the way of the beam.

3. The inverse square law (ISL) is then employed to calculate the dose to the point of interest (within the patient or phantom).

4. The final dose to the point of interest is then calculated by combining the dose from the previous step with the scatter contribution from the attenuator.

The EPIgray reconstructed dose is used to provide the percentage dose difference (%DD) between the TPS planned dose and the delivered dose calculated by EPIgray at the point of interest as shown in equation 1.1 [40].

$$\%DD = \frac{D_{EPIgray} - D_{TPS}}{D_{TPS}} \cdot 100\% \tag{1.1}$$

Where,

$D_{EPIgray}$ is the dose calculated by EPIgray

D_{TPS} is the dose planned on the TPS

1.4.1 EPIgray for EPID-Based IVD at Christchurch Hospital

EPIgray is an independent analysis system. Therefore EPIgray can be used for error detection in both dose delivery and patient positioning. EPIgray only requires an EPID image that was acquired during treatment and the initial plan data. Therefore most modern linacs with a built-in EPID can obtain the benefit of treatment verification following each fraction. Additionally, setup time associated with a lot of other in-vivo dosimeters currently in use can be avoided. Currently at Christchurch Hospital, curative-intent 3DCRT patients with limited low density tissue in the treatment field will have EPID images acquired on treatment for treatment verification using EPIgray. A tolerance of $\pm$5.0% has been set between the planned dose and the EPIgray reconstructed dose based on commissioning data. This baseline tolerance was set to account for the inherent uncertainties associated with EPIgray and other treatment-related uncertainties. The current tolerance is a generic tolerance and is department specific. The current tolerance gives rise to false positive results, where false positives results are dosimetric results that appear to be within $\pm$5.0% but are not truly within the $\pm$5.0% tolerance. False positives occur as a consequence of a range of reasons including but not limited to: variations in patient

positioning, incorrect acquisition of EPID image acquisitions and/or dosimetric errors. False positive results limit the reliable use of EPIgray for treatment verification of 3DCRT breast patients because there are chances that the EPIgray provided %DD is not representative of the dose delivered to the patient. At Christchurch Hospital the use of EPIgray is restricted to patients with limited low density tissue in the treatment field as EPIgray is known to perform poorly for accurate dose calculations involving widely varying tissue densities [39]. The use of EPIgray for IVD has tremendous potential however, clinical experience and literature review have revealed that the optimisation of the software for specific treatment sites are necessary to ensure efficient and reliable use [40].

1.4.2 EPIgray Workflow

EPIgray requires information from the TPS and the linac for dose calculation. The information required by EPIgray from each of the inputs is described below. The EPIgray workflow is also schematically shown in Figure 1.8.

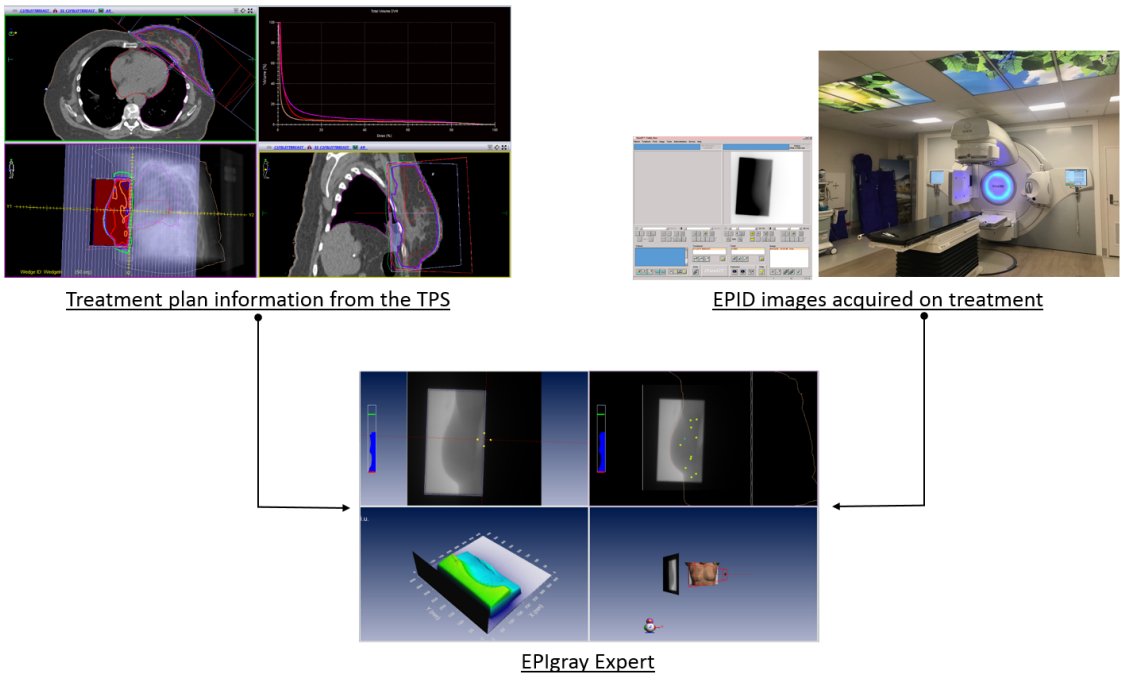

FIGURE 1.8: Schematic representation of EPIgray workflow

Exporting Information from TPS to EPIgray

EPIgray requires two inputs. The first is the treatment planning information that is exported from the TPS and directly imported into EPIgray. The information from the TPS is sent prior to treatment and includes the patient planning data in digital imaging and communications in medicine (DICOM) format. The following components of the plan are required from the TPS for EPIgray to be able to calculate the dose delivered to the patient:

- Patient CT image set.
- The radiation therapy plan with a marked point of interest at a known co-ordinate.
- The radiation therapy structure set, which includes details of the treatment volume as well as the OAR.
- Planned doses including total doses per fraction as well as individual beam doses within a fraction to the point of interest.

Exporting Information from the Linac to EPIgray

The EPID shown in Figure 1.9 will be extended throughout the treatment to acquire patient transmission images during the treatment. Figure 1.9 shows EPID position relative to the linac gantry. The EPID will oppose the linac gantry at every gantry angle to acquire transit EPID images. A transmission EPID image is acquired for every beam of radiation (treatment field) within the fraction. Once all the EPID images are acquired for a given fraction, these images are manually imported into EPIgray in DICOM format.

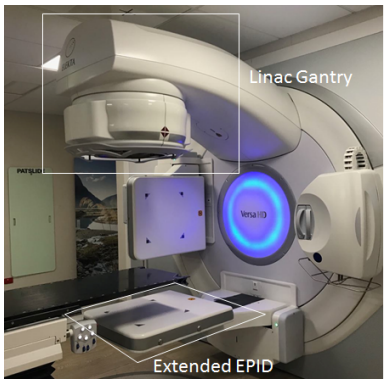

FIGURE 1.9: EPID in extended position to acquire a patient transmission image when the patient is set up on the treatment couch (black bed)

2 Aims of Research

The primary aim of this research is to optimise the use of EPIgray as an IVD system to improve the safety of 3DCRT breast radiotherapy treatments. Currently, the allowed %DD between TPS dose and the EPIgray calculated dose has been set to a tolerance of $\pm$5.0%. For specific categories of patients, it may be possible to reduce this tolerance when particular treatment conditions such as treatment volume size or laterality (side of the body treated) are met. In optimising the information obtained from EPIgray regarding breast treatments, the intention is to:

Aim 1: Use EPIgray to identify specific groups of patients at increased risk of having positional offsets on treatment

One of the aims of this research is to identify patients who are more at risk of having larger setup errors which may have the potential to compromise the treatment intent. As part of a retrospective study, patients who have previously been treated at Christchurch Hospital will be reanalysed within EPIgray. The relationship between the %DD between TPS and EPIgray doses and patient related factors such as the size of the patient's breast (target volume) and laterality of treatment volume will be considered to identify specific factors that influence the accuracy of the EPIgray calculated %DD.

Aim 2: Decrease the current tolerance between the TPS predicted dose and the EPIgray calculated dose

The current EPIgray tolerance was set based on the results of the EPIgray commissioning tests. This tolerance is not site specific and currently gives rise to false positive results in which the EPIgray provided %DD appears to be within the tolerance however the true result is not. False positive results may be decreased by decreasing the current tolerance with considerations to factors that specifically affect 3DCRT breast treatments. In addressing this aim, the optimal tolerance for 3DCRT breast treatments will be investigated and verified for clinical use with

consideration of the potential impact of the new tolerance on the clinical resources.

Aim 3: Identify more optimal points in analysis of dose difference between TPS dose and EPIgray dose

Currently the dose difference is considered for a user-specified point of interest. Other clinically relevant points will also be considered in order to decrease the %DD tolerance. With the most recent EPIgray update, 50 random points are generated within EPIgray. The doses to these points are calculated and the average dose to that volume is given [42]. This aim strives to identify whether the dose at the user-specified point of interest or the mean dose of 50 automated points provides the closest indication of the dose delivered to the patient on the day of the treatment.

Aim 4: Verify the ability of EPIgray to detect discrepancies between TPS calculated dose and the delivered dose

The entire EPID based IVD system will be tested using a phantom. The phantom will have realistic anatomical dimensions and electron densities, with comparable geometry and heterogeneities to a patient. End-to-end tests will be performed in which the phantom will be treated as a patient receiving 3DCRT breast treatment. The planned dose to the phantom and the EPIgray calculated doses for setup errors of zero and known magnitudes will be used to identify the agreement between the TPS doses and EPIgray doses.

2.1 Study Outline

This section provides a brief overview of the chapters to follow. The study has been divided into three parts:

I Retrospective study,

II Phantom study, and

III Uncertainty investigation

Chapter 3 addresses part I of this study. As part of the retrospective study, the effect of positional correction within EPIgray to account for setup errors on the %DD was examined. Previously treated patients with varying magnitude of setup errors on treatment were corrected for within EPIgray. The %DD before and after the positional correction on EPIgray were analysed for specific groups of patients. The retrospective study was designed to address research aims one, two and three.

Chapter 4 addresses part II of this study. As part of the phantom study, a phantom was designed to mimic breast and lung tissue for dosimetric measurements. The phantom study was designed in order to validate the findings of the retrospective study. Additionally, the reliability of the %DD between TPS and EPIgray doses was tested by comparing the %DD between TPS and other established dosimeters. The phantom study chapter addresses research aim four.

Chapter 5 addresses the major factors contributing uncertainties to the EPIgray reconstructed doses. In considering these factors, a new EPIgray tolerance has been proposed for 3DCRT breast treatments. The clinical impact of imposing the recommended tolerance is also discussed in this chapter. Chapter 5 addresses the second research aim of this study.

Lastly, Chapter 6 discusses the major findings and the clinical impact of this study, as well as the proposed future work of this project.

3 Retrospective Study

This chapter will address the sensitivity of EPIgray to setup errors on treatment through a retrospective study in which 30 previously treated 3DCRT breast patients were analysed using EPIgray. This study was designed to use EPIgray to identify specific groups of patients at increased risk of having setup errors on treatment. The findings of this study may be used to help justify decreasing the current clinical tolerance of $\pm$5.0% for specific groups of patients. The retrospective study grouped patients according to treatment laterality and the size of breast seen on the EPID images. Breast laterality was investigated due to the differences seen between the left and right breast fields. Left breast fields may have the presence of the heart to consider whilst the right breast fields will not. The effect of this difference was investigated in this study. Breast size was also investigated as the size of the breast will directly impact the scatter conditions and consequently the EPIgray reconstructed doses.

Following the import of all required information into EPIgray, an automatic back-projection calculation provides the %DD to a point of interest. At Christchurch Hospital the point of interest is the dosimetric reference point (DRP). The DRP location is user defined and must meet a set criteria for sensible use. The International Commission on Radiation Units and Measurements (ICRU) provides guidelines and criteria to determine an appropriate DRP. The DRP used at Christchurch Hospital is based on the recommendations of the ICRU. ICRU recommends that firstly the dose at the DRP must be representative of the treatment volume and be clinically relevant. Secondly, the DRP must be situated at a point where there are no sharp dose gradients and the dose can be accurately determined [43].

Ideally the %DD at the DRP (%DD$_{DRP}$) is expected to be 0%, indicating that there is no difference between the planned dose and EPIgray calculated dose. However deviations are likely as

a result of a number of reasons discussed in section 1.3.2 "Errors detected using EPID dosimetry". While there are several factors that influence the %DD, previous publications have identified setup errors on treatment to be the main cause of deviation between the planned and calculated doses [40]. The setup errors on treatment can be categorised into patient-related and EPID-related errors.

Patient-related errors may be systematic or random. When considering setup errors, random errors are always present in a radiotherapy setting. While the use of immobilisation devices can minimise the setup errors, the treatment of the breast does involve movable tissue. Additionally movement of the breast tissue is also likely with breathing motion. As such, the slight differences in the placement of breast tissue relative to the treatment field will affect the EPIgray calculated dose and consequently $\%DD_{DRP}$. In contrast, systematic errors are errors of similar magnitude and are likely to persist at all fractions of the treatment. For example, if the treatment staff have accidentally input incorrect numbers for patient setup, the patient will be setup at a different treatment position from the expected treatment position at every fraction. Consequently the dose received by the patient is different to the planned dose and the patient will not have received the appropriate treatment. Both random and systematic errors pose a great risk to the patient if these errors are large enough to compromise the treatment intent. Consequently, these errors highlight the importance of having an IVD system in place for identifying major set-up errors.

The study by Celi *et al.* identified EPID positioning on treatment to also have an impact on the EPIgray reconstructed dose [40]. The EPID position must be correctly aligned with the patient and the radiation source as expected by the TPS to provide the most accurate dose. However, the treatment fields associated with breast treatments may be asymmetrical to provide shielding to the nearby OAR such as the lungs. Therefore the EPID position may need to be shifted from its initial deployed position to a more appropriate position for the entire transmission image to be captured. Consequently the EPID position is different to the TPS expected position and the reconstructed dose will reflect this change in the reconstruction environment. The provided dose and consequently the %DD does not indicate dosimetric errors, as the patient could still be in the expected treatment position. Given that the patient has been set up accurately and

the linac is within the expected operating parameters, the DRP within the patient should have received the correct dose because the patient would have been setup relative to the radiation source and not the position of the EPID. With changes to the expected EPID position, the provided $\%DD_{DRP}$ would have been calculated by associating the EPID signal to the wrong plan parameters. Therefore in cases where the EPID has been shifted, the position of the EPID must be corrected for within EPIgray to ensure the $\%DD_{DRP}$ is representative of the actual treatment delivered to the patient. This concept is schematically shown in Figure 3.1.

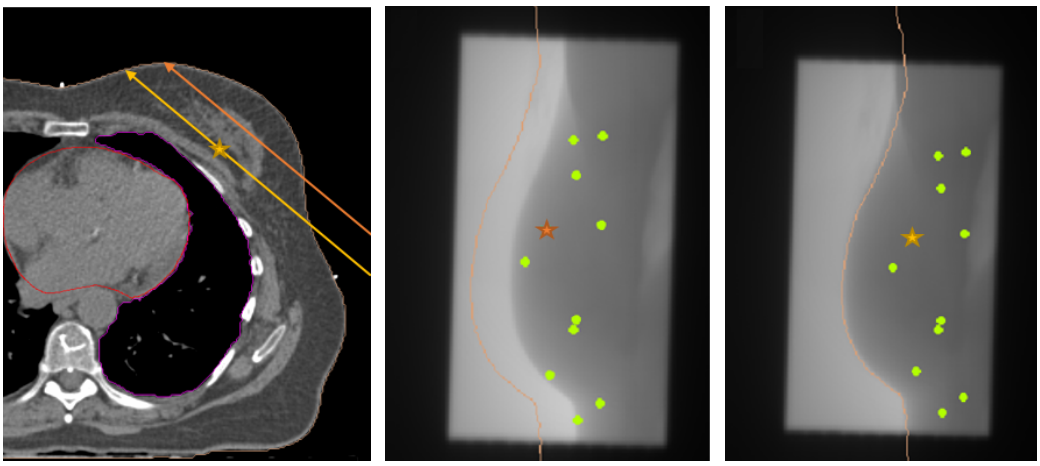

(a) (b) (c)

FIGURE 3.1: Schematic illustration of positioning errors on EPIgray results. (a) Reconstruction is expected to be performed at the yellow star, however setup errors have resulted in the dose reconstruction to be performed in a different environment (orange arrow). (b) Dose is reconstructed based on different plan parameters than expected and is evident by the lack of agreement between the shape of the breast seen on the EPID image and contours of the breast from the TPS (orange contour). (c) Manual alignment of the EPID image to the TPS contours has been performed to ensure that EPIgray calculates a dose that is dependent on the true environment present at treatment.

Subsequent to this current work, in the most recent update of EPIgray, released on 14^{th} December 2018 DOSIsoft enabled fractional dosimetric analysis using the reconstructed doses at 50 automatically generated points. After EPIgray has received all the information it requires from the TPS, EPIgray randomly generates 50 points within a volume that is representative of the treatment volume. EPIgray reconstructs the doses at these 50 points to provide a fractional mean dose to the volume, a %DD to the volume ($\%DD_{vol}$) and the standard deviation associated with the reconstructed dose. DOSIsoft now recommends the use of the $\%DD_{vol}$ rather than department specified points e.g. the currently used DRP at Christchurch Hospital. The use of $\%DD_{vol}$ in the place of $\%DD_{DRP}$ would be a significant change in practice at Christchurch Hospital. The feasibility of the use of $\%DD_{vol}$ in place of the currently used $\%DD_{DRP}$ for indication

of treatment delivery accuracy according to EPIgray was also investigated as part of this study.

3.1 Correction Methods

The EPIgray software allows the use of two methods to correct for patient and EPID positional errors to obtain a $\%DD_{DRP}$ that reflects the treatment delivered to the patient. These two methods are:

1. EPID position correction, and
2. Contour matching correction

3.1.1 Correction Method 1: EPID Position Correction

Manual adjustment of the EPID position within EPIgray allows correction of offset EPID position that has occurred on treatment. EPID position correction is performed by aligning the planned field edges that are imported directly from the TPS to the edges of the EPID image captured on treatment. Consequently the $\%DD_{DRP}$ that is obtained following correction of the EPID position is more indicative of the treatment delivered to the patient. Figure 3.2a shows an example of a misalignment between the EPID image and the field edges imported from the TPS. Following a manual adjustment of the EPID position within EPIgray, there is acceptable alignment between the EPID image and the field edges as seen in Figure 3.2b.

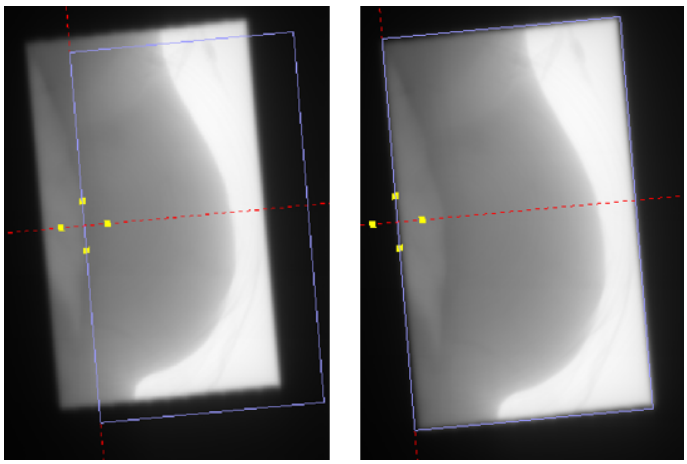

(a) (b)

FIGURE 3.2: Effect of EPID position correction (a) Misalignment seen between the field edges (purple rectangular box) and the EPID image. (b) EPID position correction performed on EPIgray to align field edge to EPID image.

3.1.2 Correction Methods 2: Contour Match Correction

The ability to position the patient in the exact position they were in during the simulation CT is difficult to achieve. Immobilisation devices customised specifically for the patient will aid in decreasing the variations in patient positioning on treatment. However, immobilisation devices will not eliminate these variations altogether. Such variations in patient positioning can be corrected for within EPIgray to provide a $\%DD_{DRP}$ that is more reflective of the treatment delivered to the patient.

Contour match correction can be performed within EPIgray by aligning the patient contour evident on the EPID image to the patient contour from the TPS. An example of contour match correction is shown in Figure 3.3. The green points in Figure 3.3 are points at which EPIgray calculates the dose. These points are automatically and randomly selected by EPIgray. The cyan asterisks seen in Figure 3.3 represents the DRP. The dose to be delivered to the patient in 3DCRT breast treatment is prescribed to the DRP when planning to provide uniform dose distribution to the entire breast volume. The DRP is user-specified within the TPS and the dose at this point is known. The dose reconstructed at the DRP is used to provide $\%DD_{DRP}$ calculated using equation 1.1. By performing contour match correction, the DRP is effectively shifted closer to the position where the TPS expects the DRP to be relative to the patient's anatomy, i.e. contour matching allows the DRP to be positioned in relation to the breast and lung tissue instead of the field edges. Therefore contour match correction is arguably better at providing an indication of treatment accuracy in comparison to EPID position correction because the former method focuses on the tissue itself instead of the reconstruction field of view.

The main limitation of contour match correction is that if patient offset on treatment has occurred, there will be a difference in the dose calculated to the DRP. However, not correcting for patient offset on treatment will lead to an overestimation in dose to the DRP due to the limitations associated with the EPIgray back-projection dose calculation algorithm. The impact on the dose to the DRP with patient offset on treatment was investigated and is presented in Chapter 4.

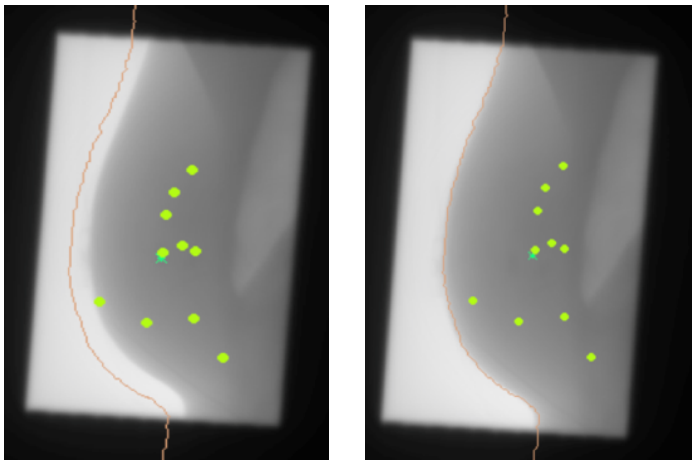

(a) (b)

FIGURE 3.3: Effect of contour match correction (a) Misalignment seen between the planning breast contour (orange contour) and the EPID image breast contour. (b) Decent alignment seen between the planning breast contour and the EPID image contour

3.2 Methods

As part of the retrospective study, positional correction and analysis was conducted for 30 previously treated 3DCRT breast patients. Due to anatomical differences between patients, and the requirement to obtain adequate dose coverage across the treatment volume, each patient had either two or three treatment fields per fraction. EPID images were acquired for a total of 255 fields across all 30 patients. EPIgray analysis was performed on all 255 EPID images.

For each field, the following data were acquired:

1. The initial $\%DD_{DRP}$.
2. The magnitude of shift required in the x and y dimensions within EPIgray to obtain the alignment between the TPS breast contour and the breast contour seen on the EPID image (correction method 2).
3. The resulting $\%DD_{DRP}$ following positional correction.
4. The width of the separation between the lung and the DRP as shown in Figure 3.4.

For the majority of this project, the accuracy of treatment delivery was analysed using $\%DD_{DRP}$ as $\%DD_{vol}$ was not available. However following the introduction of $\%DD_{vol}$ similar analysis

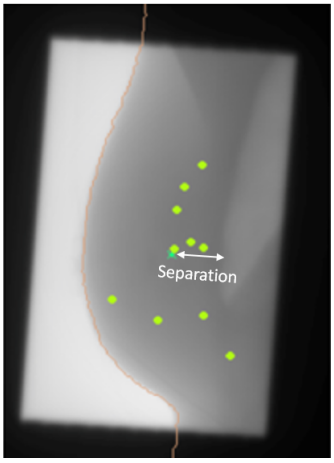

FIGURE 3.4: Separation measured between the lung and DRP

using the method above was performed for 23 of 30 patients. Seven patients were omitted from this section of the study as they could not be re-imported into EPIgray for analysis. $\%DD_{vol}$ is an indicator of fractional treatment delivery accuracy. Therefore for these 23 patients, the position corrected fractional $\%DD_{DRP}$ was obtained to draw comparisons to $\%DD_{vol}$.

The approach of the retrospective study was designed to achieve the following aims:

1. Identify specific groups of patients at risk of having positional offsets on treatment (aim 1 of Chapter 2).
2. Decrease the current tolerance between the TPS predicted dose and the EPIgray calculated dose for specific groups of patients (aim 2 of Chapter 2).
3. Verify that the use of $\%DD_{DRP}$ for treatment verification is appropriate and investigate the usability of $\%DD_{vol}$ for indication of treatment delivery accuracy at Christchurch Hospital (aim 3 of Chapter 2).

3.3 Results

The results section of the retrospective study is presented in five parts:

- Subsection 3.3.1 presents the analysis of the magnitude and direction of shifts required for patient positional correction for each group.
- Subsection 3.3.2 presents the numerical results of patient positional correction.

- Subsection 3.3.3 presents the dosimetric effect of patient positional correction.
- Subsection 3.3.4 presents the effect of low density tissue in EPIgray reconstruction window on the $\%DD_{DRP}$.
- Subsection 3.3.5 presents the results of the investigation involving the use of $\%DD_{vol}$ at Christchurch Hospital.

3.3.1 Shifts Required for Patient Positional Correction

The following subsection presents the magnitude and direction of shifts required for contour match correction to account for patient setup errors on treatment. The EPID position at which the transmission images were acquired varies from patient to patient. In order to identify specific groups of patients at risk of having positional offsets on treatment, the EPID position was corrected using the method described in subsection 3.1.1. In correcting for the EPID position, the remaining discrepancy between the breast contour on the EPID image and the breast contour from the TPS will indicate the differences in the patient positioning. EPID position correction was performed for all 255 fields to eliminate the variations in the expected EPID position. Contour match correction described in subsection 3.1.2 was then performed to obtain the shifts required for patient positional correction.

The patient is set up in 3-dimensions (3D) on treatment however the shifts for positional corrections within EPIgray are based on a 2D image. The 3D patient positional shift directions on treatment is shown in Figure 3.5. EPIgray positional corrections are performed in the x- and y-dimensions. The shifts in the x-dimension corresponds to patient movement in the anterior-posterior direction. However the patient could be offset to a position that is further away from the radiation source (distal) or closer to the radiation source (proximal). The distal and proximal shifts of the patient will also require corrections in the x-dimension as a result of performing positional corrections for 3D shifts in 2D. Shifts in the y-dimension corresponds to shifts in the superior-inferior direction of the patient. Both the magnitude and the direction of shifts were considered in the x and y dimensions for all 255 fields. The results presented below are grouped according to treatment laterality and breast size.

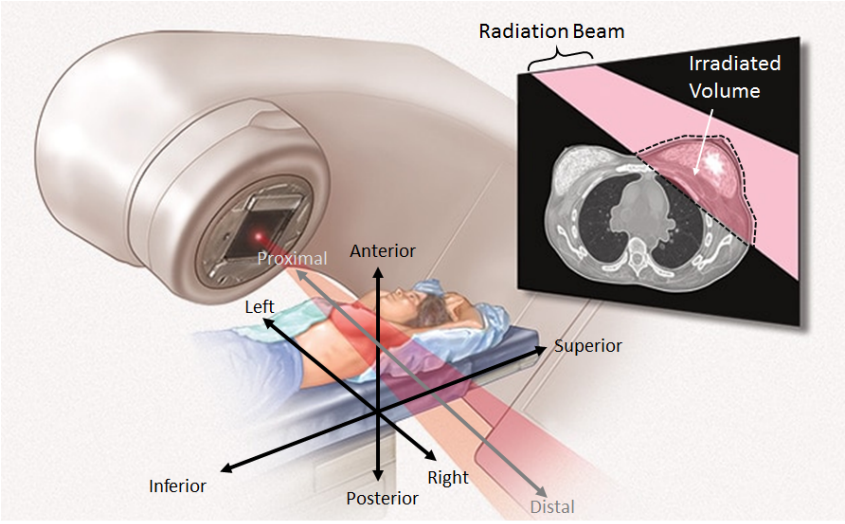

FIGURE 3.5: Directions of Patient Shifts. Note: This figure also shows an axial view of the treatment plan with the radiation beam direction and the irradiated treatment volume. The position of the radiation beam determines the linac gantry position for treatment. [44]

Breast Laterality

Shifts were implemented in the positive and negative directions for both lateralities. In order to consider only the magnitude of these shifts, the absolute values of the shifts were used to calculate the average magnitude of shift required for left and right breast fields. The average shift required for left and right breast fields were 3.1±2.9 mm and 5.4±4.2 mm respectively. The distribution of the absolute total magnitude of shift required for all fields of left and right laterality are shown Figure 3.6.

Figure 3.6 reveals that left breast fields typically required a smaller magnitude of shift in comparison to right breast fields. In considering the most common shift magnitude for both lateralities, it was found that 24% of left breast fields required an absolute shift between 0.0 mm and 1.0 mm and 15.4% of right breast fields required an absolute shift of 3.0 mm to 4.0 mm. Figure 3.6 also shows that right breast fields required a larger range of shifts in comparison to left breast fields.

x-shift

The distribution of shifts required in the x-dimension is shown in Figure 3.7. The average magnitude of shift required in the x-dimension for the left and right breast fields were 2.1±2.3 mm

FIGURE 3.6: Distribution of absolute magnitude of shift required for positional correction of fields of both lateralities

and 3.9±3.3 mm respectively. Figure 3.7 and the average magnitude of shift required in the x-dimension for patient positional correction indicate that right breast fields were not only more likely to require a shift in the x-dimension in comparison to left breast fields, but right breast fields were also more likely to require a larger shift than left breast fields. Figure 3.7 shows that majority of the left breast fields required a shift in the negative direction which corresponds to the patient offset to a position that is more posterior and/or distal from the expected position. The majority of right breast fields required a shift in the positive direction which corresponded to the patient being setup at a position that is more anterior and/or proximal than the expected position. A two-sample t-test assuming unequal variances with a significance level of 5% was conducted with the null hypothesis that there are no statistical differences between the shifts required for left and right breast fields in the x-dimension[1]. The p-value obtained was 0.20. The p-value obtained for the required x-shifts for each laterality indicates that the null hypothesis cannot be rejected and there were no statistical differences in the x-shifts required between both lateralities. Therefore the differences seen in the direction of shift required in the x-dimension between lateralities was circumstantial.

[1]Note: T-tests have been performed throughout this study to investigate the statistical significance between data. While it has been reported that t-tests are more robust for data of normal distributions, publications have revealed t-tests are valid for sample sizes above 40 [45]–[48]. The suitability of t-tests were confirmed before use in all instances throughout this study. All t-tests were performed using Microsoft Excel (2013), which employs t-test methodology from a publication by Biometrika [49].

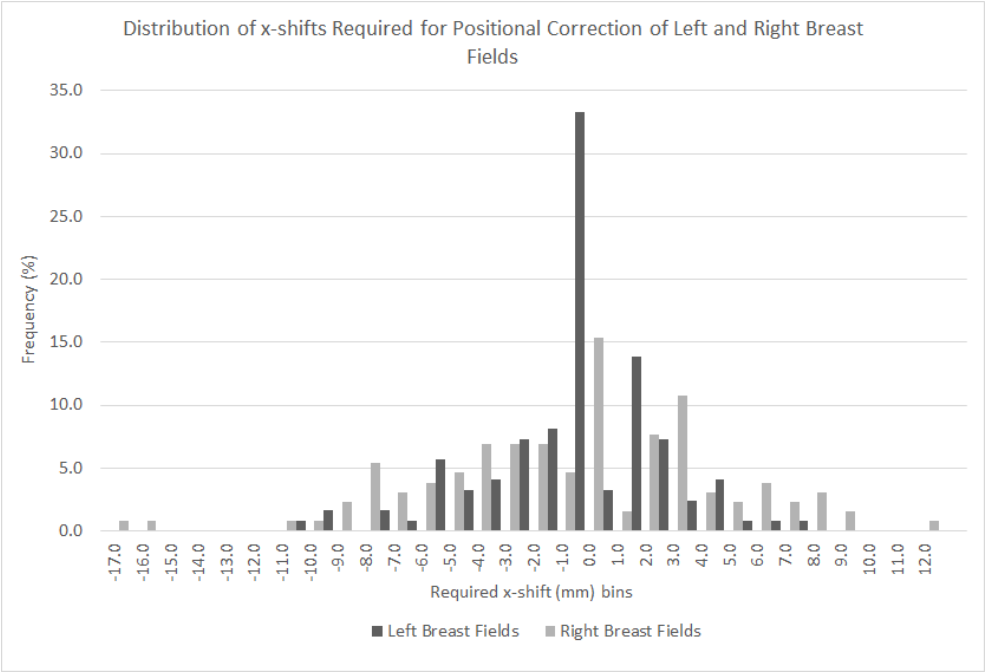

FIGURE 3.7: Breast Laterality: x-shift required for positional correction

y-shift

The average magnitude of shift required in the y-dimension for left and right breast fields were 1.5±2.5 mm and 2.5±3.8 mm. These values indicate that on average right breast fields required a larger magnitude of patient positional correction in y-dimension in comparison to left breast fields. Figure 3.8 shows the distribution of the magnitude and direction of y-shifts required for positional correction of fields within EPIgray. Figure 3.8 reveals that 60% of left breast fields required a shift between 0.0 mm and -1.0 mm while 48% of right breast fields required a shift between 0.0 and 1.0 mm. These results indicate that patient setup errors were more prominent in right breast fields. The discrepancy seen in the direction of shift required was unexpected. Results revealed that more left breast fields required a shift in the negative direction corresponding to a patient shift in the superior direction for correction. In contrast, majority of the right breast fields required a shift in the positive direction corresponding to a patient shift in the inferior direction for correction. A statistical significance test was performed to investigate the discrepancy seen in the direction of correctional shifts required for each laterality. A two-sample t-test assuming unequal variances with a significance level of 5% was conducted with the null hypothesis that there were no statistical differences between the shifts required for left and right lateralities in the y-dimension. The p-values obtained was 0.01. The p-value

obtained for the required y shifts indicate that the shifts required between left and right breast fields were statistically different.

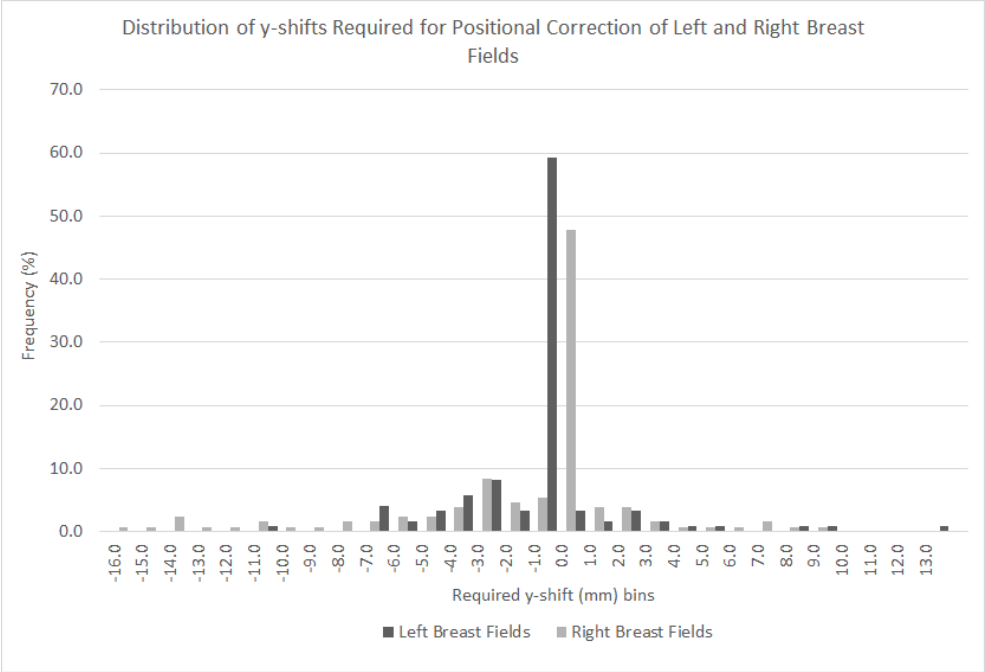

FIGURE 3.8: Breast Laterality: y-shift required for positional correction

By comparing Figures 3.7 and 3.8 it is evident that correctional shifts in the x-dimension was more likely. Figures 3.7 and 3.8 indicate that there were larger patient positional set up errors in the anterior-posterior and proximal-distal directions than in the superior-inferior direction.

Table 3.1 shows the number of fields of left and right lateralities requiring zero shifts or shifts in a specific direction in x and y dimensions. In considering the x-dimension it was found that the left breast fields do not exhibit a specific trend. That is, approximately a third of left breast fields required a negative shift, a third of left breast fields required a positive shift and a third of the left breast fields required zero shift for patient positional correction. In contrast, it was found that right breast fields required negative shift followed by a positive shift, with very few fields requiring no shift. While there were noticeable differences, the results of the t-test indicated no significant differences between the shifts required in the x-dimension for left and right breast fields. Considering the shifts in the y-dimension, it was found that majority of the fields required zero shift for both lateralities. However, the left breast field required more negative shifts than positive shifts and the opposite was true for right breast fields. This finding

suggests that left breast patients were more likely to be setup at a position that is inferior to the expected position while right breast patients were more likely to be setup at a position that is more superior to the expected treatment position.

TABLE 3.1: Number of left and right breast fields requiring negative, positive and zero magnitude shifts in x and y dimensions for positional correction

Number	x-dimension		y-dimension	
of Fields	Left Breast	Right Breast	Left Breast	Right Breast
Negative Shifts	42 (34.1%)	64 (48.5%)	34 (27.6%)	19 (14.4%)
Zero Shifts	40 (32.5%)	19 (14.4%)	72 (58.6%)	61 (46.2%)
Positive Shifts	41 (33.4%)	49 (37.1%)	17 (13.8%)	52 (39.4%)

Breast Size

The 30 breast patients were separated into two groups (small and large breasts) according to maximum breast thickness visible on the acquired EPID images. Both groups had 15 patients. The absolute magnitude of shifts required for patient positional correction were used to obtain the average magnitude of shift required for small and large breast fields, which were 3.2±2.9 mm and 5.4±4.2 mm respectively. The distribution of the total magnitude of shift required for small and large breast size fields is shown in Figure 3.9.

Figure 3.9 shows that small breast fields typically required smaller magnitude of shift with approximately 21% of small breast fields requiring a shift between 0.0 mm to 1.0 mm. Similarly majority of large breast fields, although smaller in percentage in comparison to small breast fields also required a shift between 0.0 mm and 1.0 mm. The range of shifts required is noticeably larger for large breast fields. This observation indicates that large breast fields were more prone to setup errors on treatment.

x-shift

The distribution of shifts required in the x-dimension is shown in Figure 3.10. The average magnitude of shift required in the x-dimension for small and large breast fields were 2.2 ± 2.0

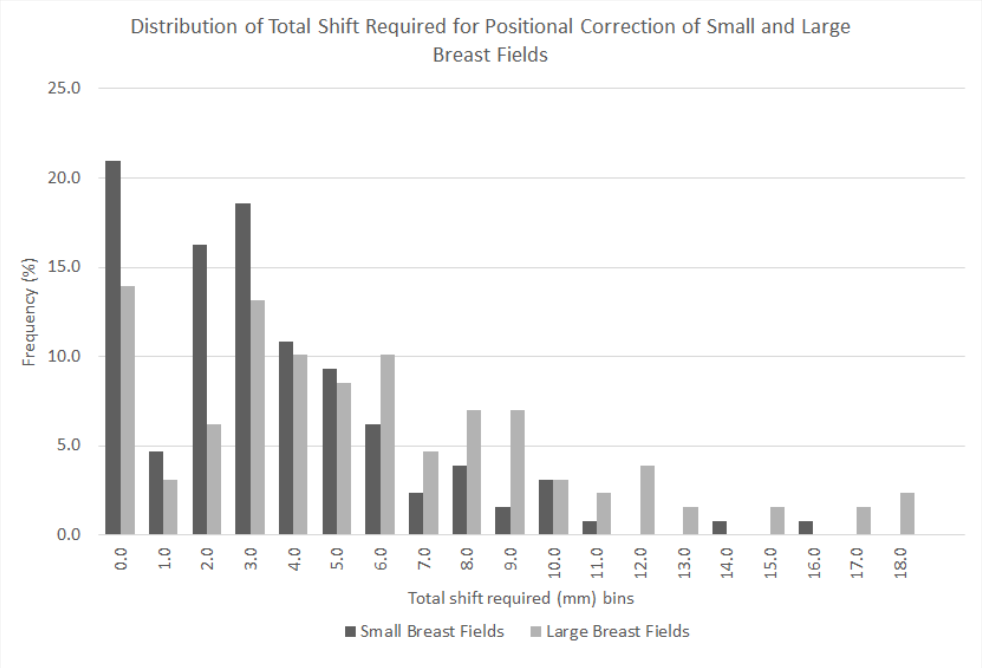

FIGURE 3.9: Distribution of total magnitude of shift required for positional correction of fields grouped according to breast size

mm and 4.0 $\pm$ 3.4 mm respectively. The average magnitude of shift in the x-dimension indicates large breast fields to require a larger shift than small breast fields. Figure 3.10 shows that majority of the small breast fields required a shift between -1.0 mm and 0.0 mm whilst majority of the large breast fields required a shift between 0.0 mm and 1.0 mm. Figure 3.10 also shows that there was a larger range of shifts associated with the large breast fields in comparison to small breast fields.

In order to investigate the differences in the direction of shift in the x-dimension, a t-test assuming unequal variance with a significance level of 5% was conducted with the null hypothesis that shifts required in the x-dimension between small and large breast fields were not statistically significant. The obtained p-value was <0.05. Therefore the null hypothesis can be rejected and the shifts required in the x-dimension for small and large breast fields were statistically different.

y-shift

The average magnitude of shift required in the y-dimension for small and large breast fields were 1.7$\pm$2.7 mm and 2.4$\pm$3.7 mm. This result indicated that large breast fields on average

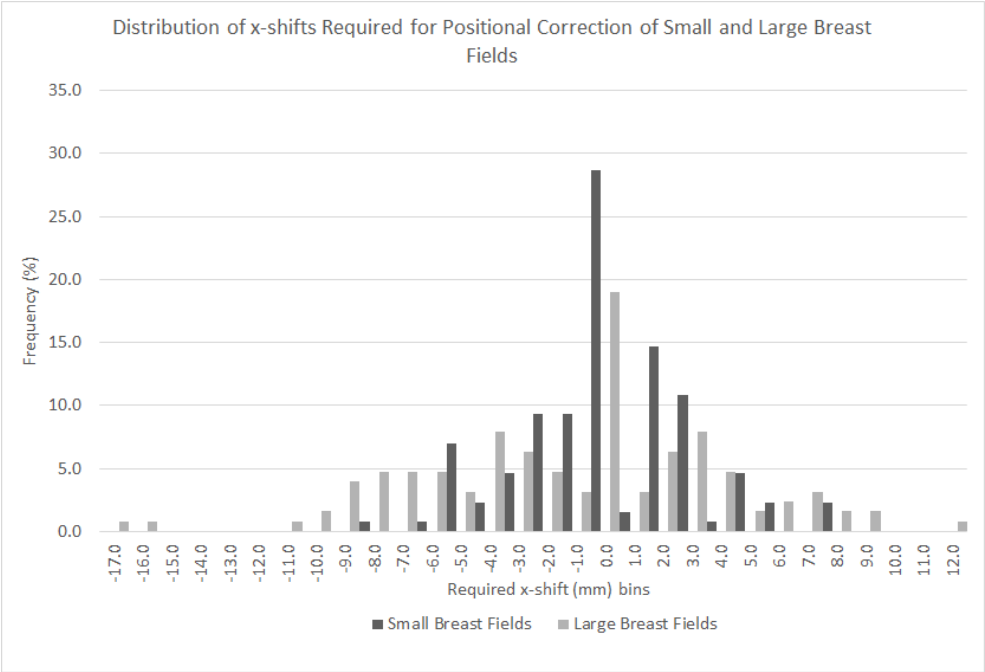

FIGURE 3.10: Distribution of x-shift required for positional correction of fields groups according to breast size

required a larger magnitude of shift in the y-dimension than small breast fields. Additionally, in drawing comparisons to the average magnitude of shift required for small and large breast fields in the x-dimension, it was found that shifts in the y-dimension for both breast sizes were of smaller magnitude. From Figure 3.11 it is evident that majority of small breast fields required a shift between -1.0 mm and 0.0 mm whilst majority of the large breast fields required a shift between 0.0 mm and 1.0 mm. These shifts indicate that small breasts were more likely to be setup at a position that is inferior to the expected position and large breasts were more likely to be setup at a position that is more superior to the expected treatment position. In comparing Figures 3.10 and 3.11 it is found that in 3DCRT breast treatment there were more shifts in the x-dimension for positional correction than in the y-dimension. This observation is in agreement with the calculated average magnitude of shifts required for both breast sizes in the x and y-dimensions. The results in this section therefore indicate that the setup errors were more likely in the anterior-posterior and distal-proximal planes than in the superior-inferior plane for both breast size groups.

In order to investigate the differences seen in the direction of shift in the y-dimension, a t-test assuming unequal variance with a significance level of 5% was conducted with the null

hypothesis that shifts required in the y-dimension for small and large breast fields were not statistically different. The obtained p-value was <0.05. Therefore the null hypothesis can be rejected and the shifts required in the y-dimension between small and large breast fields were statistically different.

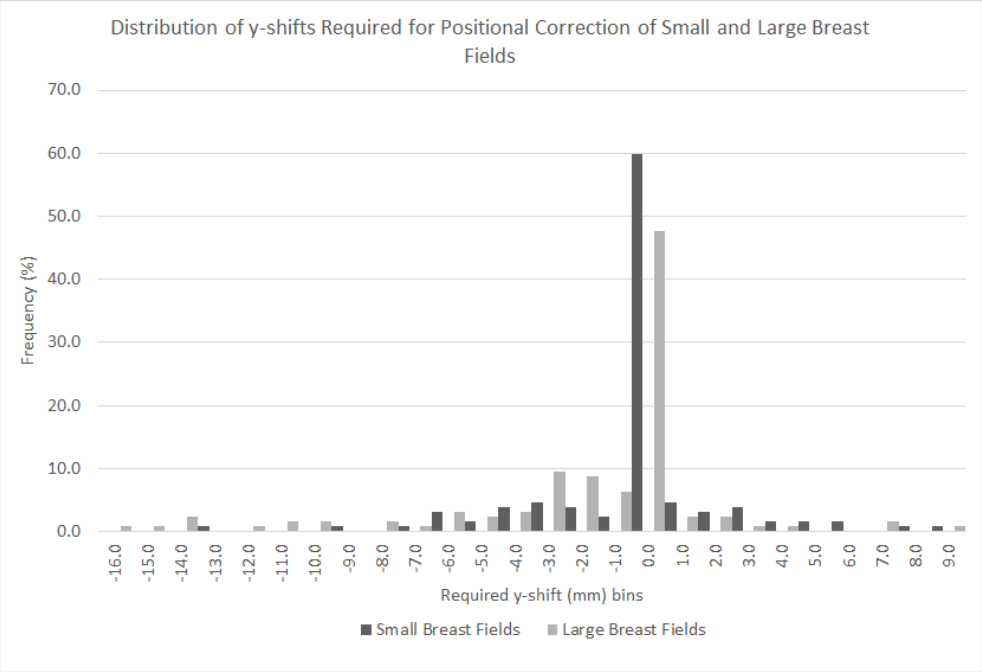

FIGURE 3.11: Distribution of y-shift required for positional correction of fields groups according to breast size

Table 3.2 shows the number of fields grouped according to breast size requiring 2D shifts in the positive and negative directions, as well as the number of fields that did not require any shifts to correct for setup errors. In considering shifts in the x-dimension, the results in table 3.2 reveal that small breast fields were more likely to require a positive shift than a negative shift, indicating small breast fields were more often setup at a position that was more anterior and/or proximal than the expected position. In contrast, large breast fields were more likely to require a negative shift than a positive shift, indicating large breast fields were more often setup at a position that was more posterior and/or distal from the expected treatment position. Results in table 3.2 also reveal that small breast fields were less likely to require a shift in the x-dimension than large breast fields by approximately 10%. In considering y-dimensional shifts shown in table 3.2, it was found that a large percentage of small breast fields required zero shift while positive and negative shifts were approximately equivalent. Large breast fields were similar to small breast fields in that a large number of fields did not require shifts in the y-dimension.

However, table 3.2 shows that a large number of fields required a negative shift than a positive shift, indicating that large breast fields were more often setup at a position that was more inferior than the expected position. These results indicate that large breast fields were more prone to setup errors as indicated by the smaller number of fields requiring no shifts in comparison to small breast fields.

TABLE 3.2: Number of small and large breast fields requiring negative, positive and zero magnitude shifts in x and y dimensions for positional correction

Number	x-dimension		y-dimension	
of Fields	Small Breast	Large Breast	Small Breast	Large Breast
Negative Shifts	45 (34.9%)	61 (48.4%)	30 (23.3%)	56 (44.4%)
Zero Shifts	36 (27.9%)	23 (18.3%)	74 (57.3%)	59 (46.9%)
Positive Shifts	48 (37.2%)	42 (33.3%)	25 (19.4%)	11 (8.7%)

3.3.2 Numerical Results of Positional Correction Performed Within EPIgray

Following patient positional correction on EPIgray, the effects of contour match correction on the resulting $\%DD_{DRP}$ for differing treatment lateralities and breast sizes was investigated. $\%DD_{DRP}$ obtained from EPIgray before and after positional correction were used to categorise the fields into one of four categories:

1. True pass[2] (TP) - A field that was initially within $\pm 5.0\%$ tolerance before positional correction and remains within $\pm 5.0\%$ tolerance following positional correction.
2. True fail[3] (TF) - A field that was initially outside of $\pm 5.0\%$ tolerance before positional correction and remains outside of $\pm 5.0\%$ tolerance following positional correction.
3. False pass[4] (FP) - A field that was initially within $\pm 5.0\%$ tolerance before positional correction and falls outside of $\pm 5.0\%$ tolerance following positional correction.
4. False fail[5] (FF) - A fields that was initially outside of $\pm 5.0\%$ tolerance before positional correction however falls within $\pm 5.0\%$ tolerance following positional correction.

[2]The terms 'true positive' and 'true pass' will be used interchangeably in this thesis.
[3]The terms 'true negative' and 'true fail' will be used interchangeably in this thesis.
[4]The terms 'false positive' and 'false pass' will be used interchangeably in this thesis.
[5]The terms 'false negative' and 'false fail' will be used interchangeably in this thesis.

Breast Laterality

Of 255 fields analysed, 123 fields were left breast fields and 132 were right breast fields. Table 3.3 shows the initial number of passing and failing fields before positional correction and the number of passing and failing fields following positional correction. Results of table 3.3 show no major differences between the lateralities. However it was found that with positional correction the left breast fields in this study produced more falsely failing results as indicated by an increase in the number of corrected passes. In contrast, right breast fields produced more falsely passing fields as indicated by a decrease in the number of corrected passes. Table 3.3 provides the number of initial passing and failing fields and corrected passing and failing fields. However these numbers do not provide field specific information following positional correction. That is, table 3.3 does not provide any indication of the number of fields that have truly passed or failed or falsely passed or failed following positional correction on EPIgray. The fate of the fields following positional correction is presented in table 3.4. Table 3.4 shows the specific statistics that identify the fields that have truly passed and failed along with the fields that have falsely passed and failed as a consequence of performing positional correction within EPIgray.

TABLE 3.3: Initial number of passing and failing fields and corrected number of passing and failing fields of left and right laterality

Numbers	Left	Right
Total number of fields	123	132
Initial Passes	108 (87.8%)	121 (91.7%)
Initial Fails	15 (12.2%)	11 (8.3%)
Corrected Passes	112 (91.1%)	115 (87.1%)
Corrected Fails	11 (8.9%)	17 (12.9%)

TABLE 3.4: The effect of positional correction on the fields of left and right laterality

Numbers	Left	Right
True Pass	101 (82.1%)	107 (81.1%)
True Fail	4 (3.3%)	3 (2.3%)
False Pass	7 (5.7%)	14 (10.6%)
False Fail	11 (8.9%)	8 (6.1%)

The statistics shown in table 3.4 do not show any significant differences between left and right breast fields in the number of true passes, true fails and false fails. However, the number of false passes between the two lateralities reveal that right breast fields were almost twice as likely to produce a falsely passing result than left breast fields. Following investigation of these failing results it was found that six of the falsely passing right breast fields have come from one patient. This particular patient had three fields per fraction. Inaccurate acquisition of EPID images over two fractions had led to six falsely passing results. Inaccurate acquisition of EPID images refer to not acquiring the entire field within the image. Therefore ignoring the EPIgray results for this patient, there were no significant differences between the lateralities when considering the number of truly passing and failing fields and the number of falsely passing and failing fields. However, these results emphasise the need for verification of proper alignment between the EPID image and the TPS contours to ensure that the given $\%DD_{DRP}$ is reflective of the treatment delivered to the patient.

Breast Size

Table 3.5 shows the initial and the positional corrected number of passing and failing fields. Initial observation of table 3.5 reveals that the effect of positional correction on EPIgray is not breast size dependent. Both small and large breast fields show similar number of passes and fails both before and after positional correction within EPIgray. However for in depth analysis, it is important to categorise these fields as true passes and true fails as well as false passes and false fails to truly examine the effect of positional correction on the $\%DD_{DRP}$ for each breast size. Table 3.6 shows specific statistics that identify the fields that have truly passed and failed as well as fields that have falsely passed and failed following positional correction on EPIgray.

TABLE 3.5: Initial number of passing and failing fields and corrected number of passing and failing fields of small and large breast size groups

Numbers	Small	Large
Total number of fields	129	126
Initial Passes	117 (90.7%)	112 (88.9%)
Initial Fails	12 (9.3%)	14 (11.1%)
Corrected Passes	116 (89.9%)	112 (88.9%)
Corrected Fails	13 (10.1%)	14 (11.1%)

TABLE 3.6: The effect of positional correction on the fields of small and large breast sizes

Numbers	Small	Large
True Pass	109 (84.5%)	99 (78.6%)
True Fail	5 (3.9%)	1 (0.8%)
False Pass	8 (6.2%)	13 (10.3%)
False Fail	7 (5.4%)	13 (10.3%)

Results shown in table 3.6 indicate that small breast fields were more likely to truly pass than large breast fields. However the total number of passing fields for small and large breast fields was found to be 90.7% and 88.9%. Therefore, these results indicate that the breast size does not affect the $\%DD_{DRP}$ following positional correction within EPIgray as there were similar number of passing and failing fields. However results shown in table 3.6 reveal that large breast fields were more likely to produce falsely passing and falsely failing results than small breast fields. Considering the results shown in tables 3.5 and 3.6 and considering only the fields that have failed, it was found that only 7.1% of the large fields that produced a failing result were true fails, while 92.9% were falsely failing fields. In contrast, the small breast fields that produced a failing result showed more of an even divide between truly failing fields and falsely failing fields. 41.7% of the initially failing small breast fields remained as failing fields following positional correction and 58.3% of initially failing small breast fields were within tolerance following positional correction. This observation at this point could be circumstantial. A t-test was performed to identify significant differences between small and large breast fields. The result of the t-test will be discussed in subsection 3.3.3.

3.3.3 Dosimetric Effect of Positional Correction Within EPIgray

The $\%DD_{DRP}$ is expected to change following positional correction within EPIgray because the environment over which the reconstruction is performed has changed. This section presents the dosimetric results of performing positional corrections. The dosimetric effects of the positional correction were subsequently analysed according to treatment laterality and breast size.

Breast Laterality

The $\%DD_{DRP}$ is calculated using equation 1.1 from Chapter 1. It is important to note that negative and positive $\%DD_{DRP}$ indicate that EPIgray has calculated a dose to the DRP that is less than and more than the TPS planned dose respectively. Therefore in order to find the average $\%DD_{DRP}$ of each laterality, the absolute $\%DD_{DRP}$ were used. This section only addresses the magnitude of the $\%DD_{DRP}$ not whether the $\%DD_{DRP}$ indicated an underdose or an overdose.

The average $\%DD_{DRP}$ before positional correction for left and right breast fields was found to be 3.4$\pm$3.9% and 3.2$\pm$3.7% respectively. Acknowledging the inherent uncertainties associated with the EPIgray dose calculation algorithm, these numbers are comparable to each other. Following positional corrections within EPIgray, it was found that the average $\%DD_{DRP}$ is 2.4$\pm$1.8% for left breast fields and 2.7$\pm$3.0% for right breast fields. Results have indicated an improvement in the $\%DD_{DRP}$ for both left and right breast fields. In order to find evidence of statistical difference between left and right lateralities, a two-sample T test assuming unequal variances with a significance level of 5% was conducted with the null hypothesis that there were no statistical differences in the $\%DD_{DRP}$ of left and right lateralities following positional correction. The p-value obtained was 0.43. This p-value indicates that the null hypothesis cannot be rejected. Therefore the small difference in the average $\%DD_{DRP}$ values after positional correction between left and right lateralities was a result of the uncertainties associated with EPIgray itself.

Distribution of The Percentage Dose Difference

For EPIgray to be an exact indicator of the treatment delivered to the patient, the $\%DD_{DRP}$ should be 0.0%, given that there were no uncertainties associated with treatment delivery. However, underdoses and overdoses according to EPIgray are likely as a result of a range of uncertainties described in Chapter 5. Due to the complexity of radiotherapy treatments there are numerous possibilities of delivering suboptimal radiotherapy. In reality the distribution of dose delivery would take a similar appearance to the distribution shown in Figure 3.12.

Previously only the absolute magnitude of the $\%DD_{DRP}$ was considered. Figures 3.13 and 3.14 show the distribution of the $\%DD_{DRP}$ of left and right breast fields, before and after positional correction. These figures address the magnitude of the $\%DD_{DRP}$ calculated by EPIgray as well as whether the $\%DD_{DRP}$ indicated an underdose or an overdose at the DRP according to EPIgray.

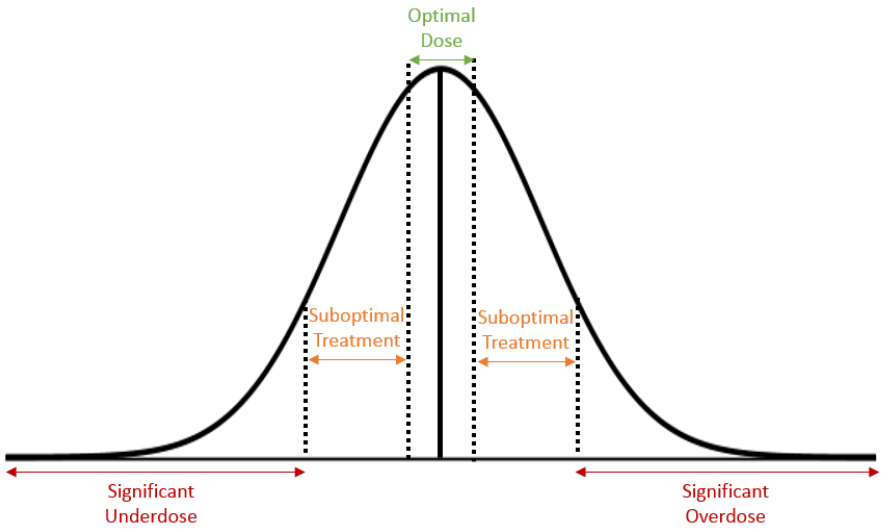

FIGURE 3.12: Realistic distribution of dose delivery in radiotherapy

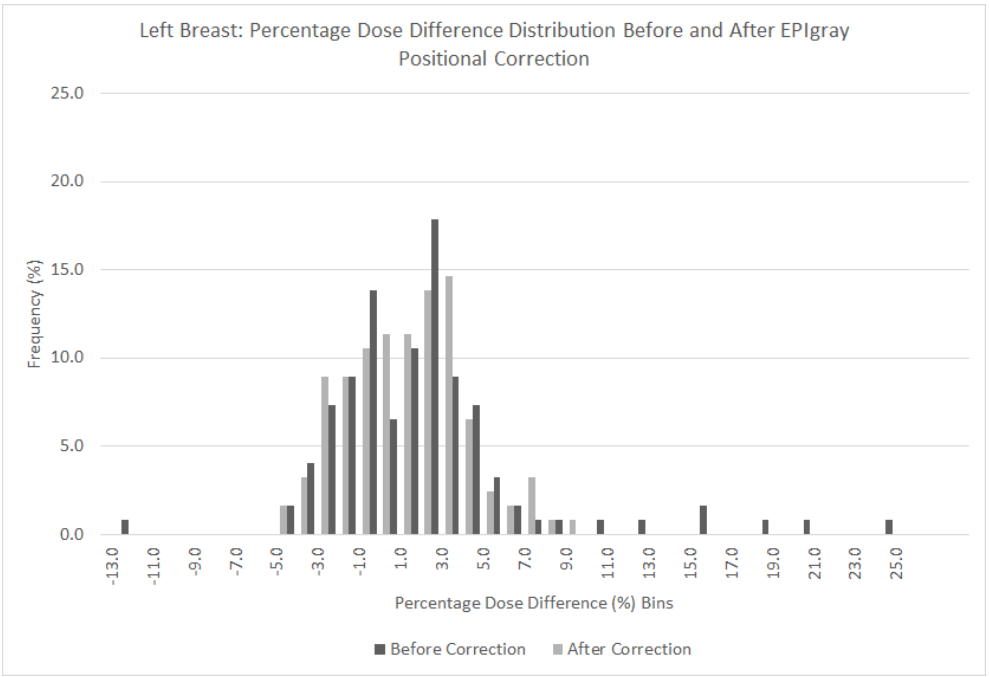

FIGURE 3.13: Distribution of percentage dose difference of left breast before and after positional correction

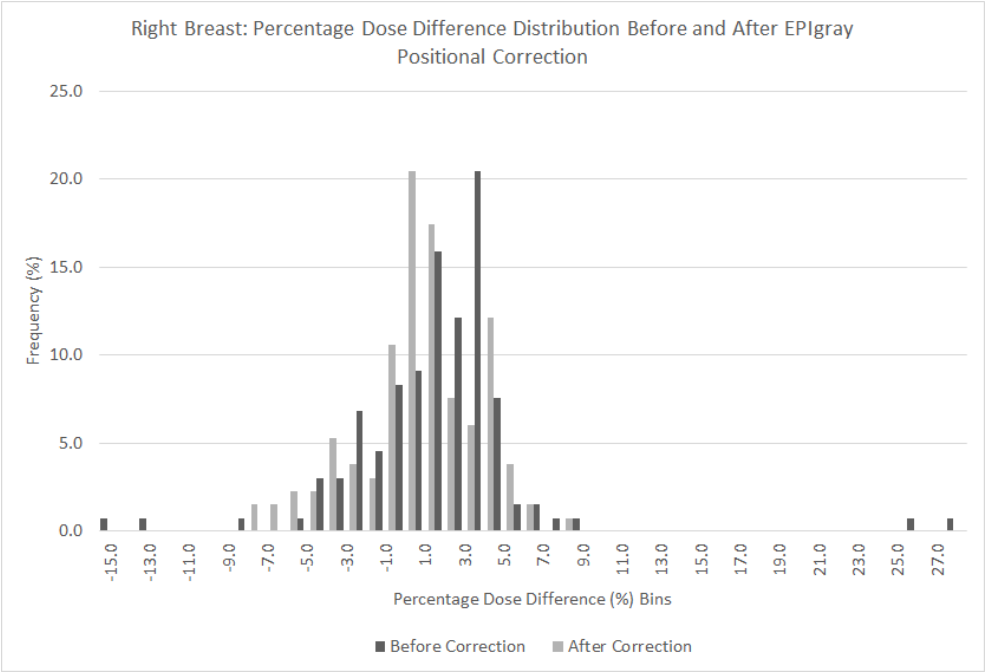

FIGURE 3.14: Distribution of percentage dose difference of right breast before and after positional correction

Initial observation of Figures 3.13 and 3.14 revealed that following positional correction the $\%DD_{DRP}$ of both lateralities lie closer to 0%. Fields that have a $\%DD_{DRP}$ greater than 10% were considered outliers. It was found that most outliers following positional correction presented a $\%DD_{DRP}$ of less than $\pm$5.0% tolerance.

Following the positional correction, it was found that 8.9% of the left breast fields and 11.4% of the right breast fields indicated out of tolerance results that required further investigation to prove they are clinically acceptable. All left breast fields that exceeded clinical tolerance indicated an overdose at the DRP. Right breast fields in contrast, indicated both underdoses (5.3% of right breast fields) and overdoses (6.1% of right breast fields) lying outside the clinical tolerance. Regardless of whether EPIgray indicated underdoses or overdoses at the DRP, both lateralities exhibited similar rates of passing and failing fields overall. Following investigation, it was determined that the failing fields failed as a result of inaccurate acquisition of the EPID image itself (where the entire EPID image had not been properly captured on treatment), rather than a dosimetric inaccuracy in the treatment delivery.

Figures 3.15 and 3.16 show the relationship between the TPS dose and the position corrected EPIgray dose of all left and right breast fields respectively. These figures also show the line of best fit for each laterality along with the equation for the line of best fit and the R^2 value. The gradient of the line of best fit of both lateralities indicated a near one-to-one relationship between the TPS and EPIgray doses. The y-intercepts of the line of best fits was found to be -2.6 for left breast fields and -5.1 for right breast fields. These numbers indicate the offset between the TPS dose and the EPIgray doses for the population under investigation. This finding suggests and supports the earlier observations that there were larger offsets between the TPS and EPIgray doses for right breast fields than left breast fields. The R^2 values provide statistical indication of how close the data were fitted to the regression line. The larger, the R^2 the better the model fits the data [50]–[52]. The R^2 values of the line of best fit of both lateralities indicated a direct linear relationship between the TPS doses and the EPIgray doses. Figure 3.16 shows the presence of an outlier. This outlier will cause R^2 to be lower than the currently displayed value for right breast fields. Investigation of this outlier revealed an issue associated with the EPID image itself and therefore will be ignored. Ignoring this single outlier, the gradient of the line of best fit remained as 1.0 however, the R^2 value increased, indicating a stronger direct linear relationship between the TPS dose and the EPIgray dose.

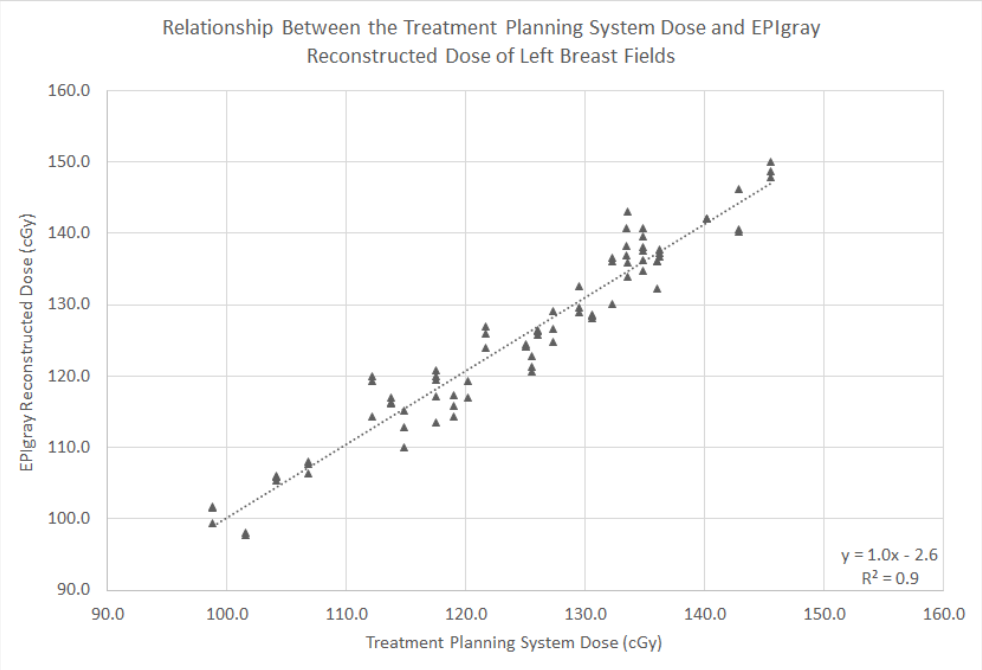

FIGURE 3.15: TPS dose and EPIgray doses of all left breast fields (dotted line represents the line of best fit)

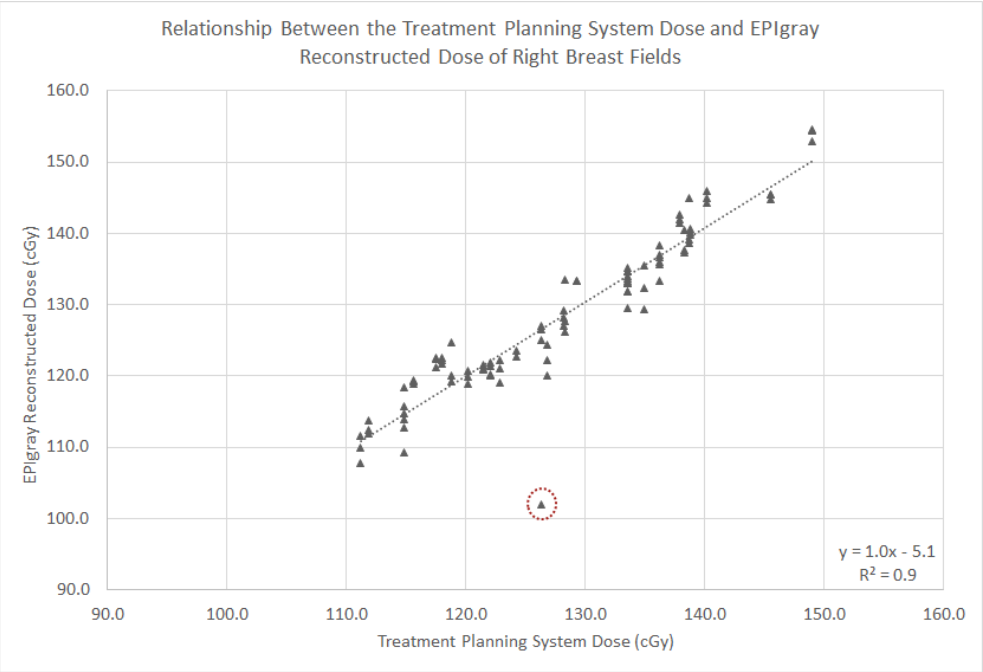

FIGURE 3.16: TPS dose and EPIgray doses of all right breast fields (dotted line represents the line of best fit). The circled point is an outlier.

Breast Size

The initial average $\%DD_{DRP}$ between the TPS dose and the EPIgray dose for small and large breast fields was found to be 2.9±2.1% and 3.6±4.9% respectively. Following positional correction the average $\%DD_{DRP}$ was found to be 2.6±1.9% for small breast fields and 2.4±2.8% for large breast fields. While the average $\%DD_{DRP}$ was initially larger for large breast fields, this value may be a consequence of $\%DD_{DRP}$ outliers skewing the data set. Following positional correction however, both small and large breast fields had comparable average $\%DD_{DRP}$.

A two-sample T test assuming unequal variances with a significance level of 5% was conducted for small and large breast fields in order to obtain evidence of statistical difference. The null hypothesis assumed that there were no statistical differences between position corrected $\%DD_{DRP}$ of small and large breast fields. The p-value obtained was 0.63. This p-value indicates that the null hypothesis cannot be rejected and therefore the differences seen in the average dose differences between small and large breast fields may have occurred by chance and these samples were not statistically different.

Figures 3.17 and 3.18 show the distribution of the $\%DD_{DRP}$ of small and large breast fields before and after positional correction respectively. These figures indicate that small breast fields have smaller range of $\%DD_{DRP}$ than large breast fields. Following positional correction the $\%DD_{DRP}$ range was comparable for both breast sizes. This finding provided an explanation for the higher average $\%DD_{DRP}$ observed for the large breast fields before positional correction. Following positional correction, the $\%DD_{DRP}$ of small breast fields range from -7.0% to 10.0% and the $\%DD_{DRP}$ for large breast field range from -7.0% to 9.0%. It is evident through Figures 3.17 and 3.18 that positional correction within EPIgray is effective for both breast sizes.

Investigation of outliers post positional correction, revealed that these fields have come from two patients. Investigation has revealed improper acquisition of EPID image for dose calculation. Significant dosimetric errors have not occurred.

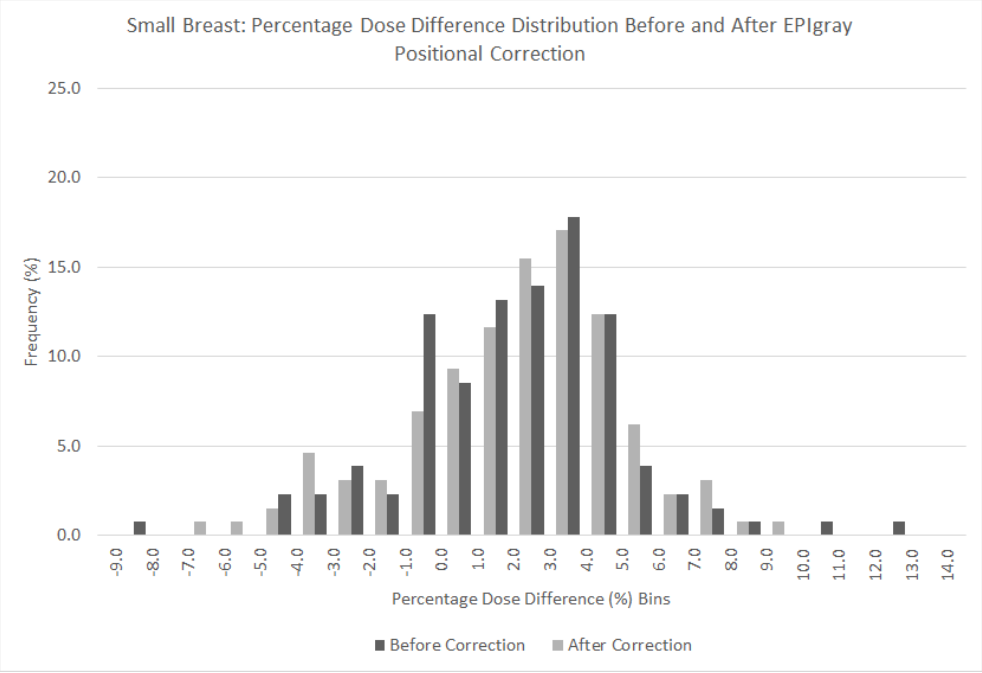

FIGURE 3.17: Distribution of percentage dose difference of small breast fields before and after positional correction

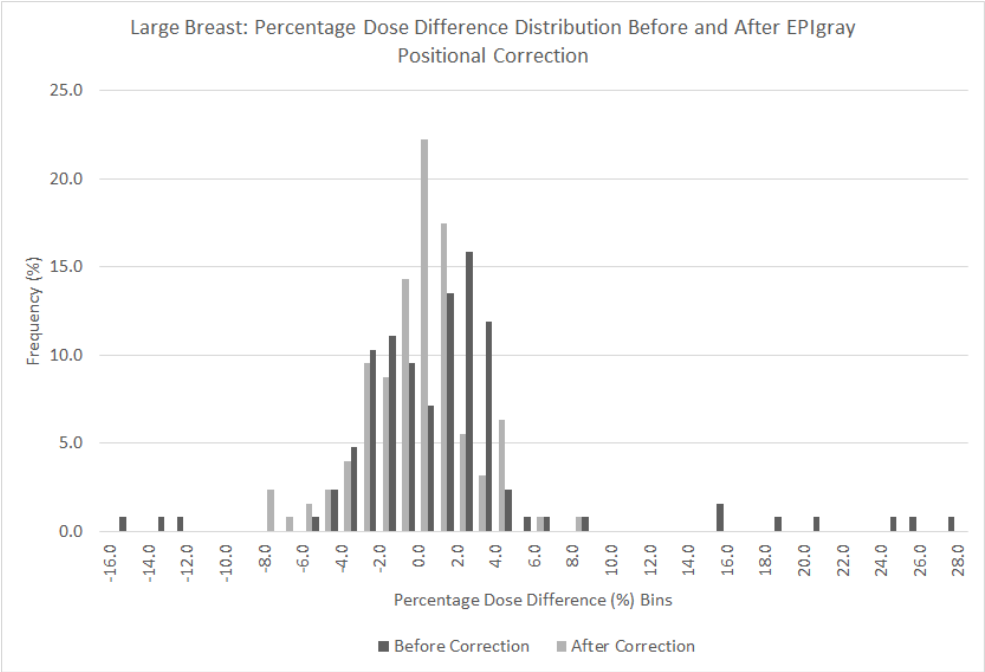

FIGURE 3.18: Distribution of percentage dose difference of large breast fields before and after positional correction

Figures 3.19 and 3.20 show the relationship between the TPS doses and position corrected EPIgray doses of all small and large breast fields respectively. These figures also display the line of best fit for each breast size and the corresponding equation for the line of best fit. The gradient of the line of best fit was found to be 1.00 for small breast fields and 1.05 for large breast fields. These values are sufficiently close to one indicating that there is a direct linear relationship between the TPS and EPIgray doses. The y-intercepts of the line of best fits was found to be 1.5 for small breast fields and -6.9 for large breast fields. These numbers indicate the offset between the TPS and the EPIgray doses for small and large breast fields. It was found that there was a larger difference between the TPS dose and the EPIgray dose for large breast fields than small breast fields. The R^2 values of the line of best fit for small and large breast fields was found to be 0.9. The magnitude of these R^2 values support the strong linear relationship indicated by the gradient between the TPS and the EPIgray doses for both breast sizes.

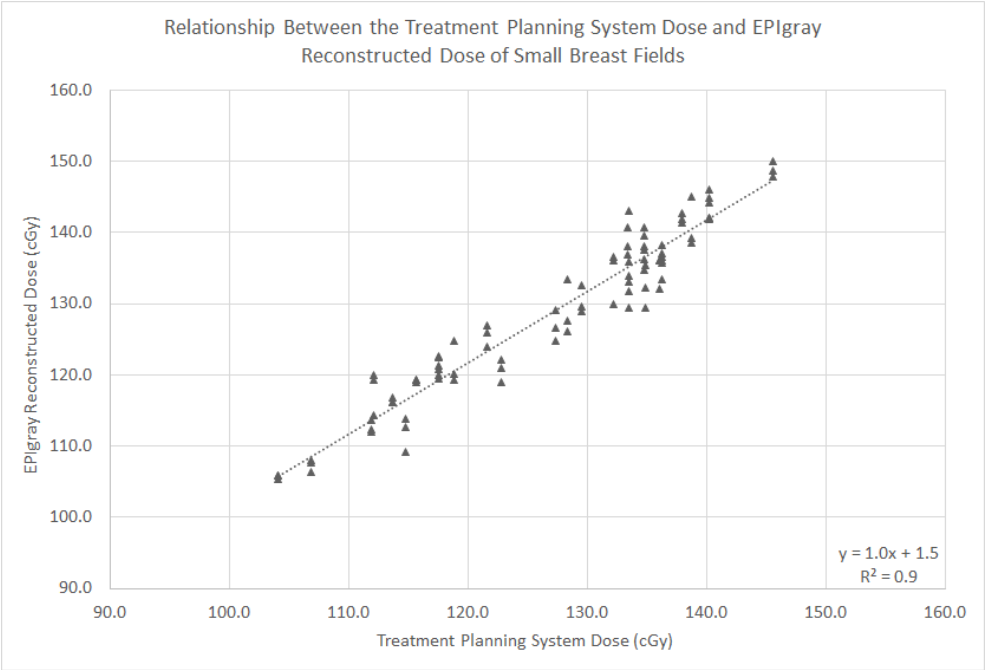

FIGURE 3.19: TPS dose and EPIgray doses of all small breast fields (dotted line represents the line of best fit)

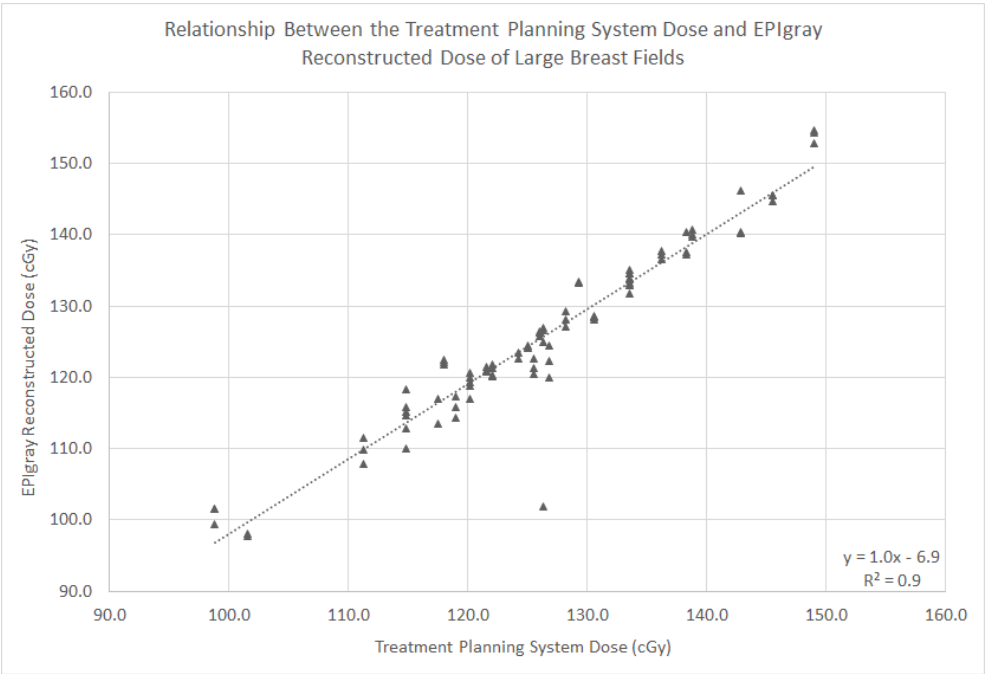

FIGURE 3.20: TPS dose and EPIgray doses of all large breast fields (dotted line represents the line of best fit)

3.3.4 Effect of Low Density Tissue on EPIgray Reconstructed Dose

Publications in the literature have revealed that the dosimetric accuracy of EPIgray determined doses decrease in areas of highly variable tissue densities [40]. The presence of lung tissue near the treatment volume of breast treatments does to a certain extent affect the reconstructed dose at the DRP. Additionally, the position of the DRP is also variable from patient to patient. This section presents the results obtained in the investigation of the EPIgray reconstructed dose dependency on the position of the DRP. The relationship between the lung and DRP separation and the position corrected $\%DD_{DRP}$ was analysed and the results are shown in Figure 3.21.

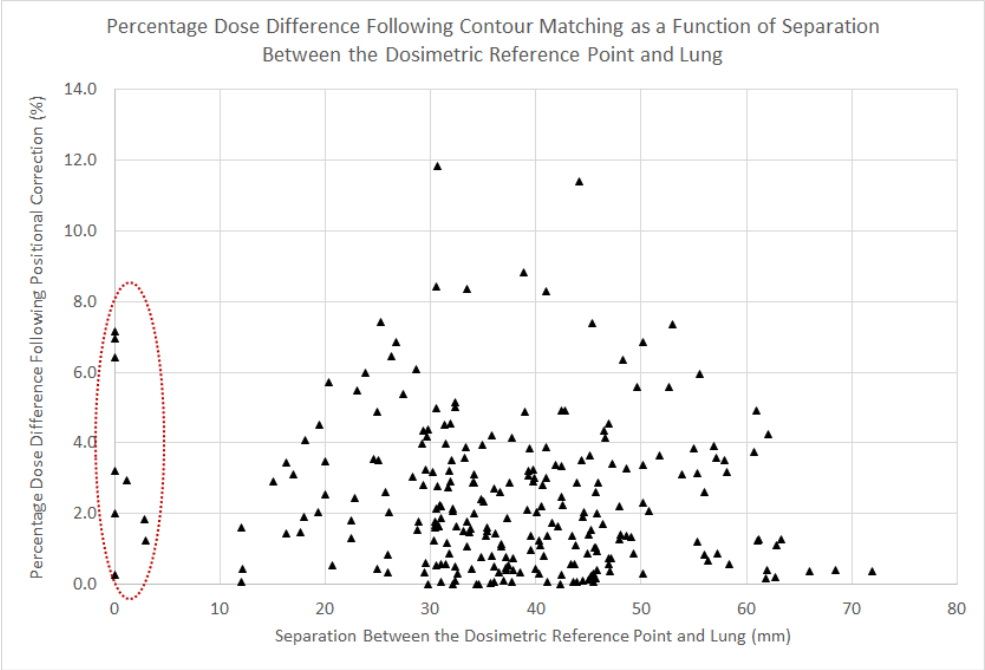

FIGURE 3.21: Relationship between the DRP and lung separation and position correction %DD. The points in the oval are %DD measured on the lung-breast tissue interface and therefore will be ignored

Figure 3.21 shows no significant relationship between $\%DD_{DRP}$ following positional correction and the separation between the DRP and the lung. It was expected that the closer the DRP is to the lung, the larger the absolute magnitude of $\%DD_{DRP}$, however Figure 3.21 does not reveal a specific trend. Other relevant measurements made to investigate the effect of lung on the EPIgray reconstructed doses were the width of the lung seen on the EPID image and the distance between the DRP and the anterior breast surface.

The width of the lung on the EPID images did not show much variation as treatments are actively planned to avoid lung in field. The width of the lung in field did not show any trends with the EPIgray reconstructed dose and therefore results are not shown here. The distance between the DRP and the anterior breast surface strongly correlates with breast size and therefore results will not be presented to avoid repetition.

3.3.5 Alternative Method for EPIgray Dosimetric Analysis

The distribution of the resulting fractional $\%DD_{vol}$ and $\%DD_{DRP}$ following positional correction for 23 of 30 patients are shown in Figure 3.22. From this figure, it is evident that the volume analysis had indicated the treatment volume to have consistently received a lower dose than the intended fractional dose, while the DRP method had indicated fractional doses that were mostly larger than the intended doses. From this figure, it is evident that there is a bias in the selection of the DRP. Additionally, the disagreement between $\%DD_{vol}$ and $\%DD_{DRP}$ indicated that the DRP may not be representative of the treatment volume. The DRP is chosen to be at a point where the dose is reproducible and is also in an area where the dose is not highly variable. The DRP will also be located in a region with minimal variation in tissue densities. In contrast, the 50 points generated by EPIgray is based on the maximum isodose that covers 50% of the treatment volume. These points are randomly generated and therefore there is minimal bias associated with the selection of these points. Consequently some points may be located near low density regions which will add to the statistical uncertainty of the $\%DD_{vol}$.

Currently, the tolerance for $\%DD_{vol}$ has been automatically set to $\pm 5.0\%$. In order to investigate the effectiveness of this tolerance to indicate falsely passing fields and potential inaccurate treatments, the fractional $\%DD_{vol}$ magnitude was checked against the $\%DD_{DRP}$ of each field for the patients of the retrospective study. A total of 66 fractions were analysed. Results have revealed that 20 of 23 patients remained within $\pm 5.0\%$. Two of the three failing $\%DD_{vol}$ patients had falsely passing fields following analysis using $\%DD_{DRP}$ method. The remaining patient produced a failing $\%DD_{vol}$ result however did not have failing results both before and following positional correction. While there was a failing $\%DD_{vol}$ patient with no failing result, it not advisable to increase the $\%DD_{vol}$ tolerance as this may permit the passing of other failing

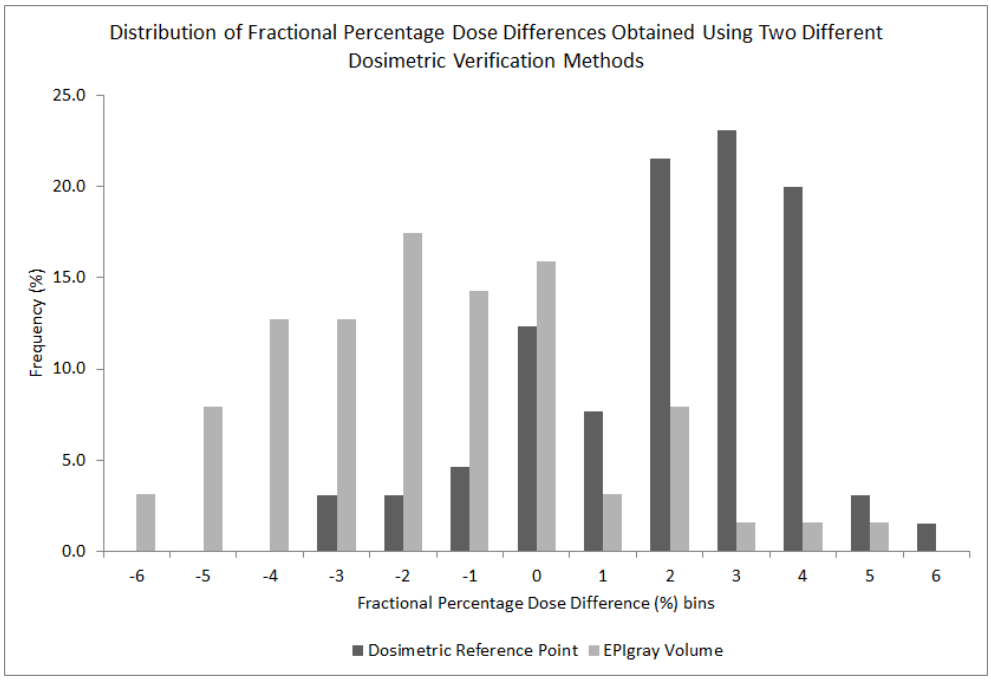

FIGURE 3.22: Percentage dose difference distribution acquired for fields using the dose to the DRP and the average dose of the EPIgray volume

results. It must be accepted that the set tolerance will never entirely encompass the entire population seen in the clinic. Consequently identifying a falsely passing field over falsely failing field is of more importance as the former would have the most significant dosimetric impact if it was missed clinically.

Additionally during the investigation of the $\%DD_{vol}$, the standard deviation associated with the reconstructed doses were also noted for each fraction. It was found that fractions of patients that exceeded a standard deviation of 0.1 Gy had at least one falsely passing field within the fraction following positional correction using $\%DD_{DRP}$ analysis. This finding allows the standard deviation of the reconstructed dose to also indicate that an unexpected treatment may have occurred.

3.4 Discussion

This section will combine the results from subsections 3.3.1 to 3.3.3 and present the discussion for breast laterality and breast size separately. This will be followed by a discussion of the effect of having low density tissue in the EPIgray reconstruction environment on the $\%DD_{DRP}$.

Lastly, the clinical use of $\%DD_{vol}$ will be discussed through comparisons to current practice at Christchurch Hospital.

3.4.1 Breast Laterality

The average magnitude of the total shift required for positional correction indicated that right breast fields on average required larger positional corrections than left breast fields. Shifts analysis performed separately in x and y-dimensions found right breast fields to not only require corrections more frequently in both dimensions but these corrections were also found to be of larger magnitude in comparison to left breast fields. These results have suggested that right breast patients were more at risk of having positional offsets on treatment. X-dimensional shift analysis revealed differences between left and right breast fields. A t-test conducted to investigate whether the shifts required between right and left breast fields were statistically different from each other revealed that the data sets were not significantly different. Therefore the differences observed were concluded be circumstantial.

Y-dimensional shift analysis revealed right breast fields to require positional corrections more frequently than left breast fields. Right breast fields on average also required positional correction of larger magnitude in comparison to left breast fields. The direction of shifts required were in the opposite direction for each laterality. The results of the t-test to test for statistical significance revealed that the shifts required in the y-dimension for left and right breast fields were statistically different. Following consultation with the treatment staff there were no obvious differences in the setup of the patients of different lateralities on treatment. Therefore the observed differences in the shifts required in the y-dimension was unexpected. Consequently, the cause of this result currently remains inconclusive and requires further investigation. A possible cause for this difference may be how the patient is setup at simulation and consequently at every fraction. Patients are asked to clasp one of their hands to the other arm's wrist above the their head to prevent their arms from receiving unnecessary radiation. At treatment, the patient will be asked to place their arms above their head at a position they find the most comfortable. Consequently, the clasping hand may vary between fractions. This may give rise to a small patient shift in position with a slight rotation depending on which arm is holding the other. This positional variation may give rise to the differences seen between right and left

breast fields. Another proposed cause may be a result of which side of the patient the radiation therapist is standing on when setting up the patient in the treatment position. Parallax error at the position the radiation therapist is at when setting up the patient may also contribute to the differences seen between the shifts required for both lateralities. As there were no apparent biases in the planning, setup or treatment of left and right breast patients, the current differences seen between the lateralities remains inconclusive until further investigation on future patients. However, analysis of shift directions as part of this study have suggested that left breast patients were more likely to be setup in a position that is inferior to the expected treatment position and right breast patients were more likely to be setup in a position that is superior to the expected treatment position. The setup offsets of patients in the anterior-posterior direction and the proximal-distal planes were more prominent than setup offsets in the superior-inferior directions for both lateralities. The shift analysis has revealed that right breast patients were more at risk of having setup errors on treatment.

Numerical analysis of fields following positional correction has revealed that there were no significant differences between truly passing and failing fields and falsely passing and failing fields of both lateralities, ignoring improper EPID image acquisitions. Nevertheless, it was found that false results were likely for both lateralities. Therefore these results emphasise the need for the verification of proper alignment of the EPID image to the TPS contours to ensure that the given $\%DD_{DRP}$ is reflective of the treatment delivered to the patient.

Dosimetric analysis of the effect positional correction has on the $\%DD_{DRP}$ between lateralities reveals that the average $\%DD_{DRP}$ of left and right breast fields were comparable before and after positional correction. In both laterality groups, it was found that the average $\%DD_{DRP}$ improved with positional correction within EPIgray. A test for statistical difference has revealed that there were no significant differences between the positional corrected $\%DD_{DRP}$ of both lateralities. This finding is in agreement with the results found in the numerical statistics section in which there were comparable number of passing and failing fields before and after positional correction.

Figures 3.13 and 3.14 have provided evidence that positional correction within EPIgray results in a smaller magnitude of $\%DD_{DRP}$. This indicates a better agreement between the TPS planned dose and the dose delivered to the patient according to EPIgray. Investigation of failing fields following positional correction of both lateralities indicated incorrect acquisition of EPID images for EPIgray analysis. It was found that both left and right breast fields had similar rates of passing and failing fields. 3DCRT treatments of the breast are planned to avoid dose to the heart and the ipsilateral lung. Therefore the treatment process should result in very minor differences seen in the $\%DD_{DRP}$ between the left and right lateralities. The dosimetric analysis of the effect positional correction has on the $\%DD_{DRP}$ has identified no significant differences between the left and right lateralities. This finding is consistent with the results of the shifts required for positional correction and the results of the numerical analysis in that there are no major discrepancies between the breast lateralities.

The $\%DD_{DRP}$ provided by EPIgray is an indication of the treatment delivery accuracy according to EPIgray. The dosimetric analysis of left and right breast fields also established the level of agreement between the TPS planned dose and the EPIgray reconstructed dose to the DRP. The relationship between the TPS dose and the EPIgray dose was a direct, linear one-to-one relationship. The R^2 values obtained for the relationship between the TPS and the EPIgray doses of both lateralities showed strong statistical agreement. Therefore the dosimetric analysis of the $\%DD_{DRP}$ has revealed that EPIgray does not indicate significant differences between left and right breast fields.

3.4.2 Breast Size

The average magnitude of the total shift required and the distribution of the magnitude of positional correction indicated that large breast fields required a larger positional correction than small breast fields. Analysis of the magnitude of shift required in the x- and y-dimensions revealed large breast fields to not only require corrections more frequently but also to require a larger magnitude of shift than small breast fields. These results have suggested that large breast patients were more at risk of having setup errors on treatment in both x- and y-dimensions. Results have shown that there was a difference in the direction of shift required in the x-dimension and y-dimensions between small and large breast fields. In the x-dimension it was found that

small breast patients were more likely to be setup at a position that is more posterior and/or distal from the expected treatment position and large breast patients were more likely to be setup at a position that is more anterior and/or proximal from the expected treatment position. Similarly in considering the shifts in the y-dimension it was found that small breast patients were more likely to be set up at a position that is inferior to the expected position and large breast patients were more likely to be setup at a position that is more superior to the expected treatment position. A t-test indicated that shifts required for positional correction of small and large breast fields were statistically different.

Following consultation with the treatment staff it was the general consensus that larger breast patients were more difficult to setup on treatment. While the planning processes and the patient processes through the radiotherapy clinic are the same for breast patients of all breast sizes, it was found that CT simulation stages and the treatment setup are more difficult for large breast patients. At the CT simulation stages, the patient would receive tattoos at points where the CT room lasers are incident upon their skin with the patient in their treatment position. These are the reference markers the staff on treatment will use to setup the patient in the same position for treatment delivery. With larger breast patients, CT simulation staff have indicated that placement of tattoo is often made difficult with having more tissue in the tattoo region. Additionally with ageing patients, there is a loss of tissue elasticity and therefore the position of the tattoo is more prone to sag. Consequently when the patient is being setup on treatment, the treatment staff have difficulty aligning all reference tattoos to the lasers of the treatment room. The treatment staff have more frequently identified notable uncertainties associated with patient setup of larger breast size. However, these positional uncertainties are within clinical tolerance and therefore treatment proceeds without considerable risk to the patient.

The results of numerical analysis of small and large breasts fields before and after positional correction do not indicate significant differences between the breast sizes. Both breast sizes indicate similar rates of passing and failing fields. However it was found that large breasts were more likely to produce false results. Nevertheless, both small and large breast groups

have shown false results. Falsely failing fields are not of major concern as treatment professionals will be alerted to these fields as initially failing fields and therefore an investigation is initiated to confirm that accuracy of the treatment. However, the falsely passing fields are of major concern as these fields present as clinically passing fields and may go unnoticed. Currently there are no measures in place to ensure that the dose has been reconstructed over the correct environment for accurate representation of dose delivered to the patient. The implication of this result is that while majority of the initial passes within EPIgray remain a pass following positional correction, a method of identifying falsely passing fields is required. This may be achieved by either implementing a more sensitive $\%DD_{DRP}$ tolerance or by performing positional correction within EPIgray for all fields regardless of breast size. Both these options would require a change in the current clinical practice.

Dosimetric analysis of the effect positional correction has on the $\%DD_{DRP}$ between breast sizes reveals that the average $\%DD_{DRP}$ before positional correction is smaller in magnitude for small breast fields than large breast fields. With positional correction the average $\%DD_{DRP}$ improved for both small and large breast fields and were comparable. It was found that while the average $\%DD_{DRP}$ for small breast fields decreased in magnitude indicating a better agreement of the EPIgray dose with the TPS dose, the decrease in the $\%DD_{DRP}$ following positional correction is negligible. In contrast a considerable decrease in the average $\%DD_{DRP}$ was seen for large breast fields. This finding is in agreement with the findings of the shifts required for positional correction. Large breast fields required shifts more frequently and the magnitude of these shifts were also larger in comparison to small breast fields. Therefore, with larger magnitude of positional correction, the environment over which the dose reconstruction is performed within EPIgray is more drastically changed. This results in a larger difference between the initial $\%DD_{DRP}$ and position corrected $\%DD_{DRP}$. Following positional correction, the average $\%DD_{DRP}$ between small and large breast fields were comparable. The result of a t-test conducted with the null hypothesis that there were no statistical differences between the positional corrected $\%DD_{DRP}$ of small and large breast fields indicated that there were no significant differences between the breast sizes. Therefore this result indicates that EPIgray does not exhibit any bias associated with breast size.

Figures 3.17 and 3.18 have provided evidence that positional correction within EPIgray results in a smaller magnitude of $\%DD_{DRP}$ for most fields. Consequently this indicates a better agreement between the TPS planned dose and the dose delivered to the patient according to EPIgray. Investigation of failing fields following positional correction of both lateralities indicated incorrect acquisition of EPID images for EPIgray analysis therefore no further investigation was necessary.

The dosimetric analysis of small and large breast fields also established the agreement between the TPS planned dose and the EPIgray reconstructed dose to the DRP. The relationship between the TPS dose and the EPIgray dose was a direct, linear one-to-one relationship. The R^2 values obtained for the relationship between the TPS and the EPIgray doses for both breast sizes showed strong statistical agreement. Therefore the dosimetric analysis of the $\%DD_{DRP}$ has revealed that EPIgray does not indicate significant differences in dose calculations between small and large breast fields.

3.4.3 Low Density Tissue Effect on Reconstructed Dose

Literature has revealed that the potential presence of the ipsilateral lung, a low density tissue within the reconstruction environment may contribute to the uncertainty associated with the EPIgray reconstructed dose. To investigate this effect in 3DCRT breast treatments, the separation between the lung and the DRP was investigated as a function of position corrected $\%DD_{DRP}$. The results section has revealed that the presence of the lung in the reconstruction window does not have a significant relationship with $\%DD_{DRP}$. Previous publications have revealed that with low density tissues in field, the reconstructed dose given will be smaller than expected as a result of decrease in scatter in the reconstruction environment [39]. With this hypothesis, the expected result of this section of the study was that with increasing separation between the DRP and the lung, the lower the $\%DD_{DRP}$ will be. However 3.21 shows that there was no significant relationship between the DRP and lung separation and the $\%DD_{DRP}$ for breast fields of both lateralities and sizes. This finding provides clinical evidence that the current placement of the DRP with reference to the lung position was not significantly affected by the limitations of EPIgray reconstruction algorithm in 3DCRT breast treatments.

3.4.4 Alternative Methods of Dosimetric Verification

Analysis using the fractional $\%DD_{DRP}$ and the $\%DD_{vol}$ has revealed that there is a bias associated with the selection of the DRP. The DRP is typically chosen to provide the most reliable dose. While it is clinically useful to reliably quantify the accuracy with which the treatment has been delivered to the patient, the $\%DD_{DRP}$ is an indicator of the dose delivered to a single point dose. The use of $\%DD_{vol}$ could be clinically beneficial because it provides an indication of treatment accuracy to a volume rather than a single point. The %DD obtained using both methods has revealed that the DRP dosimetric analysis typically provides a dose that is greater than the expected dose whilst the $\%DD_{vol}$ obtained using the volume method provides a dose that is lower than expected dose. Both $\%DD_{DRP}$ and $\%DD_{vol}$ can be simultaneously true, in that the dose to the DRP was greater than expected dose while the dose to a treatment volume was lower than expected and therefore it is difficult to claim one method to be more reliable than the other.

Unlike the dosimetric analysis using the DRP method which provides a $\%DD_{DRP}$ for every field within a fraction, the $\%DD_{vol}$ only provides the fractional %DD due to EPIgray software limitations. Therefore, in clinical situations when a failing fraction has occurred, the $\%DD_{vol}$ will not provide additional information regarding which fields are responsible for the failed result. Results show that the use of $\%DD_{vol}$ may be clinically beneficial however its limitations of providing only fractional information means that other dosimetric methods must also be in place to provide other immediate information if necessary. A $\%DD_{vol}$ tolerance of $\pm 5.0\%$ and a ± 0.1 cGy tolerance for reconstructed dose standard deviation has been recommended following analysis of the retrospective study patients using $\%DD_{vol}$. These tolerances have shown to effectively identify falsely passing fields.

3.5 Conclusions

From the retrospective study, it was found that when considering treatment laterality and breast size, right and large breasts were more at risk of having setup errors respectively. The

direction of the shift required for positional correction varied based on the breast size and laterality. For all breast patients, it was found that patient positional offsets in the anterior-posterior and proximal-distal directions were more common than patient offsets in the superior-inferior direction.

Numerical and dosimetric analysis of the $\%DD_{DRP}$ of fields of different lateralities and breast size have indicated that false results are a possibility across both treatment lateralities and breast groups. Currently there are no measures in place to ensure that $\%DD_{DRP}$ automatically calculated by EPIgray has been calculated over the appropriate treatment environment using the correct treatment parameters. Therefore it becomes important to verify patient and EPID position with EPIgray before using $\%DD_{DRP}$ as an indicator for treatment accuracy. It is recommended that either a new tolerance for the $\%DD_{DRP}$ that is more sensitive to false results is implemented or positional verification is performed for every field for at least the first fraction to ensure no major errors have occurred and to reliably use EPIgray as an IVD system.

The retrospective study has revealed that the $\%DD_{DRP}$ provided by EPIgray is unaffected by the treatment laterality and breast size following positional correction within EPIgray. There were similar numbers of passing fields following positional correction on EPIgray between lateralities and breast sizes. This result provides clinical evidence that the EPIgray dose calculation algorithm does not exhibit significant biases for a particular treatment laterality or breast size. The relationship between the TPS and the EPIgray doses also indicated a direct linear relationship. Therefore, evidence from the retrospective study provides clinical validation for using EPIgray as an IVD system. However, the agreement between EPIgray and TPS doses is not sufficient. An independent dosimetric system must verify the doses delivered to the patient to ensure that the EPIgray reconstructed doses are sufficiently accurate and are representative of the dose delivered to the patient, as found in Chapter 4.

The effect of having low density tissue in the field on the EPIgray reconstructed dose was investigated using the lung and DRP separation. This investigation was launched following literature review which indicated that the accuracy of EPIgray reconstructed doses is diminished with decreasing distance between the point of dose reconstruction and rapidly varying

tissue densities. Following analysis of a range of separations between DRP and lung, it was found that the presence of the ipsilateral lung tissue in the field of reconstruction does not significantly affect the $\%DD_{DRP}$.

Investigation of using $\%DD_{vol}$ at Christchurch Hospital revealed that there is a bias associated with the selection of the DRP. Results of this investigation have indicated that it would be clinically beneficial to implement $\%DD_{vol}$ which provides an indication of treatment accuracy using volume rather than a single point. However, the limitation of this method is such that $\%DD_{vol}$ will need to be used in conjunction with $\%DD_{DRP}$. Additionally the investigation of using $\%DD_{vol}$ as a treatment accuracy indicator involved $\%DD_{vol}$ analysis of patients who have previously been treated at Christchurch Hospital. Whilst these patients had small positional errors associated with their treatment, these errors were not dosimetric errors. The $\%DD_{vol}$ obtained were for positional corrected fields and were compared to fractional $\%DD_{DRP}$ of positional corrected fields. A tolerance of $\pm 5.0\%$ is recommended for implementation of $\%DD_{vol}$ for routine clinical use. Additionally the use of the standard deviation associated with the mean reconstructed dose using the volume method is also recommended for identification of falsely passing fields. It is recommended that for a fractional standard deviation of greater than 0.1 Gy, positional correction should be performed with EPIgray and the $\%DD_{DRP}$ of each field is verified to have truly passed. Investigation of the relationship between $\%DD_{DRP}$ and $\%DD_{vol}$ with positional offsets will need to be tested before using the DOSIsoft recommended volume based dosimetric analysis for verification of the dose delivered to the patient.

4 Phantom Study

The retrospective study showed that patient setup errors on treatment result in EPIgray providing an inaccurate $\%DD_{DRP}$ as a result of the dose reconstruction performed over an incorrect environment. Positional correction within EPIgray minimises the uncertainties associated with EPID and patient positioning on treatment. Consequently, positional correction within EPIgray provides a $\%DD_{DRP}$ that is more representative of the dose delivered to the patient. Additionally, the retrospective study has provided confirmation that there is acceptable agreement between the TPS dose and the delivered dose regardless of treatment laterality or breast size. However validation that the $\%DD_{DRP}$ is sufficiently close to the delivered dose using an independent dosimetry system is required to reliably use EPIgray as an IVD system. The retrospective study has also identified differences between routinely used $\%DD_{DRP}$ and the DOSIsoft recommended $\%DD_{vol}$ for dosimetric analysis. Therefore, an investigation of the use of $\%DD_{vol}$ with setup errors will need to be conducted to verify the recommended clinical tolerance.

A phantom study was undertaken to achieve the following aims:

1. To quantify the effects of setup errors on the $\%DD_{DRP}$ in order to decrease the current $\%DD_{DRP}$ tolerance of $\pm 5.0\%$ between the TPS dose and the EPIgray reconstructed dose for 3DCRT breast treatments if indicated.
2. To verify the fractional $\%DD_{vol}$ tolerance to minimise the number of false results.
3. To verify the ability of EPIgray to detect discrepancies in patient positioning on treatment through identification of discrepancies between the TPS dose and the EPIgray reconstructed dose.

The phantom study was performed using a phantom specifically designed to achieve the aims listed above.

4.1 Breast-Lung Phantom

4.1.1 Purpose

In order to validate the use of EPIgray as an IVD system, the breast-lung phantom was designed to allow dosimetric measurements to be acquired using two established dosimeters: an IC and radiochromic film. The breast-lung phantom would therefore allow comparisons to be made between the TPS predicted dose, EPIgray calculated dose and the delivered dose measured on treatment. The results from this investigation would validate the use of EPIgray as an IVD system.

The phantom would also be used to isolate patient setup errors on treatment in terms of direction and their effects on $\%DD_{DRP}$. The phantom would be shifted by a known distance on treatment and the doses at these corresponding offsets would be measured. The comparison of the EPIgray doses to the IC and film doses at the offset positions would provide information regarding EPIgray reliability with patient setup errors on treatment.

Lastly, the phantom would be used to investigate the relationship between $\%DD_{DRP}$ and $\%DD_{vol}$ with setup errors to validate the recommended fractional $\%DD_{vol}$ tolerance for treatment verification of 3DCRT breast treatments.

4.1.2 Phantom Design Aims

1. In order to use the proposed phantom in place of a patient receiving radiation treatment to the breast, the phantom must be representative of a patient. The phantom would have two components. The first component would represent the target volume, the entire breast and the second component would represent the main OAR, the ipsilateral lung.
2. The phantom should allow dosimetric measurements to be made during treatment delivery and therefore it must allow placement of an IC and radiochromic film in relevant locations without significantly affecting the dose to be measured.

3. The phantom would be used to investigate the effects of setup errors on the $\%DD_{DRP}$ and therefore the phantom must be easy to move and position on treatment in order to simulate changes in the patient position.

4.1.3 Phantom Design

Tissue-Substitute Materials

In order for the phantom to be used in the place of a patient receiving radiation treatment to the breast, the phantom must achieve tissue equivalency in terms of its radiation absorption and scatter properties. In considering tissue equivalency the physical density, electron density, attenuation coefficient and the stopping power of the phantom materials must closely match that of the tissue it is replacing for the dosimetric measurements to be meaningful. Deviations in these properties between the phantom and tissue would lead to different radiation interactions, resulting in a measured dose that has limitations for comparisons between the phantom and patients. The phantom was designed to have tissue substitutes for breast and lung. The tissue substitutes used were selected based on their similar absorption and scatter properties as their tissue counterparts [53].

Considering both physical and dosimetric properties, the most commonly used breast tissue substitute according to literature is wax [54]–[56]. The relative physical density of wax to water is 0.94, which approximately corresponds to that of breast tissue taking into account both glandular and adipose tissues of the breast [53]. Wax was consequently used as the breast tissue substitute.

Chang *et al.* investigated and compared the physical properties of natural cork, composition cork, rubber cork and the reference lung material (ICRU-44 lung tissue) [35]. The physical properties investigated were physical density, electron density and effective atomic number. Chang *et al.* found that the physical properties and dosimetry properties of composition cork was the most similar to the ICRU-44 lung tissue. Composition cork was therefore used as the lung-tissue substitute for the breast-lung phantom.

Phantom Morphology

The size and shape of the phantom was designed to mimic breast and lung. However, the materials proposed above for simulating breast and lung tissue were more rigid than their tissue counterparts. While this difference did not simulate the exact treatment conditions as if it were a patient, the relative increase in rigidity of the phantom served as an advantage as phantom positioning during the acquisition of the measurements were more reproducible [55].

Figure 4.1 shows the phantom design in side and birds eye views. The white region represents the breast tissue and the orange region represents the lung. The blue horizontal lines indicated in Figure 4.1a show slabs of wax making up the breast tissue. The black cross seen in Figure 4.1b represents the isocentric treatment position and the blue crosses seen in Figure 4.1b show the lateral and longitudinal shifts of magnitude $\pm$0.5 cm, $\pm$1.0 cm and $\pm$2.0 cm to be performed to simulate patient shifts on treatment. Vertical shifts of $\pm$0.5 cm, $\pm$1.0 cm and $\pm$2.0 cm were also implemented but are not diagrammatically shown.

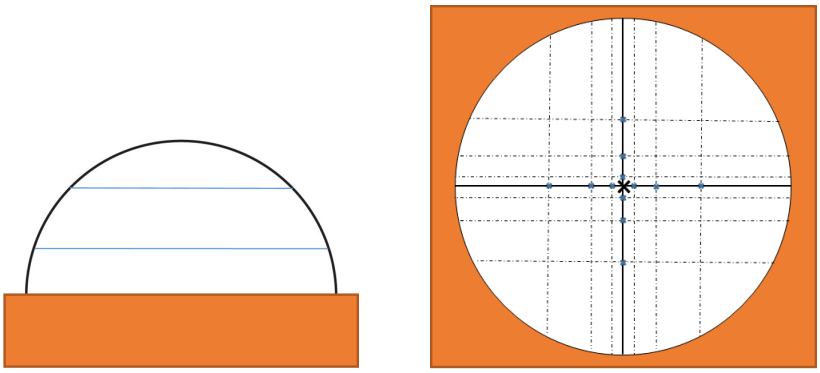

(a) Side view (b) Birds eye view

FIGURE 4.1: Different views of the breast-Lung phantom

Figure 4.3a shows the breast-lung phantom design for measurements using an IC. As seen in this figure, there were three slabs of wax representing the breast. The middle slab had an insert in which the IC was placed for measurement during treatment delivery. The IC insert was designed specifically for a CC13 IC shown in Figure 4.2. The dimensions of this chamber were taken into consideration to minimise the air gaps within the cavity with the chamber in place. The introduction of air gaps would alter the dosimetry and consequently affect the dose measurement. Therefore this insert was only suitable for use with a CC13 chamber (iba

FIGURE 4.2: CC13 IC used for dosimetric measurements

Dosimetry, Germany). For measurement of dose using radiochromic film, the middle slab was replaced with two smaller slabs that can be separated at the indicated dashed line shown in Figure 4.3b. For measurement of the EPID image, the middle slab was replaced by a solid wax slab. Therefore, in addition to the top and bottom slabs a total of four middle slabs were made:

- One solid middle slab for EPID image acquisition.
- One middle slab with IC insert.
- Two middle slabs that can be separated at the reference depth and sum to the equivalent thickness of the other middle slabs for film measurement.

The breast size of the phantom from the base of the breast to the breast apex (as shown in Figure 4.4) was 4.5 cm. The dimensions of the breast phantom were based on the average breast dimensions of patients from the retrospective study. The depth of the DRP was based on the average depth of DRP for patients from the retrospective study. The DRP was placed centrally at a depth of 2.2 cm from the breast apex. The placement of DRP was checked to ensure appropriate placement to minimise the uncertainties associated with both the measured and calculated doses.

The dimensions of the phantom are shown in table 4.1 and Figures 4.4a and 4.4b. The three versions of the phantom are shown in Figure 4.5.

TABLE 4.1: Breast-Lung phantom dimensions

Phantom Dimensions		
Breast Size		4.5 cm
Reference depth		2.2 cm
Slab Dimensions	Top	1.5 cm
	Middle	1.5 cm
	Bottom	1.5 cm

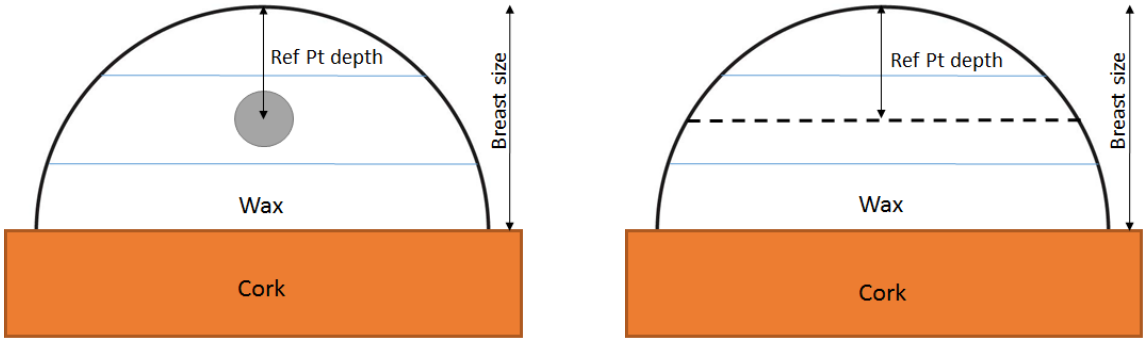

(a) Placement of IC (b) Film placement

FIGURE 4.3: Breast-Lung Phantom Design

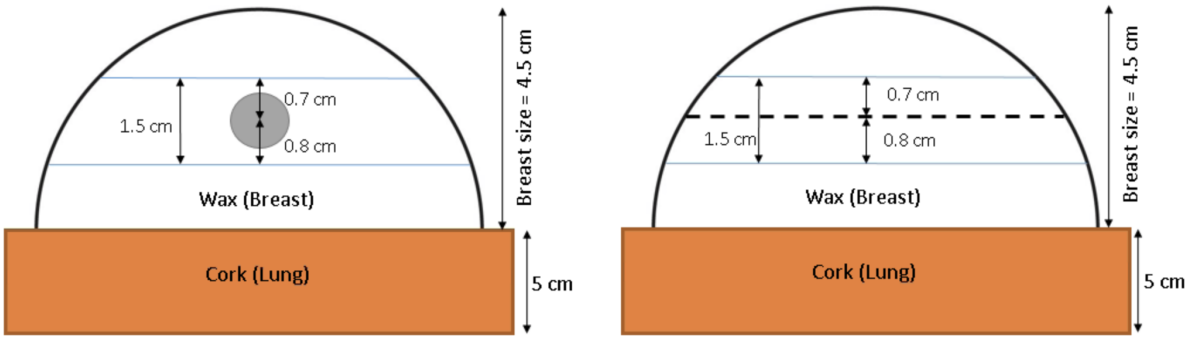

(a) EPID phantom (b) Film phantom

FIGURE 4.4: Phantom dimensions. Note: This figure is not to scale, the breast geometry has been emphasised to show more details regarding the dimension of breast portion of the phantom

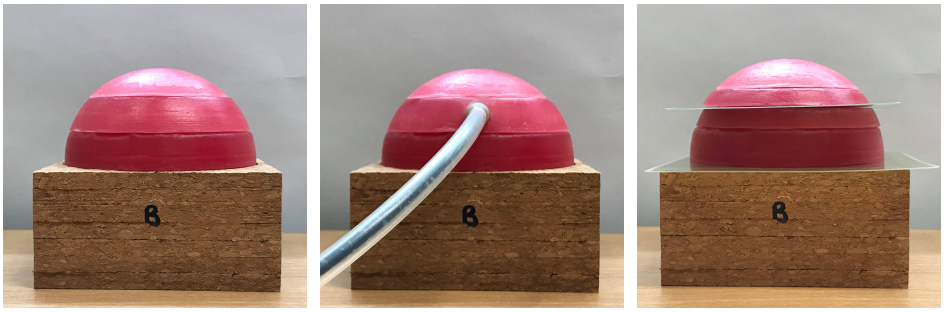

(a) EPID phantom (b) IC phantom (c) Film phantom

FIGURE 4.5: Breast-Lung Phantom used for validation measurements.

4.2 Methods

The breast-lung phantom will serve as an end-to-end test for reliable clinical use of EPIgray for IVD of 3DCRT breast treatments. The entire treatment process was performed on the breast-lung phantom.

CT simulation was performed on the phantom positioned using the CT lasers as shown in Figure 4.6. The overhead lasers were set to the centre of the phantom and the lateral lasers were set to be coincident on the breast-lung interface. A typical patient would receive a skin reference tattoo at the laser incidence on their skin however, there was no need for the placement of a reference mark as the treatment position of the phantom already corresponded to specific and reproducible points.

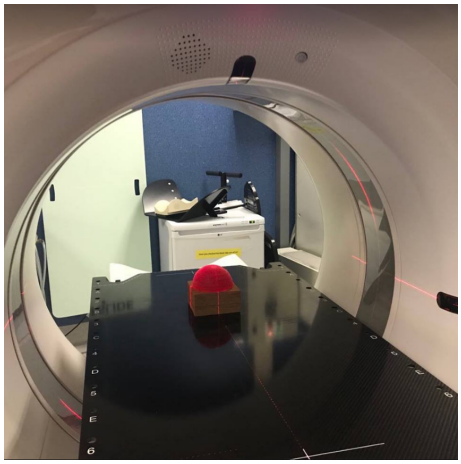

FIGURE 4.6: Setup of Breast-Lung phantom aligned to the lasers at CT simulation

The acquired CT simulation images were imported into Monaco version 5.1 (Elekta CMS, Maryland Heights, MO, USA), the TPS employed at Christchurch Hospital. The treatment was planned in a similar manner to an actual 3DCRT breast patient except with varied gantry angles. Different gantry angles were employed to isolate and quantify the effects of lateral, longitudinal and vertical shifts. The treatment plan consisted of two beams (treatment fields) each delivering 1 Gy from linac gantry angles of 90° and 270°. Figure 4.7 shows a CT slice of the phantom on the treatment couch. This figure shows the two opposing beams from linac gantry angles of 90° and 270°.

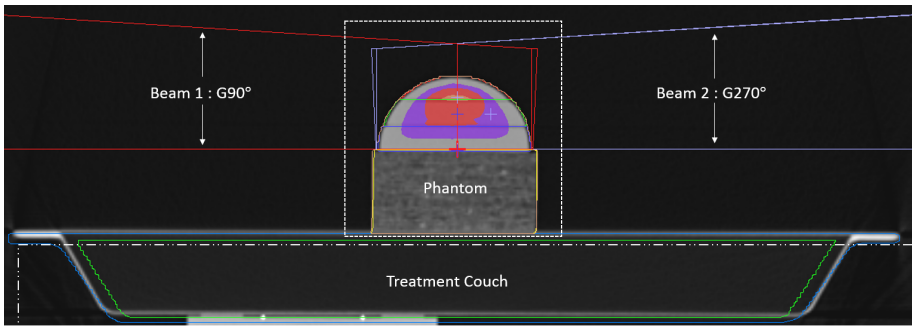

FIGURE 4.7: Treatment Plan of Breast-Lung Phantom

The dose to the DRP per fraction can be obtained from the TPS. This dose will be used to draw comparisons between the EPIgray reconstructed doses as well as the doses that will be measured using the IC and the film.

4.2.1 Film Calibration for Dosimetric Measurements

To obtain absolute dosimetric measurements from the radiochromic film, proper calibration of the film is required. In order to achieve consistency in the film measurements and to minimise the uncertainties associated with using a film scanner for dose readout, specific recommended protocols were followed. The protocols used were taken from literature and were adjusted accordingly for this specific application [57]–[61].

FilmQAPro software (Ashland Inc., Covington, Kentucky, USA) was used to perform triple-channel dosimetry using EBT3 GAFchromic film (Ashland Inc., Covington, Kentucky, USA). EBT3 film type can provide absolute dose for dose ranges between 0.2 Gy and 10 Gy. FilmQAPro allows dose measurement result comparisons from three colour channels, red, blue and green. Given that the calibration protocols are correctly followed, the radiochromic film would convert the measurement to absolute dose.

In order to perform an absolute dose measurements using the GAFchromic film, a calibration curve for the specific batch of radiochromic film must first be established within the FilmQAPro software. The method followed for establishing such a curve was based on previous recommendations and published results of the medical physics community. Publications have demonstrated that if the protocols are closely followed, the uncertainties associated with the

dose measurements should be within ±2.0% [60].

The film calibration procedure is outlined below:

1. Nine 3 cm strips were cut using a film cutter.
2. Eight strips were exposed to known radiation doses shown in table 4.2.
3. Irradiated strips were then scanned using the 48-bit flatbed Epson 10000XL film scanner.
4. The dose delivered to each calibration strip was specified within the FilmQAPro software.
5. The FilmQAPro software registered the red, blue and green channel values for these film strips and provided the calibration curve for the particular batch of film that was used for dosimetric measurements in this study.

TABLE 4.2: Doses delivered to the calibration film strips

Doses Delivered To Calibration Film Strips	
Strip Number	Dose Delivered (Gy)
0	0
1	0.07
2	0.13
3	0.26
4	0.52
5	1.03
6	2.06
7	4.12
8	8.25

Note, although the calibration curve would be valid for doses up to the highest dose delivered to the calibration film strips, it was recommended in literature that at least two strips receive doses that are equal to or greater than the highest dose to be measured. Additionally, FilmQAPro software makes a recommendation of selecting doses to provide an asymptotic fit and to also have a strip that receives zero dose. Therefore the doses delivered to calibration strips increased in geometric progression i.e. x, dX, d^2X, d^3X and etc. The calibration curve

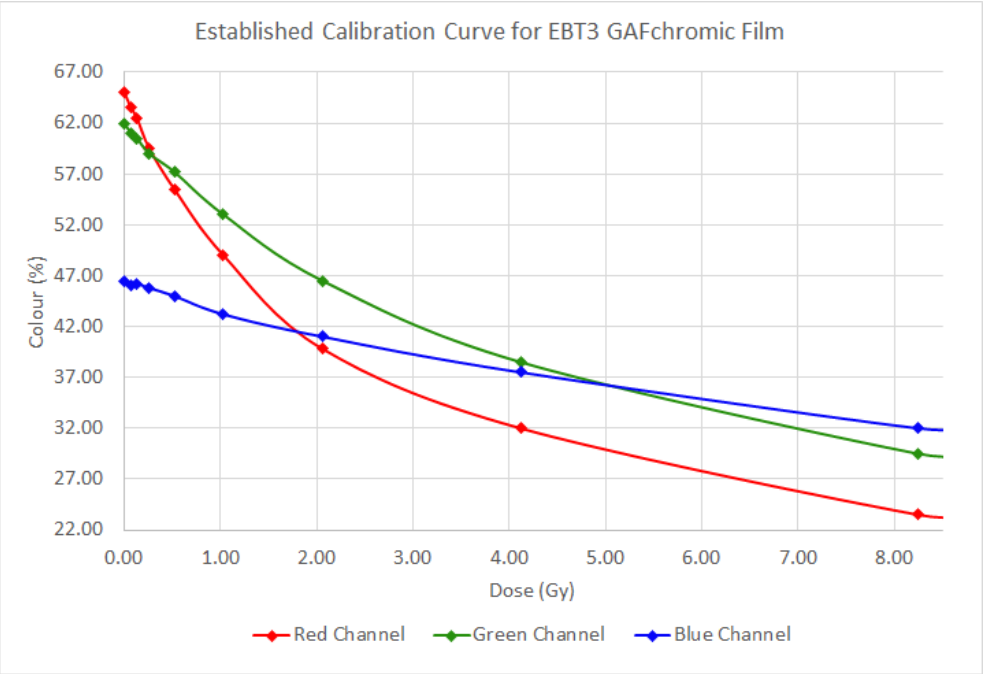

FIGURE 4.8: Calibration curve established for GAFchromic film used for dosimetric measurements

established for the batch of films used for dosimetric measurements is shown in Figure 4.8.

The treatment for the breast-lung phantom was planned to deliver a total fractional dose of 2 Gy. As per literature recommendations, the red channel dose calibration was used for dosimetric analysis [60], [61]. Figure 4.8 facilitates that the red channel had the most pronounced change in the optical density measured by the scanner for the dose output of 2 Gy. Therefore using the the red channel dose values minimised the uncertainties associated with the measured doses.

4.2.2 Simulation of Patient Setup Errors

Expected Treatment Position

The breast-lung phantom was setup on treatment at the expected treatment position using the treatment room lasers. The middle wax slab of the breast was replaced with the corresponding insert suitable for the type of measurement to be acquired. Dosimetric measurements were acquired using an IC, film and EPID to calculate the dose delivered to the phantom.

Offset Treatment Position Measurement

The phantom was intentionally offset from the expected treatment position by a known magnitude to simulate patient setup errors on treatment. The phantom was offset in the lateral (patient left to right), longitudinal (patient head to toe) and vertical (patient anterior to posterior) planes by $\pm$0.5 cm, $\pm$1.0 cm and $\pm$2.0 cm. These shifts were implemented using the treatment couch which had a calibrated digital read-out indicating the couch position and consequently the phantom position. The systematic setup error of the treatment couch was $\pm$0.5 mm [62]. Additionally the lasers present in the treatment bunker were also used to verify the shift magnitude.

4.2.3 Effect of Patient Setup Errors on the Percentage Dose Differences Provided by Different Dose Verification Methods

The EPID images acquired for dosimetric analysis at the expected treatment position and offset positions were used to calculate the fractional $\%DD_{DRP}$ and $\%DD_{vol}$ to analyse the effects of patient setup errors on the %DD provided by the different dosimetric analysis methods available.

4.3 Results

The results section of the phantom study will be presented in two parts:

- Subsection 4.3.1 presents the doses measured and calculated at the DRP using the IC, film and EPIgray at the expected and offset treatment positions.
- Subsection 4.3.2 presents the resulting fractional $\%DD_{DRP}$ and $\%DD_{vol}$ at the expected and offset treatment positions.

4.3.1 Dosimetric Results at Expected and Offset Treatment Positions

Expected Treatment Position

At the expected treatment position the TPS predicted a dose of 2.008 Gy to the DRP. The doses acquired using EPIgray, IC and radiochromic film at the expected treatment position are shown

in table 4.3.

TABLE 4.3: Doses measured at expected treatment position by different dosimeters

Dosimeter	Measured Dose (Gy)	%DD from TPS (%)
IC	2.001 ± 0.000	-0.35 ± 0.00%
Film	2.001 ± 0.060	-0.35 ± 0.06 %
EPIgray	2.001 ± 0.070	-0.35 ± 0.07%

Table 4.3 shows strong agreement between the doses acquired using different dosimetric systems. All dosimetry systems indicated minor deviations between the planned treatment and delivered treatment. This result indicates that at the expected treatment position, the EPIgray dose was consistent with the doses measured by other dosimeters.

Whilst the accuracy of the average dose calculated using different dosimeters were equivalent at the expected treatment position, the standard deviation associated with these measurements indicate IC measurements to be the most precise, followed by film and lastly EPIgray. These results therefore show a higher variability associated with EPIgray doses than the other dosimeters. However, results from this section indicate that EPIgray reconstructed doses at the DRP can be reliably used for verification of treatment delivery accuracy.

Offset Treatment Positions

Lateral Offsets

Figure 4.9 shows the $\%DD_{DRP}$ measured using different dosemeters for lateral offsets. For all positional shifts, the IC measurements have indicated an underdose to the DRP. The absolute magnitude of the IC $\%DD_{DRP}$ increased with increasing magnitude of positional shift. Shifts of equal magnitude and opposite directions provided comparable $\%DD_{DRP}$. For positional shifts of $\pm$0.5 cm film measurements suggested an underdosing to the DRP. However, this result is within the expected uncertainty and therefore whether the dose registered was an overdose or an underdose was not of significance. For other positional shifts, film measurements have indicated an overdose to the DRP. The EPIgray $\%DD_{DRP}$ have indicated an overdose to the DRP for all positional shifts. EPIgray also has the largest magnitude of $\%DD_{DRP}$ for all positional

shifts in comparison to other dosimetric systems. Unlike other dosimetric systems however, the absolute magnitude of $\%DD_{DRP}$ indicated by EPIgray does not increase in magnitude with increasing magnitude of shift.

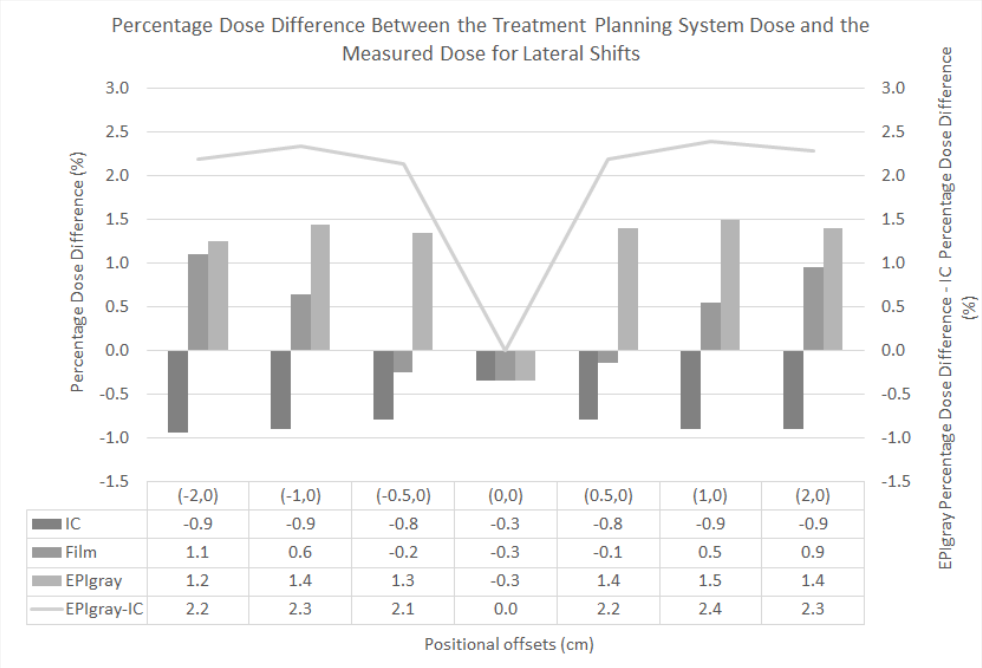

FIGURE 4.9: Dose measured by different dosemeters for lateral offsets

IC are routinely used for absolute point dose measurements. The geometry of these chambers allow accurate point dose measurements [63]. The uncertainties associated with IC measurements are smaller in comparison to the uncertainties associated with the film measurements [22]. Therefore the IC measurements for each positional shift was used as the benchmark to draw comparisons to EPIgray measurements. The difference between the IC $\%DD_{DRP}$ and the EPIgray $\%DD_{DRP}$ is also shown in Figure 4.9. It is evident that at any given shifted position, the absolute EPIgray $\%DD_{DRP}$ was noticeably larger than the $\%DD_{DRP}$ at the expected treatment position. However, the changes in the $\%DD_{DRP}$ with shifts of differing magnitudes were not as pronounced for EPIgray as they were with IC measurements. This result indicates that EPIgray was able to indicate a shift from the expected treatment position however, the magnitude of the shift that had occurred in the lateral direction was not reflected in the calculated $\%DD_{DRP}$.

Longitudinal Offsets

Figure 4.10 shows the $\%DD_{DRP}$ measured using different dosimeters following positional shifts of the phantom in the longitudinal plane. The longitudinal shift results were similar to the results of the lateral shift. The IC doses consistently provided a $\%DD_{DRP}$ that indicated an underdose. The IC $\%DD_{DRP}$ also demonstrated that with increasing magnitude of setup error, regardless of the shift direction the absolute magnitude of $\%DD_{DRP}$ would increase. For all positional offsets, the film measurements have indicated an overdose to the DRP. The EPIgray measurements indicated a noticeable increase in the absolute magnitude of $\%DD_{DRP}$ with longitudinal positional offsets from the expected treatment position. The EPIgray $\%DD_{DRP}$ for positional offsets do not mirror the trend seen for other dosimeters. EPIgray results have indicated that with increasing magnitude of offset from the expected treatment position, the $\%DD_{DRP}$ generally decreased. While this result was not expected, it may be explained by a range of uncertainties associated with the EPIgray dose reconstruction. Inherent uncertainties associated with the EPIgray dose reconstruction including variations in treatment parameters, acceptable setup errors, and the uncertainties associated with the linac on the day of treatment are a few factors that largely influence the EPIgray reconstructed doses. The influence of these factors on the $\%DD_{DRP}$ will be addressed in Chapter 5.

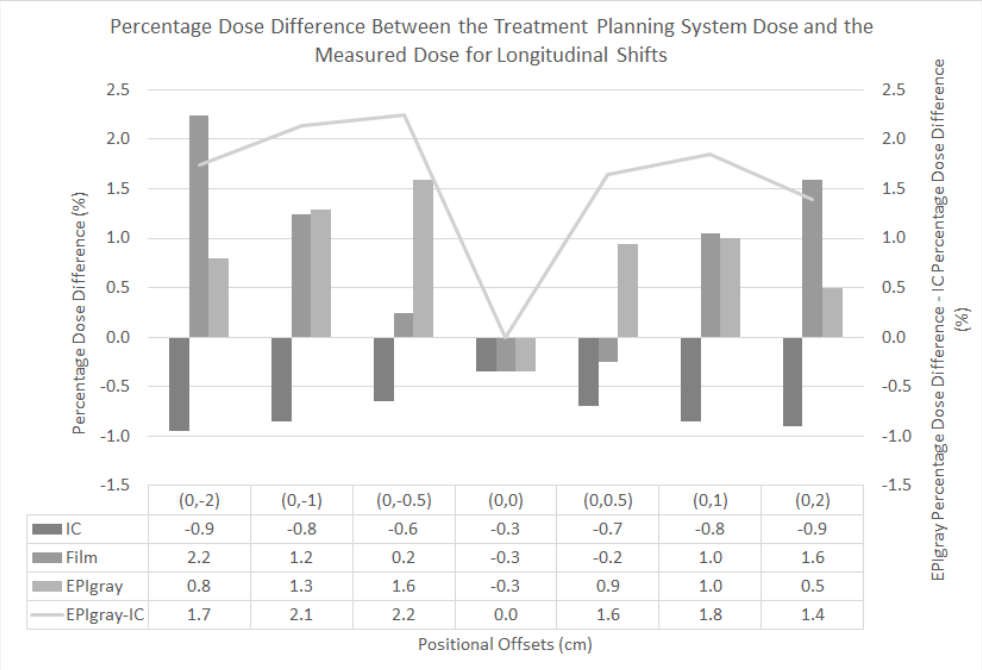

FIGURE 4.10: Dose measured by different dosemeters for longitudinal offsets

Vertical Offsets

The resulting $\%DD_{DRP}$ of different dosimeters following vertical positional offsets of the phantom are shown in Figure 4.11. From Figure 4.11 it is evident that the IC consistently indicated an underdose at all shifted positions. This observation for IC was consistent with the resulting $\%DD_{DRP}$ for setup errors of the phantom in other planes. Film $\%DD_{DRP}$ generally indicated an overdose to the DRP. Film $\%DD_{DRP}$ results were consistent with $\%DD_{DRP}$ results of setup errors in other planes, i.e. at any given position from the expected treatment position resulted in a noticeable increase in the $\%DD_{DRP}$. The resulting EPIgray $\%DD_{DRP}$ with vertical offsets mainly indicated an overdose trend with an underdose only occurring for a vertical downward shift of 2 cm. In comparing the EPIgray $\%DD_{DRP}$ with IC $\%DD_{DRP}$ for vertical offsets, it was evident that EPIgray consistently indicated a larger delivered dose to the DRP than intended. The exception to this observation was seen with a vertical downward shift of 2 cm. EPIgray calculated a -48.0% decrease in dose from the expected dose while the IC measured a $\%DD_{DRP}$ of -21.8%. The overshooting of the EPIgray $\%DD_{DRP}$ with a downward shift of 2 cm is explained by EPIgray dose reconstruction algorithm's difficulties in calculating dose to a point with highly variable densities in the reconstruction field of view. The noticeable increase in the magnitude of $\%DD_{DRP}$ can be attributed to the differences in the way the TPS and EPIgray handle heterogeneities in dose calculations. This finding is consistent with literature [64].

In comparing the IC $\%DD_{DRP}$ to the EPIgray $\%DD_{DRP}$ for positional shifts, with the exception of downward 2 cm shift, it was found that EPIgray $\%DD_{DRP}$ was typically approximately 2% higher than the $\%DD_{DRP}$ given by the IC measurements.

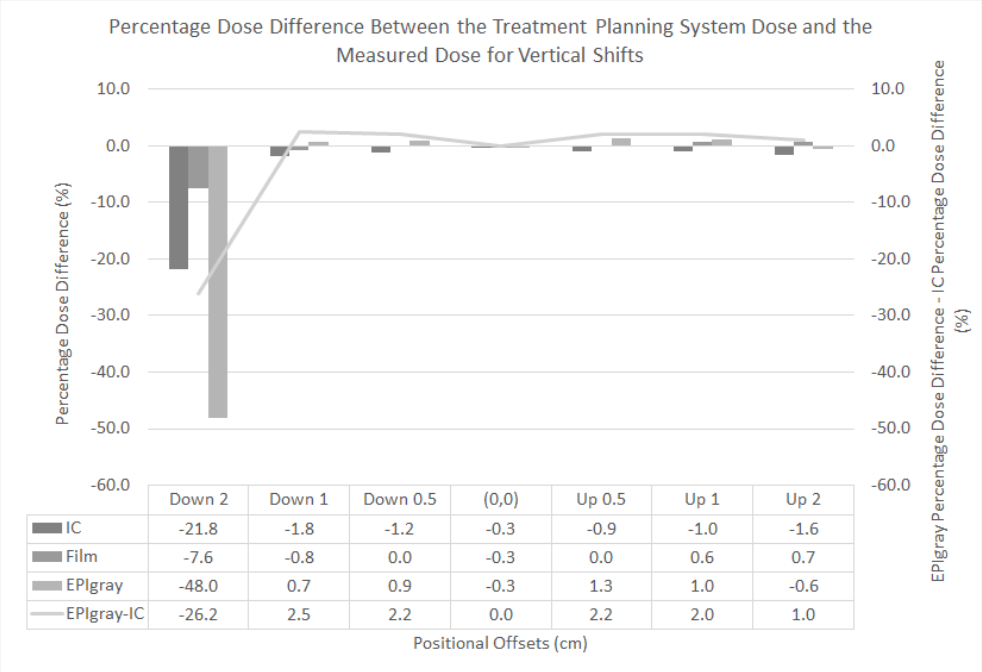

FIGURE 4.11: Dose measured by different dosemeters for vertical offsets

4.3.2 Effect of Patient Setup Errors on $\%DD_{DRP}$ and $\%DD_{vol}$

The fractional $\%DD_{DRP}$ and $\%DD_{vol}$ before and after positional correction on EPIgray analysed using the DRP method and the volume method is presented in this section.

Figure 4.12 and Figure 4.13 show the $\%DD_{DRP}$ and $\%DD_{vol}$ for lateral positional offsets before and after positional correction within EPIgray [1]. From these figures, it is found that the $\%DD_{vol}$ was larger than $\%DD_{DRP}$ both before and after positional correction. The standard deviation associated with the $\%DD_{vol}$ was found to be the smallest at the expected treatment position. The standard deviation associated with the $\%DD_{DRP}$ at each positional offset was found to decrease following positional correction.

[1] Figures showing the effects of positional correction (before and after) on $\%DD_{DRP}$ and $\%DD_{vol}$ were intentionally not combined. The scales of these graphs are different and therefore combining these figures will affect the interpretation.

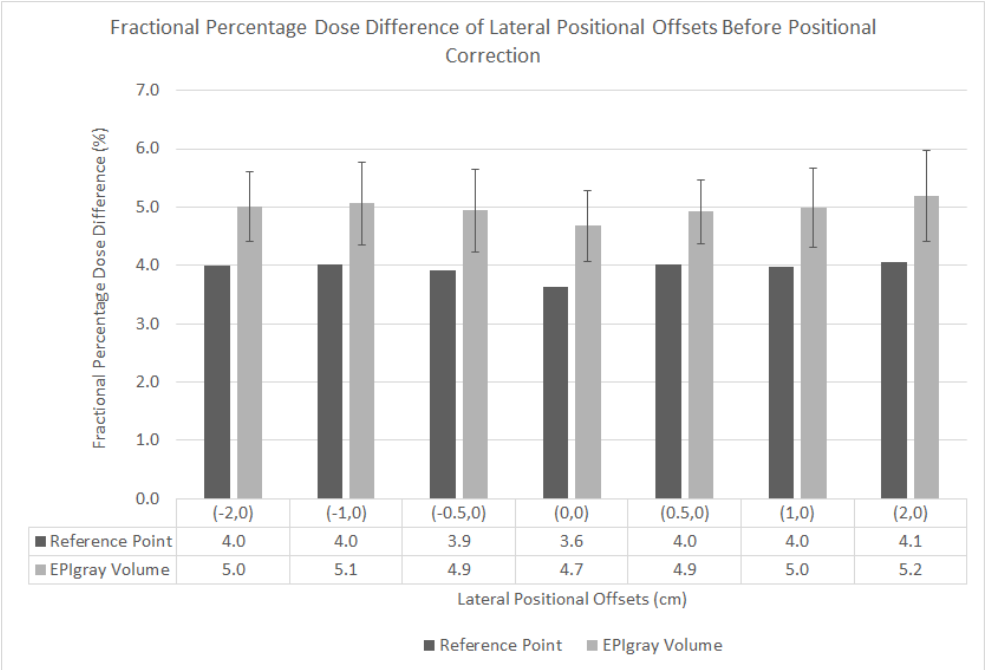

FIGURE 4.12: Fractional %DD of lateral shifts before positional correction using reference and mean volume dose method

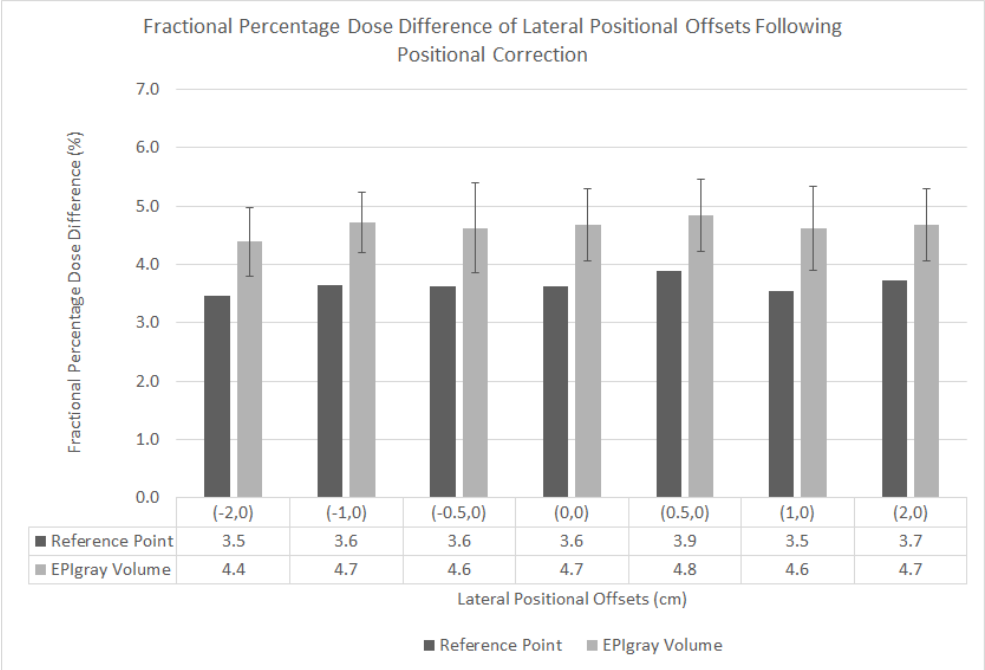

FIGURE 4.13: Fractional %DD of lateral shifts following positional correction using reference and mean volume dose method

In considering the effects of longitudinal shifts, using Figure 4.14 and Figure 4.15 it was found that at each positional offset the $\%DD_{vol}$ was larger than the $\%DD_{DRP}$. Additionally it was found that with increasing magnitude of shift, the uncertainty associated with the $\%DD_{vol}$ also increased. The increasing uncertainty of $\%DD_{vol}$ with positional offset was a result of EPIgray

performing a dose calculation with increased amount of heterogeneties in the field of reconstruction. The large standard deviation with these measurements can immediately alert the treatment professional that an unexpected event has occurred and positional verification within the EPIgray will need to be performed. With positional correction within EPIgray, the $\%DD_{vol}$ still remained larger in magnitude for every positional shift in comparison to $\%DD_{DRP}$. Following positional correction, the magnitude of $\%DD_{DRP}$ and $\%DD_{vol}$ both decreased. Furthermore it was found that the uncertainty associated with $\%DD_{vol}$ at each phantom position has also noticeably decreased. The standard deviation associated with each positional offset is similar in magnitude regardless of the magnitude of offset. This finding emphasises the limitations of EPIgray in reconstructing dose with highly varying densities in the field of reconstruction. The smallest magnitude of $\%DD_{vol}$ uncertainty was at the expected treatment position.

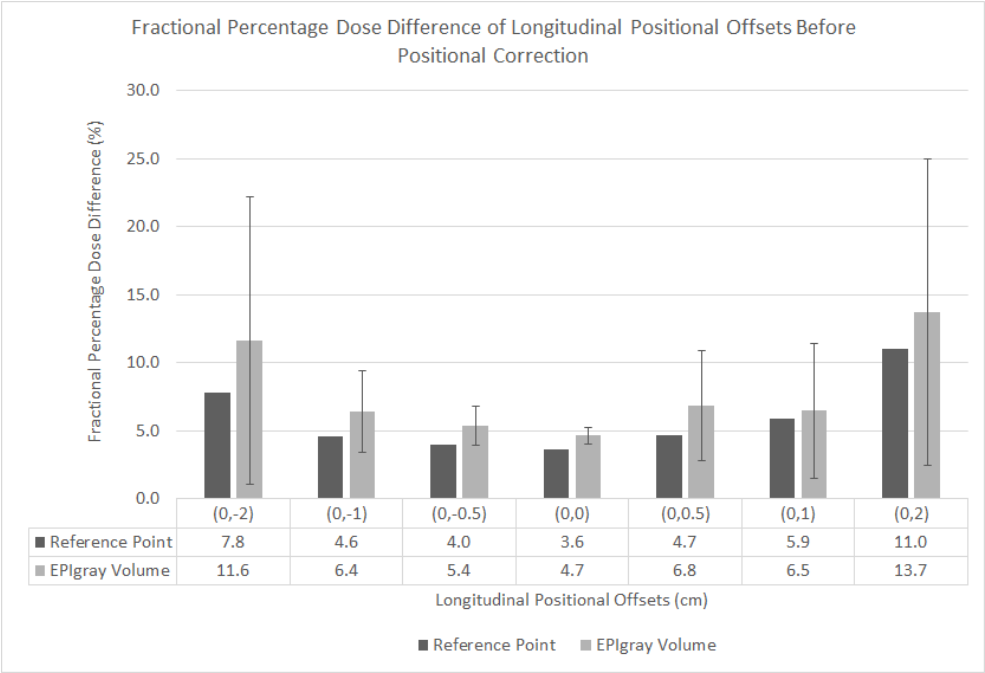

FIGURE 4.14: Fractional %DD of longitudinal shifts before positional correction using reference and mean volume dose method

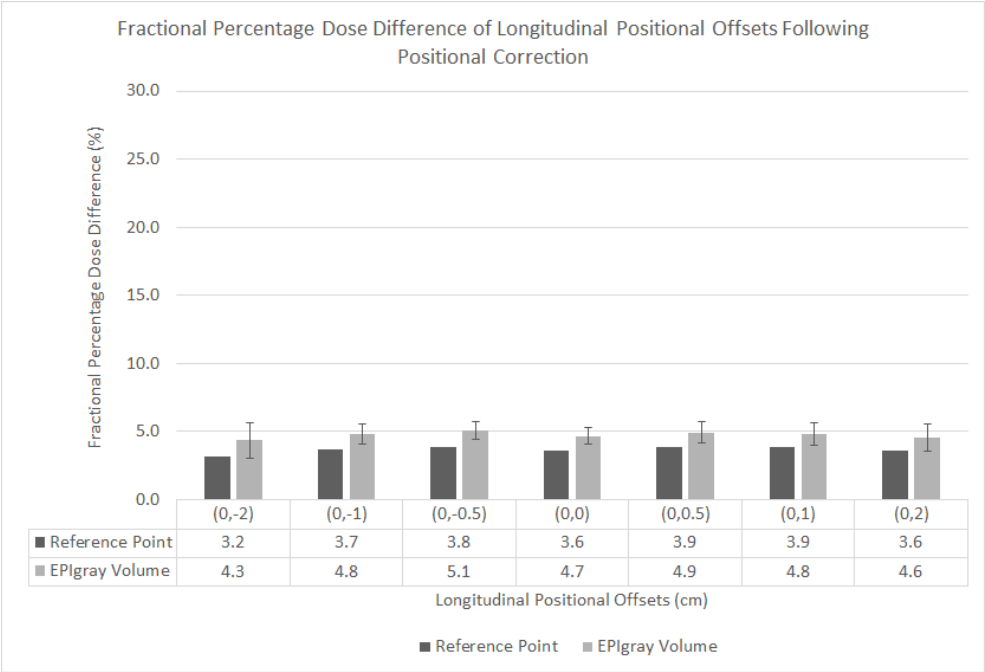

FIGURE 4.15: Fractional %DD of longitudinal shifts following positional correction using reference and mean volume dose method

In considering vertical shifts, Figures 4.16 and 4.17 indicate that of all positional offsets, the most significant changes to the %DD was seen with vertical shifts. The absolute magnitude of $\%DD_{vol}$ for vertical shifts was mostly found to be the greater than $\%DD_{DRP}$ both before and after positional correction within EPIgray. The standard deviation associated with $\%DD_{vol}$ measurements at each position increased with increasing magnitude of offset as expected. Following positional correction, the uncertainty associated with the $\%DD_{vol}$ decreased for all positional offsets with the exception of downward shifts of 1.0 and 2.0 cm.

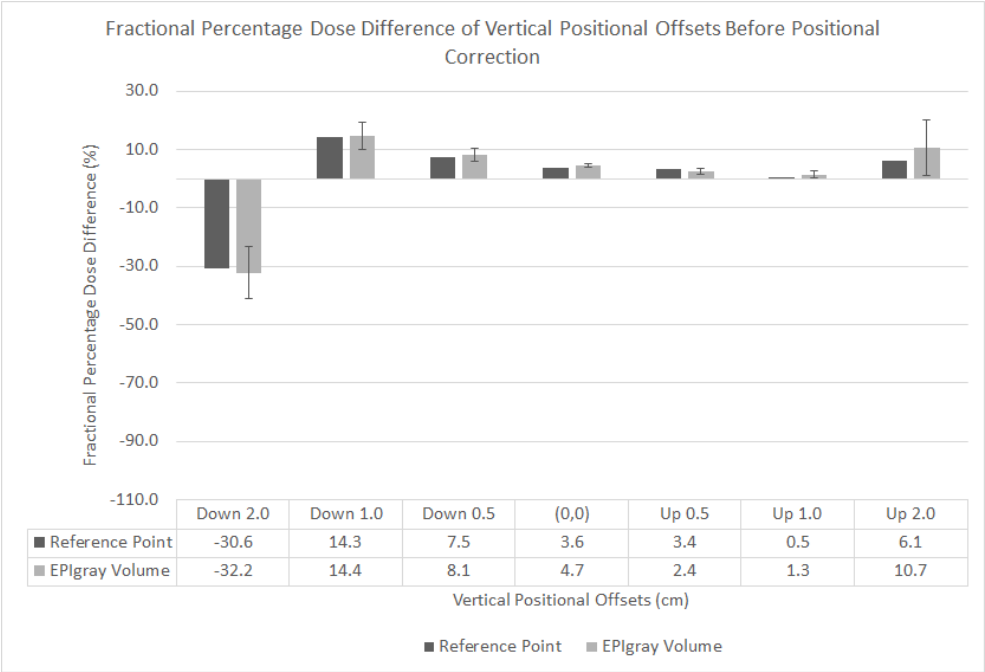

FIGURE 4.16: Fractional %DD of vertical shifts before positional correction using reference and mean volume dose method

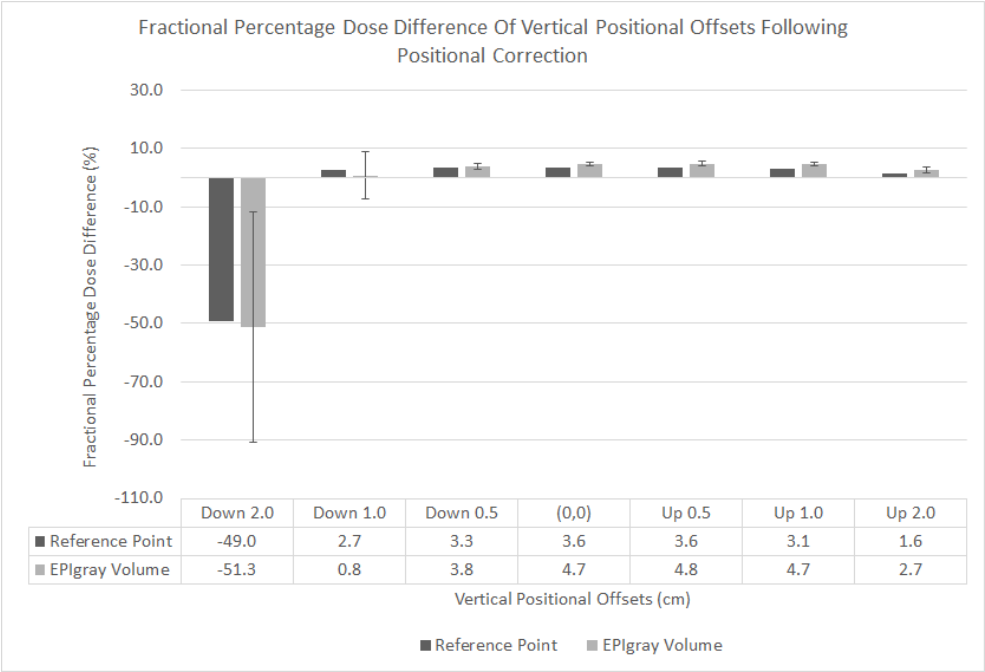

FIGURE 4.17: Fractional %DD of vertical shifts following positional correction using reference and mean volume dose method

4.4 Discussion

The results of the phantom study will be discussed in two parts. Subsection 4.4.1 will address the effects of positional offsets on the EPIgray reconstructed doses and how EPIgray doses compared to doses acquired using an IC and film. Subsection 4.4.2 will address the similarities and differences between $\%DD_{DRP}$ and $\%DD_{vol}$ with phantom positional offsets to verify the recommended clinical tolerance for $\%DD_{vol}$.

4.4.1 EPIgray vs. Established Dosimeters

Expected Treatment Position

The dosimetric results obtained at the expected treatment position revealed that the accuracy of EPIgray doses were comparable to the doses acquired using other dosimeters. However the standard deviations associated with these measurements revealed EPIgray reconstructed doses to have larger uncertainty than the routinely used clinical dosimeters. The doses shown in table 4.3 are the average doses measured and calculated across three irradiations. Except for dosimetric measurements using film, which required placement of an unirradiated film between each irradiation, no changes were made to the setup. Therefore the uncertainty associated with the EPIgray reconstructed doses was a consequence of the uncertainties associated with the treatment and EPIgray itself. The effects of the treatment-related and EPIgray-related uncertainties will be investigated and discussed in Chapter 5.

The dosimetric results obtained using EPIgray and other routinely used dosimeters provided quantifiable evidence to reliably use EPIgray at the expected treatment position for 3DCRT breast treatments following positional correction.

Lateral Positional Offsets

The $\%DD_{DRP}$ provided by all dosimetry systems were expected to be smallest at the expected treatment position as all calculations were made with the geometry associated with the expected treatment position, and thus was shown to be true for lateral shifts.

An increase in the absolute magnitude of $\%DD_{DRP}$ was expected with increasing magnitude of shift from the expected treatment position. The dependency of $\%DD_{DRP}$ on the shift magnitude is based on the changes to the position of the point at which the dose was calculated. With lateral shifts, the depth of the DRP is effectively shifted, changing the geometry of the treatment. This difference in the phantom position would alter the scatter environment resulting in the delivery of a different dose to the DRP. The two fields of the treatment were planned to be incident with the phantom from gantry 90° and 270°. Therefore the lateral shifts that were performed would result in the movement of the phantom towards one field and further away from the other depending on the direction of shift, i.e. if the phantom was shifted in the positive lateral direction the phantom would be moved closer to the field at 90° and further away from the field at gantry 270° and a negative shift would have the opposite result. During treatment planning, the treatment planner would assign the required dose to the point of interest, in this case the DRP. The TPS would then calculate the number of monitor units (MU) required to achieve the assigned dose at the DRP. At Christchurch Hospital, the MU as deliverable radiation quantities are usually defined as follows. 1 MU is equivalent to 1 cGy under reference conditions of source-to-detector distance of 100 cm, 10 cm depth in water-equivalent material, for a treatment field size of 10 x 10 cm [63]. The TPS uses beam models of the linac to calculate the number of MU required to achieve a particular dose requested from the TPS by the planner. However, the TPS calculations are dependent on the set geometry of the treatment. That is, the TPS uses patient setup factors such as the distance between the patient and the radiation source and the thickness of patient before the DRP. For the phantom treatment plan, the expected treatment position has been setup such that the DRP within the phantom sits in the middle of the lateral distance between 90° and 270°. However, with positional offset the phantom position relative to the field is shifted for both fields. This shift in the depth of the DRP will result in a different dose to be deposited at the DRP. This concept is best explained using Figure 4.18, which shows the percentage depth dose (PDD) curve for a typical 6 MV photon beam. The PDD curve shows the percentage of maximum dose deposited by a radiation beam as a function of depth. Using Figure 4.18, an increase or decrease in depth would alter the dose to the DRP. Therefore with larger magnitude of shift, the $\%DD_{DRP}$ from the TPS calculated dose would be greater.

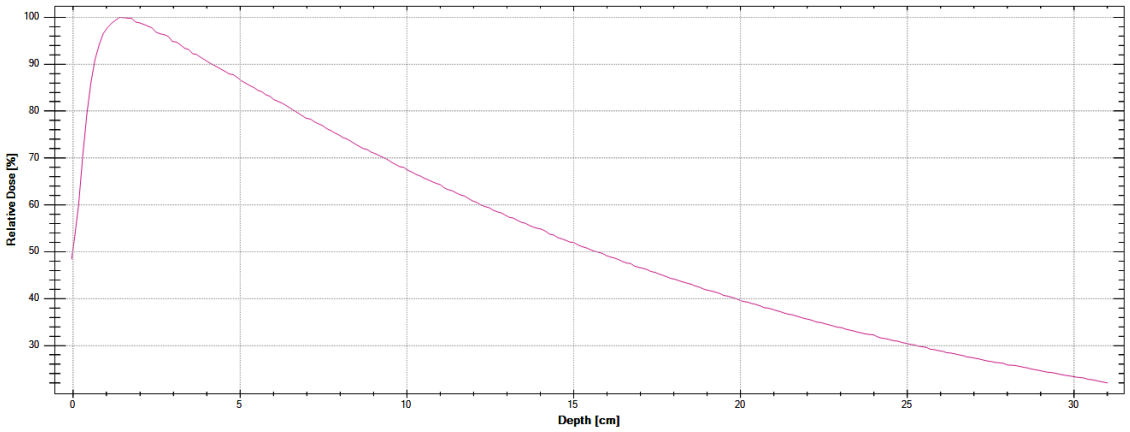

FIGURE 4.18: 6 MV Percentage Depth Dose

The increase in the absolute magnitude of $\%DD_{DRP}$ with increasing magnitude of shift was seen for IC and film measurements but not with EPIgray. This finding suggests that while EPIgray is capable of identifying that a treatment setup error has occurred by a noticeable increase in the $\%DD_{DRP}$, the magnitude of EPIgray $\%DD_{DRP}$ does not indicate the magnitude of setup error. A setup error of $\pm$2.0 cm is highly unlikely and patients will be setup again to correct for this error if it is noticed on treatment. However, evidence from this section of the investigation has revealed that the $\%DD_{DRP}$ at $\pm$2.0 cm are still within the tolerance of $\pm$5.0%. These results therefore highlight the importance of either establishing a process to double check patient positioning on treatment or establishing a more sensitive $\%DD_{DRP}$ tolerance for positional correction within EPIgray to account for setup errors as a clinically significant setup error still produces an acceptable $\%DD_{DRP}$.

It was also expected that $\%DD_{DRP}$ obtained for shifts of equal magnitude but opposite directions should be comparable, i.e. the IC $\%DD_{DRP}$ at the 0.5 cm offset should be comparable to the IC $\%DD_{DRP}$ at the -0.5 cm offset. Both fields of the treatment plan had equal weighting in terms of dose delivered to the DRP and therefore the effects of positive phantom shift should be comparable to negative phantom shifts. Subject to minor variations, all three dosimetric systems exhibited this trend. This finding implies that the EPIgray dose calculation algorithm is not biased towards proximal and distal shifts of the patient.

Longitudinal Positional Offsets

Figure 4.19 shows the extent to which both fields of the treatment plan extend. The treatment

fields are shown to extend 1.75 cm beyond the phantom surface. Fields extending beyond the patient surface are often seen in radiotherapy plans that treat to the surface to ensure target movement associated with patient breathing motion and patient setup errors on treatment do not result in missing superficial part of the target volume. Flash allows the treatment to proceed with the planned fields as the target volume will still be sufficiently irradiated. In considering the magnitude of positional offsets performed on the phantom with reference to Figure 4.19, the offsets of greater than 1.75 cm would provide a pronounced effect on the $\%DD_{DRP}$. Therefore the longitudinal shifts of 2.0 cm regardless of whether it is a positive or negative shift would result in the largest $\%DD_{DRP}$. With a shift of 2.0 cm in the longitudinal direction, the treatment field would no longer be covering the entire phantom. Consequently there would be less scatter than expected by the TPS for the original treatment position leading to a lower dose calculated at the DRP.

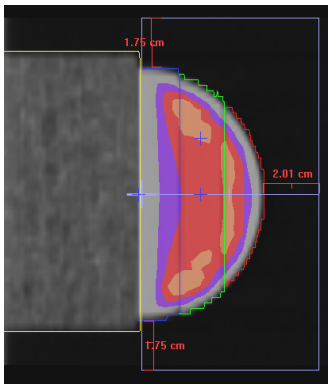

FIGURE 4.19: Sagittal view: Extended beam fields to account for patient movement

By observation of Figure 4.10 the results of the IC were the most consistent with the expected result. Film and EPIgray both revealed overdoses across the positional offsets with the $\%DD_{DRP}$ increasing with magnitude of shift. These results are consistent with the results of the lateral shifts. A systematic offset was seen between the IC doses and EPIgray doses. The overdoses indicated by EPIgray were not actual overdoses but needed to be systematically offset to be consistent with the results of the IC.

Considering only the EPIgray results, it was generally found that the $\%DD_{DRP}$ from the TPS decreased with increasing magnitude of shift. The $\%DD_{DRP}$ was not expected to change significantly for offset magnitudes of 0.5 cm and 1.0 cm regardless of the shift direction. However

the largest impact on the $\%DD_{DRP}$ was expected for the 2.0 cm offsets. With a positional shift of greater than the magnitude of field extent, the decrease in the scatter from the portion of the phantom that was missed by treatment field should have resulted in a lower dose than calculated at the DRP. This decrease in dose combined with EPIgray's tendency to calculate a larger dose to the DRP resulted in the dose to the DRP at $\pm$2 cm being smaller than the doses of other positional offsets of smaller magnitude. The variations seen across the other four longitudinal offsets were within the EPIgray dose calculation uncertainties. These results highlight the occurrence of false results as a consequence of EPIgray-related uncertainties. Consequently the results of this section provided clinical indication for verification of patient positioning within EPIgray. If the fields of the treatment were sufficiently symmetrical with reasonable field extension such as the ones used in this investigation, the DRP may have received an acceptable dose to the DRP however, the overall target coverage may be compromised if $\%DD_{DRP}$ was used without EPIgray positional correction.

Similar to the results of the lateral offsets, the resulting EPIgray $\%DD_{DRP}$ did not provide any indication of the magnitude of shift that had occurred. Small shifts such as the $\pm$0.5 cm shifts did not significantly impact the treatment outcome, however larger positional errors had the potential to compromise the treatment. The EPIgray $\%DD_{DRP}$ was within the $\pm$5.0% tolerance for larger positional offsets as seen in this section of the study. However the target coverage was significantly reduced. Consequently the results from the lateral and longitudinal shifts had indicated the need to verify the position of the patient within EPIgray to ensure that the treatment was delivered as expected and the provided EPIgray $\%DD_{DRP}$ could be reliably used.

Vertical Positional Offsets

Upward movements of the phantom result in more of the cork in the field. Consequently, the cork which had a lower density than wax should have resulted in decreased scatter leading to a lower measured dose for all dosimetric systems relative to the TPS predicted dose. However there was sufficient flash in the field and therefore an upward shift of <2 cm should also not have drastically affected the $\%DD_{DRP}$. For all vertically upward shifts of the phantom, the resulting $\%DD_{DRP}$ obtained using different dosimeters produced expected results. These results have provided evidence that EPIgray $\%DD_{DRP}$ could be reliably used for setup errors within

the magnitude of the flash available in the plane perpendicular to the source.

In contrast, a downward movement of the phantom would result in more air occupying the field and less cork. The flash only extends in the anterior direction. Therefore with a downward shift corresponding to the movement of the phantom in the posterior direction, there was a significant decrease in the scatter from the anterior direction leading to a significant decrease in dose to the DRP. It was expected that with increasing magnitude of shift in the downward direction, the magnitude of $\%DD_{DRP}$ should decrease due to reduced dose from a lack of scatter. This expected result was evident across all dosimeters. Figure 4.11 shows that downward phantom movement of 2.0 cm resulted in the greatest deviation from the predicted TPS dose for all dosimeters.

By comparing the IC measurements with the EPIgray measurements, it was found that the EPIgray $\%DD_{DRP}$ and IC $\%DD_{DRP}$ were consistently within 2.5% for all longitudinal and lateral shifts. In considering the vertical shifts, it was found that EPIgray $\%DD_{DRP}$ was consistent with IC $\%DD_{DRP}$ granted that the field of reconstruction did not have largely varying tissue densities. With downward movement of the phantom, there was a noticeable change in density as air would occupy the volume that was previously occupied by cork and wax on the captured EPID image. For downward movement of 2.0 cm the $\%DD_{DRP}$ difference between IC and EPIgray was 26.2%. This result indicated that EPIgray was capable of providing a $\%DD_{DRP}$ that would alert the treatment professional to a potential error that may have occurred, although the magnitude of the $\%DD_{DRP}$ was not entirely proportional with the shift magnitude that had occurred.

4.4.2 DRP Dose vs. Mean Volume Dose

Investigation of the effect setup errors on treatment had on $\%DD_{DRP}$ and $\%DD_{vol}$ suggested that $\%DD_{DRP}$ was consistently smaller in magnitude than $\%DD_{vol}$. The advantage of using $\%DD_{vol}$ for dosimetric analysis was that $\%DD_{vol}$ provided an indication of the treatment delivery accuracy to a sensible volume and not to a single selected point. Additionally $\%DD_{vol}$ was provided with a standard deviation. Large uncertainties associated with the $\%DD_{vol}$ could be

used as an indicator of an unexpected treatment delivery. The use of DRP for dosimetric analysis provided a different set of advantages in that although the dose was only reconstructed to a single point, this point was appropriately chosen such that the uncertainties associated with the $\%DD_{DRP}$ were minimised. Secondly, the investigation of potential errors was made easier with the DRP analysis because the dose to the DRP was known within the TPS and could be simulated at different points within the TPS if necessary. This was not an option with the $\%DD_{vol}$ because the 50 points are randomly selected by EPIgray and the position of these points are not directly transferable to the TPS.

The trend of $\%DD_{DRP}$ and $\%DD_{vol}$ with clinically appropriate positional shifts were found to be similar. The dose offset seen between both $\%DD_{DRP}$ and $\%DD_{vol}$ were not directly comparable as one %DD was to a single point and the other considered multiple points. Results of this section of the phantom study indicated that it would be clinically beneficial to have both $\%DD_{DRP}$ and $\%DD_{vol}$ in place and not one over the other for the reasons mentioned above.

With the exception of a downward shift of 2 cm, it was found that following positional correction all positional shifted $\%DD_{vol}$ were within $\pm$5.0%. Considering that the $\%DD_{vol}$ was consistently larger than $\%DD_{DRP}$, the most conservative approach would be to set the fractional $\%DD_{vol}$ clinical tolerance to $\pm$5.0%. Having a narrow tolerance placed on the $\%DD_{vol}$ would also aid in the reduction of false positive results. In considering the $\%DD_{DRP}$, the initial tolerance of $\pm$5.0% was retained based on the evidence from the retrospective study and the phantom study. The $\%DD_{DRP}$ analysis can be performed for each field, whilst the $\%DD_{vol}$ only considers the overall fraction. Therefore the use of $\%DD_{vol}$ would be more sensitive to failures, as this tolerance would take into account all the fields within each fraction. The standard deviation associated with the mean reconstructed dose of the volume analysis should also be considered when using $\%DD_{vol}$ as an indicator for treatment delivery accuracy. Fractional DD_{vol} exceeding the $\pm$5.0% tolerance could be investigated using the dose to the DRP to identify the specific field(s) that may have caused the failing result for the overall fraction. No significant differences were found between breast lateralities and size and therefore this proposed change is for all 3DCRT breast patients.

4.5 Conclusion

The retrospective study confirmed that there was good agreement between the TPS doses and the EPIgray reconstructed doses at the DRP. However validation was necessary to confirm that the EPIgray reconstructed doses were representative of the doses delivered to the patient on treatment. Results from subsection 4.3.1 reveal that there was a strong agreement between the EPIgray reconstructed doses and the doses measured by other dosimeters at the expected treatment position. While there were small differences between the TPS doses and the EPIgray calculated doses, accurate EPIgray calculation of the dose was affected by a range of uncertainties discussed in Chapter 5. These uncertainties may be minimised however could not be eliminated altogether. The results section of this chapter had revealed that EPIgray could be reliably used for in-vivo dosimetric verification of 3DCRT breast patients.

Results of the phantom study revealed that in the presence of phantom shift EPIgray consistently calculated a dose that is larger than the doses measured using the IC and film. A range of positional shifts were applied to the phantom to simulate patient setup errors. The greatest shift applied in each direction was 2.0 cm. IC measurements were the most consistent with the expected results based on the scatter and absorption properties. Additionally IC measurements had the best agreement with the TPS and had the smallest uncertainties. Uncertainties for IC measurements and film measurements were able to be reduced based on routine use of these dosimeters clinically. The uncertainties associated with EPIgray doses will be explored in the next chapter to be able to quantify and minimise these uncertainties. In drawing comparisons between IC and EPIgray, it was evident that there was a positive offset in the calculated EPIgray dose and IC measured doses for all offset positions. Across all planes and shifts in both directions, it was found that EPIgray $\%DD_{DRP}$ was systematically offset by 2.5% with a downward phantom shift of 2 cm being an exception. The phantom study provided further evidence of EPIgray limitations with increasing amount of heterogeneities in the field of the dose reconstruction. EPIgray provided a more pessimistic dose difference than what had occurred on treatment. While EPIgray did not directly indicate the dose delivered, the pessimistic EPIgray $\%DD_{DRP}$ in comparison to the IC $\%DD_{DRP}$ provided confidence that treatment accuracy was achieved or would be more likely detected by the tolerance.

Investigation of $\%DD_{DRP}$ and $\%DD_{vol}$ has revealed that the magnitude of $\%DD_{vol}$ was consistently larger than $\%DD_{DRP}$. Evidence from the retrospective study and the phantom study indicated that a tolerance of $\pm 5.0\%$ placed on $\%DD_{vol}$ was restrictive however effective. The treatment fractions that fail to meet this tolerance could be analysed using the $\%DD_{DRP}$ $\pm 5.0\%$ tolerance. Based on the findings of the retrospective study and the phantom study, the $\pm 5.0\%$ $\%DD_{DRP}$ was retained. The primary reason for reducing this tolerance was to reduce the number of false passes. Whilst the tolerance on $\%DD_{DRP}$ did not change based on the results of this section, having $\%DD_{vol}$ as another metric for dosimetric analysis of the treatment accuracy with tighter tolerances would aid in limiting the number of false passes without significantly changing the current clinical practice. Additionally the standard deviation associated with mean reconstructed doses of the volume method was also shown to be a good indicator of unexpected treatment events. Therefore the standard deviation associated with the mean reconstructed dose should also be used as an indicator for treatment delivery accuracy.

5 EPIgray Uncertainties

5.1 Factors Contributing to EPIgray Reconstructed Dose Uncertainty

The $\pm$5.0% tolerance placed on the $\%DD_{DRP}$ is the uncertainty associated with the EPIgray reconstructed dose. The second objective of this project aims to decrease this tolerance to more effectively identify unexpected treatment. The current tolerance was set based on measurements acquired during commissioning of EPIgray. This tolerance is generic and applies to all treatment sites. In order to decrease this tolerance specifically for 3DCRT breast treatments, the factors contributing to this uncertainty must be identified and quantified.

The major factors that influence the magnitude of $\%DD_{DRP}$ are discussed in the following sections:

1. Within 3DCRT breast treatments, treatment plan parameters are subject to vary from patient to patient depending on numerous factors including the patient's anatomy. The variations associated with these plan parameters affect the $\%DD_{DRP}$. Section 5.3 identifies and quantifies the effects of 3DCRT breast treatment plan parameters and its effects on the $\%DD_{DRP}$.

2. The setup of a patient on treatment will typically not be identical to the setup of the patient at CT simulation. The presence of random errors associated with setup is always present in a radiotherapy setting. Consequently radiotherapy treatments are planned to minimise and account for these errors. As such the setup errors that may occur have treatment tolerances. If the setup errors on treatment are within the given tolerances, the treatment can proceed and is still considered to be effective treatment. Section 5.4 presents the differences in the setup of the patient and the EPID on treatment within the acceptable tolerance and its corresponding effects on the $\%DD_{DRP}$.

3. The EPIgray software itself provides an inherent uncertainty to the EPIgray reconstructed dose based on the accuracy of the beam model under specific treatment parameters. These EPIgray related factors contributing to the differences in $\%DD_{DRP}$ are discussed in section 5.5.

4. Lastly, the retrospective study has shown that positional correction within EPIgray affects the magnitude of the $\%DD_{DRP}$. Positional correction involves the operator performing the correction to find the most appropriate alignment between the EPID and TPS contours. Consequently variations in the matching between operators will result in differences in $\%DD_{DRP}$. Section 5.6 will present the operator-related errors associated with positional correction within EPIgray.

The purpose of this section of the study is to quantify the major factors causing deviations in the EPIgray reconstructed doses. The findings of this chapter will determine the feasibility and implications of decreasing the current $\pm 5.0\%$ tolerance for 3DCRT breast treatments.

5.2 Defining Uncertainties of Dosimetric Measurements

The uncertainties of dosimetric measurements like other measurements, are expressed with reference to accuracy and precision. The precision of dosimetric measurements refers to the reproducibility of the measurements in similar conditions. The precision of measurements can therefore be estimated using the results of repeated measurements. The magnitude of the standard deviation of the measurements will provide an indication of the precision, where high precision relates to a low standard deviation and vice versa. The accuracy of dosimetric measurements refers to the closeness of the measured quantity to the true or expected quantity. The inaccuracy associated with the measurement is referred to as the 'uncertainty'. The uncertainties associated with measurements may be estimated using statistical methods (type A uncertainties) or other methods (type B uncertainties).

Type A Uncertainties

The best estimate for a dosimetric quantity D, would be the arithmetic mean for repeated measurement of D given by equation 5.1.

$$\bar{D} = \frac{1}{N}\sum_{i=1}^{N} D_i \tag{5.1}$$

The standard deviation for the set of repeated measurements quantifies the average uncertainty of each individual measurement assuming gaussian variability. The standard deviation of the dosimetric quantity is given in equation 5.2.

$$\sigma_D = \sqrt{\frac{1}{N-1}}\sum_{i=1}^{N}(D_i - \bar{D})^2 \tag{5.2}$$

The standard deviation of the mean dosimetric measurement is given by:

$$\frac{1}{\sqrt{N}}\sigma_D = \sqrt{\frac{1}{N(N-1)}}\sum_{i=1}^{N}(D_1 - \bar{D})^2 \tag{5.3}$$

Type A standard uncertainty (u_A) is the standard deviation of the mean value ($u_A = \sigma_{\bar{D}}$). The standard type A uncertainty can be evaluated using statistical analysis of repeated measurements and the uncertainty associated with the dosimetric quantity is reduced with increasing number of repeated measurements.

Type B Uncertainties

Type B standard uncertainty is not obtainable through repeated measurement. Rather, type B standard uncertainty is determined through scientific judgement of non-statistical uncertainties of the dosimetry quantity to be measured. Type B standard uncertainties include consequences of the measurement process, use of literature defined physical data and application of correction factors to the measured quantity. The type B standard uncertainties is given as a fraction of the limits beyond which there is no probability of occurrence. The chosen fraction is therefore taken as the limits of the assumed distribution.

Combined Uncertainty Of Dosimetric Measurements

The equation for measuring the dosimetric quantity D at point P is given by:

$$D_P = M \prod_{i=1}^{N} C_i \tag{5.4}$$

Where,

M is the measurement given by the dosimetry system,

N is the number of repeated measurements,

C_i is the correction factor.

The dosimetric quantity therefore involves the combination of u_A and u_B uncertainties. The standard uncertainty of dosimetric uncertainties is given by u_C, the combined uncertainty.

$$u_C = \sqrt{u_A^2 + u_B^2} \tag{5.5}$$

The distribution of u_C is assumed to be a normal distribution [14]. The product of u_C and a coverage factor (k) is used to obtain the expanded uncertainty, U, given in equation 5.6. A coverage factor of 2, corresponds to 95% confidence level and is typically used to represent the overall uncertainty.

$$U = k u_C \tag{5.6}$$

Therefore the dosimetric measurement will be expressed as $D_P \pm U$.

5.3 Treatment Parameter Uncertainties

Radiotherapy treatments are individualised to the patient. There are numerous treatment plan-related factors that may differ from patient to patient and therefore it is important to quantify the error contribution from each of these treatment parameters to determine an appropriate

uncertainty tolerance. The major treatment plan parameters of 3DCRT breast treatments contributing to the uncertainty associated with the EPIgray reconstructed dose are discussed below.

Dose Linearity

An ideal IVD system should provide a response that is linearly proportional to dose. The EPID images that were used as input for dose calculations using EPIgray were acquired using an aSi EPID. Previous publications have identified non-linear dosimetric responses of the aSi EPID [65]. Since doses of 3DCRT breast treatment fields are subject to variations, the relationship between $\%DD_{DRP}$ and dose was investigated.

Dose Rate Linearity

Radiotherapy treatments using linacs provide the capability of delivering the prescribed dose faster or slower by adjustment of the dose-rate (MU/min). Increasing the dose rate will result in faster treatments and decrease the potential of patient movement during the treatment. However, Winkler *et al.* have shown that the dose-rate affects the EPID response and consequently the EPIgray reconstructed dose. The relationship between $\%DD_{DRP}$ and dose rate was investigated to quantify the uncertainties arising as a consequence of variable dose rate [65].

Gantry Angle

Gantry angles used for treatment of breast patients are subject to variations and are dependent on the treatment laterality and the anatomy of the patient. The gantry angles of 3DCRT breast treatments are specifically chosen to provide dose to the breast and to avoid dose to the underlying lung tissue and contralateral breast. The variations in the $\%DD_{DRP}$ with gantry angles were investigated to quantify the error contribution arising from variable gantry angles of 3DCRT breast treatments.

Source-Surface Distance (SSD)

The SSD is defined as the distance between the radiation source and the surface of the phantom/patient. The SSD is subject to change between breast patients and is dependent on the

breast size and the positioning on treatment. The effects of the expected range of SSD on the EPIgray reconstructed doses were investigated to quantify the effects of SSD on the $\%DD_{DRP}$.

Field-size Dependency

The field sizes chosen for treatment are dependent on the patient anatomy. The larger the target volume, the larger the field size. A wide range of breast sizes are seen in 3DCRT treatment of the breast. Consequently, the fields employed to irradiate the target volume are also extensive. Therefore it is important to identify the effects of field-size on the EPIgray reconstructed doses and consequently the $\%DD_{DRP}$. The effect of field size on the $\%DD_{DRP}$ was investigated using a range of field sizes typically used for the treatment of 3DCRT breast patients.

5.3.1 Methods

In order to investigate the effects of the factors mentioned above on the $\%DD_{DRP}$, a reference plan was generated for a phantom with simple geometry. A stack of 30x30x15 cm^3 solid water was used for these measurements. Solid water was chosen as the phantom for this investigation because it is relatively water equivalent and therefore has similar scattering properties to that of a patient. Additionally solid water is convenient for measurements because it can be easily handled. The parameters of the reference plan for the stack of solid water are shown in table 5.1.

The reference plan shown in table 5.1 was altered with different treatment parameters that have the potential to cause deviations in the EPIgray reconstructed doses. Table 5.2 shows different versions of the reference plan that were generated by changing a single treatment parameter at a time to investigate their effects on the EPIgray reconstructed doses. The changes implemented on each treatment parameter of the reference plan were based on the typical ranges seen in 3DCRT breast treatments.

TABLE 5.1: Reference plan for treatment of solid water

Treatment Plan Parameters	Set Value
Gantry angle	0°
Source-surface distance	90 cm
Dose	100 cGy
Dose rate	440 cGy/min
Field size	10 cm x 10 cm

TABLE 5.2: Altered versions of the reference plan to investigate the effects of these treatment parameters on the EPIgray dose reconstruction

Dose Linearity (Changes to MU only)	Beam 2	Dose = 30 cGy
	Beam 3	Dose = 63 cGy
	Beam 4	Dose = 125 cGy
	Beam 5	Dose = 250 cGy
	Beam 6	Dose = 500 cGy
Dose-rate Linearity (Changes to the dose-rate only)	Beam 7	Dose-rate = 26 MU/min
	Beam 8	Dose-rate = 53 MU/min
	Beam 9	Dose-rate = 107 MU/min
	Beam 10	Dose-rate = 216 MU/min
	Beam 11	Dose-rate = 440 MU/min
Field Size Dependency (Changes to the field size only)	Beam 12	Field size = 9 cm x 5 cm
	Beam 13	Field size = 9 cm x 10 cm
	Beam 14	Field size = 9 cm x 15 cm
	Beam 15	Field size = 9 cm x 20 cm
	Beam 16	Field size = 20 cm x15 cm
SSD Dependency (Changes to SSD only)	Beam 17	SSD = 80 cm
	Beam 18	SSD = 85 cm
	Beam 19	SSD = 90 cm
	Beam 20	SSD = 95 cm
	Beam 21	SSD = 100 cm
	Beam 22	SSD = 105 cm
Gantry Angle Dependency (Changes to gantry angle only)	Beam 23	Gantry Angle = 0°
	Beam 24	Gantry Angle = 30°
	Beam 25	Gantry Angle = 60°
	Beam 26	Gantry Angle = 90°
	Beam 27	Gantry Angle = 120°
	Beam 28	Gantry Angle = 150°
	Beam 29	Gantry Angle = 180°
	Beam 30	Gantry Angle = 210°
	Beam 31	Gantry Angle = 240°
	Beam 32	Gantry Angle = 270°
	Beam 33	Gantry Angle = 300°
	Beam 34	Gantry Angle = 330°

5.3.2 Results

Dose To EPID Dependency

The results of the dose linearity investigation are shown in table 5.3. Figure 5.1 shows the relationship between $\%DD_{DRP}$ and the TPS planned dose. The relationship between $\%DD_{DRP}$ and the dose delivered was shown to be non-linear. It was found that with an initial increase in TPS dose, the $\%DD_{DRP}$ increased rapidly. With further increase of the TPS dose, the $\%DD_{DRP}$ increased however, the increase in $\%DD_{DRP}$ was less pronounced. As no other factors were changed other than the dose delivered to the EPID, the results of this section have suggested that the deviation in the $\%DD_{DRP}$ was caused by a change in the EPID response to dose. This result was consistent with other publications [65].

TABLE 5.3: Results of dose linearity investigation

TPS Dose (cGy)	Reconstructed Dose (cGy)	$\%DD_{DRP}$
30.00	30.13	0.44
60.00	60.42	0.70
120.00	121.19	1.00
250.00	254.64	1.86
500.00	511.64	2.33

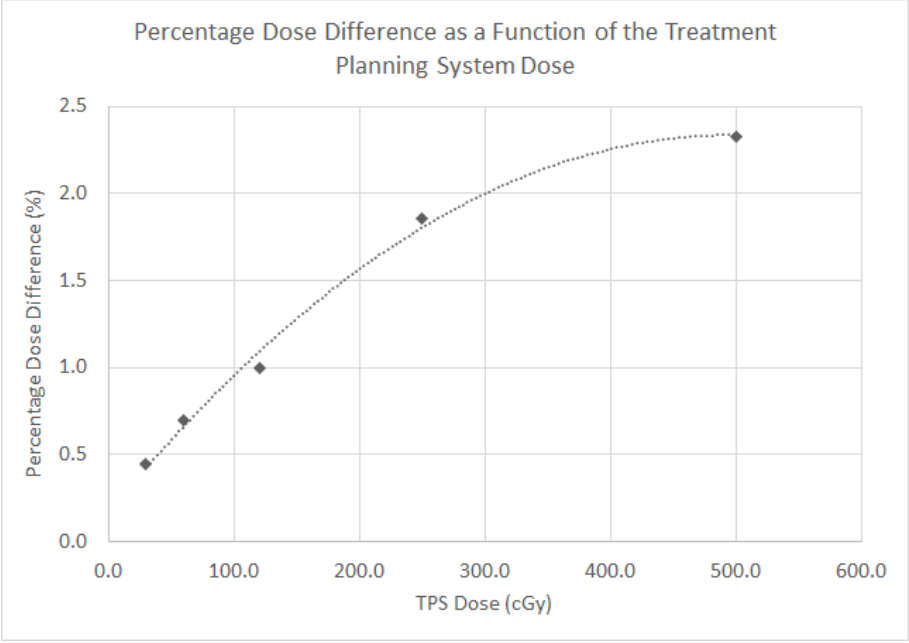

FIGURE 5.1: $\%DD_{DRP}$ as a function of TPS planned dose

Dose-Rate Dependency

The relationship between the $\%DD_{DRP}$ and dose rate was investigated by using clinical dose rates to determine the extent to which the accuracy of EPIgray dose reconstruction was affected by the dose rate. The results in Figure 5.2 show the measurements normalised to the dose rate of the reference plan. In considering the dependence of $\%DD_{DRP}$ on the dose rate, it was found that the accuracy of EPIgray reconstructed doses decreased with decreasing dose rates. The increasing $\%DD_{DRP}$ with decreasing dose rates could be explained by increasing noise over a longer image acquisition period.

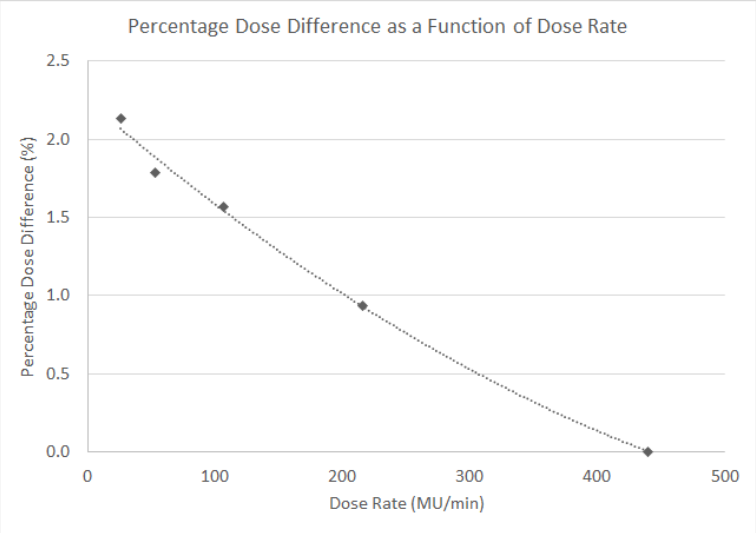

FIGURE 5.2: $\%DD_{DRP}$ from TPS as a function of the dose rate

Gantry Angle Dependency

The $\%DD_{DRP}$ for gantry angles ranging between 0° and 360° with 30° increments were measured and calculated using EPIgray. The resulting $\%DD_{DRP}$ for these gantry angles were normalised to the dose at 0° and are shown in Figure 5.3.

The gantry angle used for treatment would vary from patient to patient depending on patient anatomy. The gantry of the linac weighs several tonnes and cannot be equally balanced. Consequently the gantry is susceptible to different magnitudes of sag at different gantry angles under the influence of gravity. The gantry sag would lead to the relative offset in EPID position from the expected position. This would lead to the calculation of an inaccurate $\%DD_{DRP}$. Figure 5.3

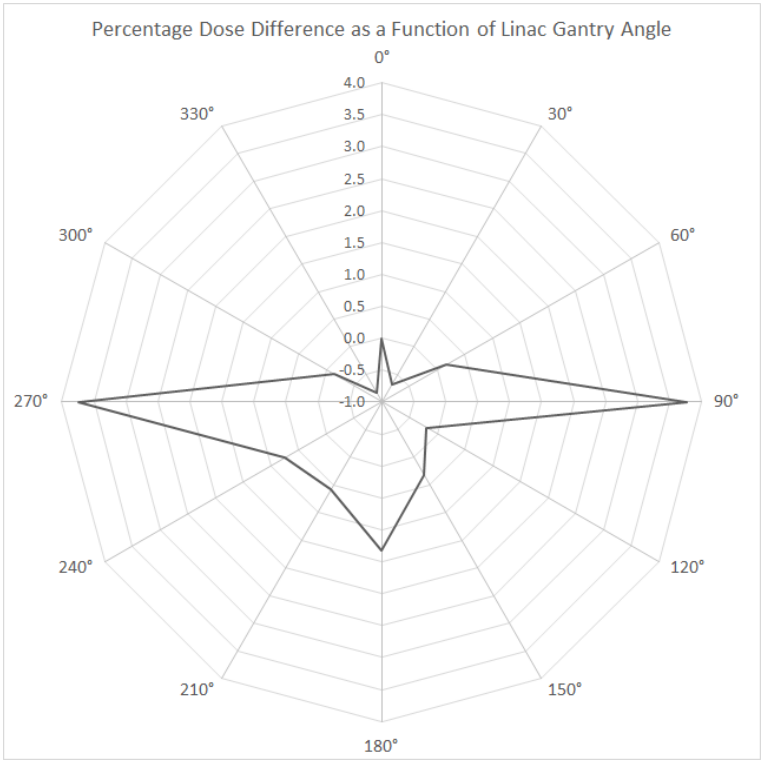

FIGURE 5.3: Effect of gantry angles on the %DD_{DRP} from TPS

shows that the %DD_{DRP} is dependent on the gantry angle. The inaccuracy of EPIgray reconstructed doses noticeably increases at gantry 90° and 270°. For majority of the gantry angles however, the %DD_{DRP} remains within 1.5%.

SSD Dependency

SSD dependency was intended to check how EPIgray dose reconstruction would deal with changes in patient thickness. Figure 5.4 shows the result of varying SSDs on the %DD_{DRP} from the TPS. The SSDs do not significantly vary for 3DCRT breast patients, however the extreme upper and lower limits were investigated.

The %DD_{DRP} of different SSDs shown in Figure 5.4 have been normalised to the dose at the 90 cm SSD of the reference plan. Figure 5.4 does not reveal an obvious trend between the SSD and EPIgray accuracy. However, it is found that at extended SSDs, the EPIgray accuracy decreases noticeably.

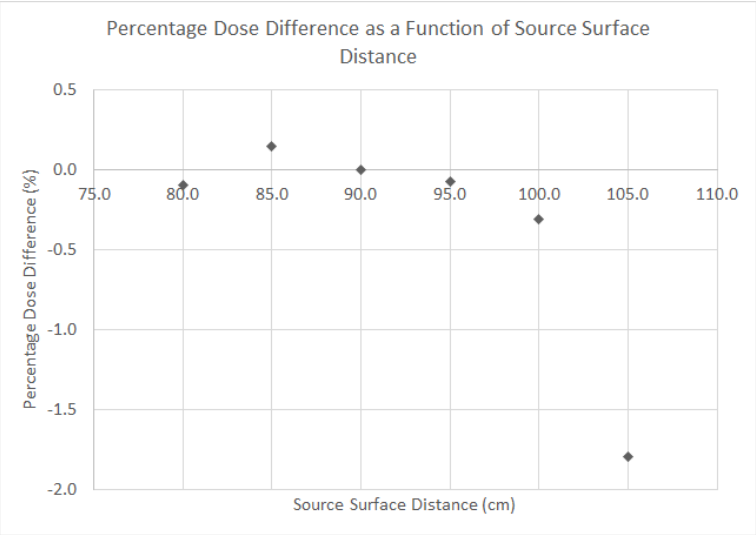

FIGURE 5.4: Effect of SSD on the %DD from TPS

Field Size Dependency

The effect of field size on the $\%DD_{DRP}$ from the TPS was investigated using field sizes that are commonly seen in 3DCRT breast treatments. The results of this investigation are shown in Figure 5.5.

The field size will affect the dose delivered to the point of interest. Delivering 100 MU and changing the field size will result in delivering a different dose. Consequently in order to draw comparisons between rectangular fields of different sizes, the concept of equivalent square field (EQS) was employed. The EQS of a rectangular field will exhibit similar scattering properties. Therefore to enable efficient analysis, the EQS was found for all field sizes considered in this investigation. The EQS was found using equation 5.7. The resulting $\%DD_{DRP}$ for each field size were normalised to the $\%DD_{DRP}$ of the reference 10 cm x 10 cm field.

$$EQS = \frac{2ab}{a+b} \tag{5.7}$$

Where, a and b are the length and width of the rectangle. The x-axis of Figure 5.5 has been labelled as EQS rather than the field sizes shown in table 5.2.

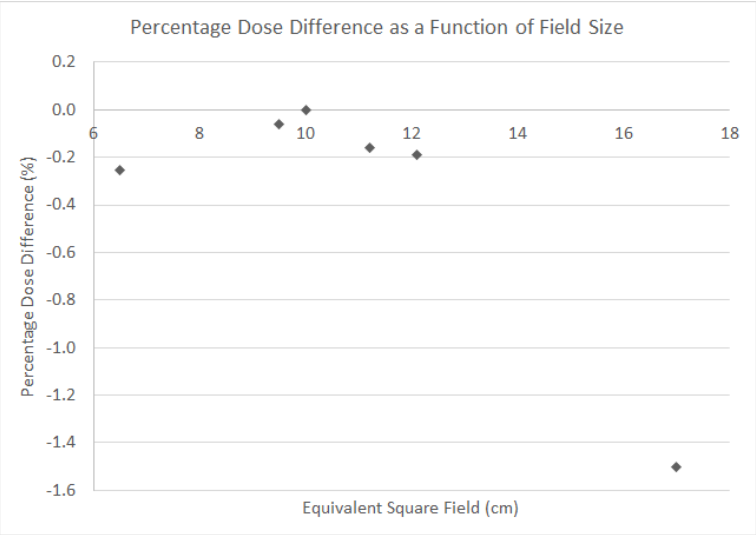

FIGURE 5.5: Effect of field size on the $\%DD_{DRP}$ from TPS

Figure 5.5 shows that the accuracy of EPIgray is affected by the field size. The absolute magnitude of $\%DD_{DRP}$ increases with deviations from the reference EQS of 10 cm. Over the typical field sizes of 3DCRT breast treatments, the $\%DD_{DRP}$ is within $\pm 1.0\%$.

5.3.3 Discussion

The results of the dose linearity investigation showed that the $\%DD_{DRP}$ increased with increasing dose. There was a non-linearity associated with $\%DD_{DRP}$ with increasing dose. At Christchurch Hospital, 3DCRT breast treatment fields are planned to deliver between 4 cGy to 350 cGy [66]. The $\%DD_{DRP}$ over this dose range was found to vary between 0.2% to 2.1%. Ideally, the $\%DD_{DRP}$ should not be dependent on dose however the results from this investigation have suggested otherwise. Consequently, the clinical tolerance should account for this dependency. The results of this section are consistent with literature. It is reported that up to 10% non-linearity can be expected with varying dose when using an aSi EPID for dosimetry [65]. EPIgray at Christchurch Hospital has been commissioned with correction factors from DOSIsoft to account for the non-linear response of the EPID to dose. While the corrections have reduced the uncertainty associated with the EPID response to dose, the clinical tolerance of $\%DD_{DRP}$ must account for the remaining inaccuracy. Based on the results of this investigation, an error contribution of $\pm 2.0\%$ is recommended to account for variations in the EPID response with dose.

Investigation of the $\%DD_{DRP}$ dependency on the dose rate has revealed that the $\%DD_{DRP}$ and dose rate do not have a linear relationship. Ideally, $\%DD_{DRP}$ should not depend on the dose rate however it was found that with decreasing dose rate, the $\%DD_{DRP}$ increased. With decreasing dose rate, the radiation delivery time increases. Therefore the decrease in EPIgray accuracy associated with decreasing dose rate can be explained by an increase in the electrical noise captured on the EPID image over a longer dose delivery period. Currently EPIgray does not contain corrections for the effects of dose rate. However, the EPID dosimetric calibrations and the linac modelling within EPIgray have been performed at the maximum dose rate and all 3DCRT breast treatments at Christchurch Hospital are delivered with the maximum dose rate and therefore significant corrections for the effect of dose rate are not necessary. However, during treatment delivery the dose rate displayed on the console is subject to minor variations, therefore an error contribution of $\pm 0.1\%$ is recommended to account for these variations.

The variations seen in the $\%DD_{DRP}$ with gantry angles were expected. The greatest $\%DD_{DRP}$ from the TPS was seen at gantry 90° and 270°. This result was expected as the magnitude of gantry and EPID sag were expected to be the greatest at these angles as a result of gravitational forces. Changes in the distance between the EPID and the radiation source within the gantry leads to different central pixels, which are perceived as an offset. Therefore the $\%DD_{DRP}$ was expected to differ between gantry angles. Additionally the variations seen in the $\%DD_{DRP}$ across different gantry angles may also be a result of beam obliquity. The TPS and EPIgray do not employ the same dose calculation algorithms. Consequently, these dose calculation algorithms may handle beam obliquity differently resulting in varying magnitudes of uncertainties associated with the reconstructed dose depending on gantry angle. The clinical tolerance for 3DCRT breast treatments will also need to account for the error associated with varying gantry angles. The nature of 3DCRT treatments means that treatment fields should never be delivered from the cardinal angles to avoid unnecessary dose to the OAR. Breast treatments are planned using tangential fields that are specifically angled to provide dose to the breast and avoid dosage to the underlying lungs and therefore the inaccuracies associated with the EPIgray reconstructed doses at the cardinal angles will not be considered for the gantry angle error contribution. An error contribution of $\pm 1.5\%$ is recommended following consideration of the clinically relevant treatment angles for 3DCRT breast treatments.

Investigation of the SSD influence on EPIgray accuracy has revealed that $\%DD_{DRP}$ was dependent on the SSD to a small extent. The SSDs of the patients in the retrospective study ranged between 85 cm to 97 cm. Over this range, the results have revealed $\%DD_{DRP}$ to vary within $\pm 0.2\%$. This error contribution encompasses majority of 3DCRT breast patients. SSDs greater than 100 cm, classified as extended SSDs are not likely, however these SSDs were incorporated into this investigation to gain understanding of the overall trend. It was found that with extended SSDs, there was a noticeable increase in the absolute magnitude of $\%DD_{DRP}$. However, the SSD error contribution to EPIgray accuracy at extended SSDs is not clinically relevant for breast patients. An error contribution of $\pm 0.2\%$ is recommended following consideration of the clinically relevant SSDs for 3DCRT breast treatments.

Results have revealed that $\%DD_{DRP}$ was also dependent on field size as expected. With deviations from the reference 10 cm x 10 cm field size, the absolute magnitude of $\%DD_{DRP}$ increases. The EQS range of the patients of the retrospective study was between 7.7 cm and 15.5 cm. Over this EQS range, the $\%DD_{DRP}$ varies by approximately 1.0%. In considering this range, a field size error contribution of ± 1.0 % is recommended.

5.4 Treatment Setup Errors

Minor setup errors associated with EPID and patient positioning on treatment are unavoidable. This section will address the consequences and contribution of these random and systematic errors on the $\%DD_{DRP}$.

EPID Positioning

The EPID on treatment is only extended into the image acquisition position when an EPID image is required. The Elekta iViewGT EPID used in this study for acquisition of EPID images has an isocentric position when deployed. The EPID will extend until the isocentric position is reached and the movement of the EPID pauses for approximately 1 second to allow the radiation therapist to identify the isocentric position. The radiation therapists may then shift the panel to a different position if required. Potentiometers are used to identify the lateral and longitudinal positions of the isocentre. The voltage of the potentiometers are compared with

a known voltage that is set at calibration to identify the isocentre position [25]. The iViewGT EPID on the Elekta linac does not have a system to indicate the EPID's exact position in space. The isocentric position voltage may drift and therefore, when the EPID is extended it may be at a slightly different position from its previous extended position even if it is assumed to be at the isocentric position. The retrospective study has indicated that EPID position has a significant effect on the $\%DD_{DRP}$. Therefore the reproducibility of the panel position was investigated.

Acceptable Setup Errors

It is unlikely a radiotherapy treatment will be delivered exactly as intended due to random and systematic errors associated with the treatment setup. The setup factors specific to 3DCRT breast treatments that need to be considered are the gantry angle, SSD, field size, the patient setup according to treatment couch positions and patient positioning e.g. rotations of the body oriented towards the linac. 3DCRT treatments are planned to account for minor variations in these factors and therefore there are acceptable tolerances for each of these factors on treatment. The tolerances placed on these setup parameters at Christchurch Hospital are shown in table 5.4 [67].

TABLE 5.4: Acceptable setup tolerances for 3DCRT breast treatments

Parameter	Tolerance Level
SSD	±1.0 cm
Gantry Angle	± 2.0°
Patient Setup	± 0.5 cm
Field Size	± 0.1 cm

The variable range associated with the acceptable setup errors will affect the magnitude of $\%DD_{DRP}$ and therefore the error contributions from these setup parameters were investigated.

5.4.1 Method

EPID Positioning Reproducibility Tests

In order to investigate the effect of minor variations in EPID position on the $\%DD_{DRP}$, the solid water phantom and the reference plan shown in table 5.1 were employed. The solid water was

setup at the expected treatment position. Without any additional changes to the setup, five EPID images were acquired using the reference plan. The resulting EPID images were used to acquire the reconstructed doses to the DRP and the corresponding $\%DD_{DRP}$. No changes were implemented between each consecutive image acquisition. The average of these measurements were used as the control for the analysis of the panel position reproducibility test.

Following acquisition of the control EPID images, the reference plan was delivered five more times to acquire five additional EPID images. However for this set of measurements, the EPID was folded away and back into acquisition position between each image acquisition. The resulting averages of these two sets of EPID images provided the uncertainty associated with the EPIgray reconstructed doses as a result of EPID positioning.

Contributions from Variations in Acceptable Setup Errors

Based on the acceptable tolerances on setup parameters shown in table 5.4, both the breast-lung phantom and the solid water phantom were used to simulate the worst-case acceptable treatment conditions to quantify the effects these factors have on the $\%DD_{DRP}$.

5.4.2 Results

EPID Positioning Reproducibility Tests

The EPIgray reconstructed doses and the corresponding $\%DD_{DRP}$ of the control measurements are shown in table 5.5.

TABLE 5.5: Control measurements: Reconstructed doses and corresponding $\%DD_{DRP}$ of the reference plan

Measurement	TPS Dose (cGy)	Reconstructed Dose (cGy)	$\%DD_{DRP}$ (%)
1	98.00	98.75	0.77
2	98.00	98.77	0.79
3	98.00	98.75	0.77
4	98.00	98.76	0.78
5	98.00	98.80	0.82
Average	98.00	98.77 ± 0.05	0.78 ± 0.05

Table 5.6 shows the resulting reconstructed doses and the corresponding $\%DD_{DRP}$ of five EPID images acquired during the EPID position reproducibility test in which the EPID was folded away and back into acquisition position between each image acquisition. Comparisons of the results in table 5.5 and table 5.6 reveal a difference between the average of controlled measurements and the average of the EPID positioning reproducibility test measurements. The average $\%DD_{DRP}$ increased with EPID movement between consecutive image acquisitions. Additionally, the associated standard deviations with these measurements also increased in the EPID positional reproducibility test. A t-test assuming equal variance with a significance level of 5% was consequently conducted with the null hypothesis that there were no statistical differences between the two sets of measurements. The obtained p-value was 0.03. The p-value indicates that there were statistical differences between the $\%DD_{DRP}$ acquired with no EPID movement between image acquisitions and the $\%DD_{DRP}$ acquired with EPID movement between each image acquisition.

TABLE 5.6: Results of panel position reproducibility tests

Measurement	TPS Dose (cGy)	Reconstructed Dose (cGy)	$\%DD_{DRP}$
1	98.00	99.07	1.09
2	98.00	99.08	1.10
3	98.00	98.85	0.87
4	98.00	98.84	0.86
5	98.00	98.79	0.81
Average	98.00	98.93 ± 0.05	0.94 ± 0.05

Acceptable Setup Errors On Treatment

Following simulation of acceptable setup errors on the breast-lung phantom and the solid water phantom, it was found that the contributions from these setup errors were comparable between both phantoms. The variations in the $\%DD_{DRP}$ as a consequence of variations in the acceptable setup errors are shown in table 5.7.

TABLE 5.7: Error contribution from acceptable setup errors of 3DCRT Breast Treatments

Parameter	Error Contribution
SSD	±0.1%
Gantry Angle	±0.2%
Patient Setup	±1.0%
Field Size	±0.1%

5.4.3 Discussion

The results of the panel position reproducibility test and subsequent comparison to the control results have revealed that there were statistical differences between the $\%DD_{DRP}$ acquired with and without EPID movement between consecutive image acquisitions. The $\%DD_{DRP}$ and the associated uncertainty was found to be smaller in magnitude with no EPID movement between each image acquisition. This result was expected and the results of this section have revealed that the minor positional variations of the EPID in space does have a quantifiable impact on the EPIgray provided $\%DD_{DRP}$. The consequences of panel movement between image acquisitions were small positional changes of the EPID. Consequently the EPIgray reconstructed doses were susceptible to slight variations with changes to the reconstruction environment and these variations were reflected in the provided $\%DD_{DRP}$. The $\%DD_{DRP}$ suggested by EPIgray following EPID movement on average was 0.16% higher than the average $\%DD_{DRP}$ with no EPID movement. Based on these findings an error contribution of ±0.2% is recommended for panel positioning reproducibility.

The results of this section have shown that the acceptable setup errors on treatment would affect the accuracy of the EPIgray reconstructed dose. The error contributions of these factors with the exception of patient setup were relatively small as expected. However, these error contributions will need to be considered when determining the uncertainty associated with the EPIgray reconstructed dose of breast treatments. The largest source of error was associated with patient positioning. This result was expected because small random errors associated with positioning are always present. The error contribution for patient setup was obtained from the results of the phantom study found in subsection 4.3.1. Therefore these measurements were not repeated in this section of the study. It must be noted that the setup errors investigated consider

the dose to the DRP only and not to the entire target volume. Consequently, there may be areas that are more significantly impacted as a consequence of these setup errors. Therefore there are possibilities for these error contributions to be greater than the given magnitudes.

5.5 Inherent EPIgray Uncertainties

Inherent uncertainties associated with EPIgray is a consequence of two major factors. These factors are errors associated with the linac modelling within EPIgray and EPID calibrations.

Linac Modelling Within EPIgray

Beam modelling of the linac within EPIgray was implemented by acquiring EPID images under specific conditions comparable to the test performed in section 5.3 to examine the effect of field size on the $\%DD_{DRP}$. The resulting EPID images were sent to DOSIsoft, and the beam model library was consequently built from user data. DOSIsoft beam modelling produced deviations within $\pm 1.0\%$ for phantom thicknesses ranging between 10 cm and 30 cm and for EQS ranging from 5 cm to 20 cm. While the DOSIsoft provided $\%DD_{DRP}$ exhibited a smaller influence of field size on the $\%DD_{DRP}$, these results were based on the identical images that were used for beam modelling. Therefore it was expected for these deviations to be noticeably smaller than the measured results. During commissioning, DOSIsoft recommended that the deviation between the delivered and the reconstructed dose be within $\pm 2\%$. The EPIgray-related errors established to be within $\pm 2\%$ by DOSIsoft also accounts for the EPID calibration deviations.

EPID Calibration

The EPIgray-related uncertainties are routinely checked as part of QA to ensure the magnitude of error remains within $\pm 2.0\%$ under calibration conditions. A calibration factor is used to convert the pixels of the transmission image registered on the EPID to dose. EPID calibrations are performed when maintenance work results in changes in the EPID response or when the $\%DD_{DRP}$ exceeds the EPIgray tolerance. If the $\%DD_{DRP}$ exceeds $\pm 2\%$ without evidence of setup errors, a drift in the EPID calibration is indicated and consequently an EPID calibration is performed.

EPID calibration involves the measurement of the output of the machine and acquisition of an EPID image. The EPID image is subsequently imported into EPIgray and the pixel values of the EPID image are related to the dose delivered to provide a calibration factor. The output measurement of the linac and consequently the dose delivered to the EPID for calibration is acquired using an IC. The primary source of uncertainty resulting from the EPID calibration comes from using the IC for the output measurement. There are a number of factors that influence the uncertainty of an output measurement made using an IC. The main sources of error for measurements acquired using an IC include the IC calibration error, the detector placement error, the linac output variations on the day of measurements and the statistical type A error associated with the measurements acquired.

IAEA TRS-398 has identified the combined standard uncertainty associated with dose to water to be within $\pm 1.5\%$ [63]. The use of IC to measure the dose to a point of interest also requires a range of correction factors outlined in IAEA TRS-398. These corrections factors are outside the scope of this project however, do provide a small contribution of $\pm 0.1\%$ to the total uncertainty [63].

Measurement of the dosimetric output of the linac is subject to variations due to a range of reasons including variations in pressure and temperature on the day of the measurement. A clinical tolerance of $\pm 0.5\%$ is routinely used to account for these variations [68].

The active region of the IC in comparison to the field size is sufficiently small such that a relatively large offset in the x or y directions would not significantly affect the dose measured. However, the changes in the dose with shifts in the z direction (movement of the chamber towards or away from the source) will need to be accounted for using the inverse square law (ISL). Positional shifts in the z direction are highly unlikely however, for a positional shift of 1 mm, the error in the dose calculated is 0.2% as shown in equation 5.8.

$$ISL = \frac{d_2^2}{d_2^2} = \frac{1.001^2}{1.000^2} = 1.002 \tag{5.8}$$

Following an audit of the output measurements of the linacs, type A measurement uncertainty associated with repeated measurements were found to be ±0.2% for a routinely used and calibrated IC. A summary of the EPID calibration related error contributions is shown in table 5.8.

TABLE 5.8: Estimated magnitude of errors related to EPID calibration

Component	Estimated Error Contribution
IC Calibration Error	±1.5%
Output Dosimetric Error	±0.5%
ISL	±0.2%
Type A Measurement Error	±0.2%

The recommended DOSIsoft EPIgray tolerance of ±2.0% accounts for inaccuracies resulting from linac-modelling within EPIgray and EPID calibrations. These factors will contribute to EPIgray reconstructed doses and therefore will need to be incorporated in the final calculation to determine the uncertainty associated with EPIgray reconstructed doses of 3DCRT breast treatments.

5.6 Operator Related Uncertainties

Following the acquisition of the EPID images on treatment, EPIgray automatically performs a dose calculation to provide a $\%DD_{DRP}$ for each field that was delivered to the patient. If this $\%DD_{DRP}$ for any field within the fraction exceeds the ±5.0% tolerance, positional correction is performed within EPIgray to ensure that the $\%DD_{DRP}$ provided is representative of the treatment delivered to the patient. Consequently, the positional corrected $\%DD_{DRP}$ provided by EPIgray is dependent on the alignment between the TPS contours and patient contours evident on the EPID images. Frequently, perfect match between the contours is unattainable and operator judgement is required for the most appropriate match. Therefore operator matching judgement to a certain degree plays an important role in the reconstructed dose. In order to quantify the effect of differential matching, seven physicists with variable experience with EPIgray were asked to perform EPIgray corrections on three patients. Three patients were selected based on the breast size seen on the EPID images as well as the laterality of their treatment to investigate how these variables affect the inter-person matching. The patient numbers

and the corresponding breast size and laterality are shown in table 5.9. The EPIgray correctional analysis instructions given to the seven participants can be found in appendix A.

TABLE 5.9: Laterality and breast size of patients used for inter-person matching variations on EPIgray

Patient Number	Laterality	Breast Size
1	Left	Small
2	Right	Small
3	Left	Large

5.6.1 Methods

Seven participants were asked to perform contour matching positional correction on EPIgray for the three patients shown in table 5.9. Participants were asked to note the shifts in x and y directions to attain the best possible alignment based on their judgement and the resulting $\%DD_{DRP}$. The patients shown in table 5.9 were selected to draw conclusions regarding matching for both breast lateralities and sizes. Comparisons of the correction results between patients 1 and 2 would reveal how the laterality of the treatment site would affect the matching results, given that the size of breast are comparable and comparisons of the correction results between patients 1 and 3 would reveal how breast size of the patient would affect the matching results given that lateralities are the same for these patients.

5.6.2 Results

Differences in the positional shifts required between different breast groups

The results of positional correction conducted by each participant was analysed individually. For each participant, a total of four paired t-tests were performed:

1. The magnitude of shifts required in the x-direction for all fields of patient 1 and patient 2 to determine differences in matching dependent on breast laterality.

2. The magnitude of shifts required in the x-direction for all fields of patient 1 and patient 3 to determine differences in matching dependent on breast size.

3. The magnitude of shifts required in the y-direction for all fields of patient 1 and patient 2 to determine differences in matching dependent on breast laterality.

4. The magnitude of shifts required in the y-direction for all fields of patient 1 and patient 3 to determine differences in matching dependent on breast size.

The paired t-test used a significance level of 5% and assumed that the two data sets were not significantly different and hypothesised a mean difference of 0. The obtained mean p-values for these paired t-tests are shown in table 5.10.

TABLE 5.10: P-values of paired t-test conducted on the magnitude of shifts required as determined by each matcher

Operator	x-direction		y-direction	
	Left vs. Right	Small vs. Large	Left vs. Right	Small vs. Large
1	0.45	0.69	0.92	0.12
2	0.57	0.79	0.37	0.16
3	0.55	0.73	0.55	0.2
4	0.08	0.39	0.75	0.07
5	0.33	0.06	0.51	0.06
6	0.62	0.67	0.7	0.37
7	0.24	0.64	0.5	0.15

Results of table 5.10 reveals that participants did not exhibit any bias in matching for both breast groups. All p-values in table 5.10 are larger than 0.05 and therefore the null hypothesis cannot be rejected as the resulting differences between the breast groups have a greater than 5.0% probability of occurring by chance.

Additionally, correlation analysis was conducted between the shifts required in the x and y directions between participants. The correlation coefficient measures the strength and direction of relationship between variables. Correlation analysis was performed for shifts in the x and y direction separately. The variables of the correlation analysis in this setting were the shifts required in each direction as determined by the seven participants. For both directional shifts, the correlation analysis has revealed a moderate to strong relationship as indicated by the correlation coefficient. Where, a moderate relationship is indicated by a correlation coefficient

between -0.3 and -0.7 or 0.3 and 0.7 and a strong relationship is indicated by a correlation coefficient between -0.7 and -1.0 or 0.7 and 1.0 [69]. This result indicates that there are no significant variations in the shifts required as determined by different operators. The average correlation coefficients obtained for each breast laterality and size revealed that right breast fields and large breast fields had higher agreement between the shifts required in x and y directions than left breast and small breast fields.

The resulting variation in the $\%DD_{DRP}$ as a consequence of differences in positional correction between participants was also considered. Figures 5.6a and 5.6b show the variation in the EPIgray $\%DD_{DRP}$ from TPS following positional correction of left and right breast fields.

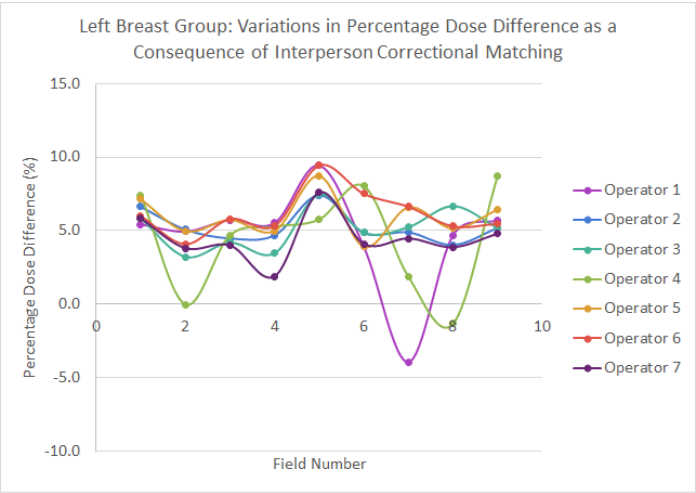

(a)

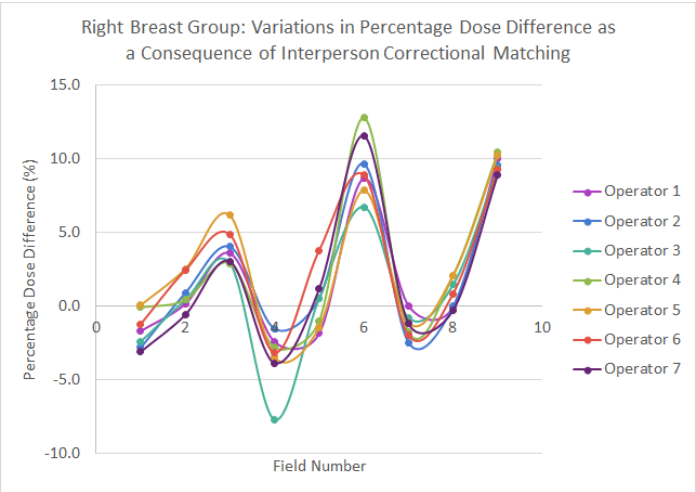

(b)

FIGURE 5.6: EPIgray $\%DD_{DRP}$ following correctional analysis on EPIgray for (a) left and (b) right breast fields.

From Figures 5.6a and 5.6b it is visually evident that there is better agreement between the operators in terms of $\%DD_{DRP}$ for right breast fields than left breast fields. The magnitude of EPIgray $\%DD_{DRP}$ post-positional correction within EPIgray is not of concern in this section, as the interest is primarily considering the grouping of $\%DD_{DRP}$. Correlation analysis revealed moderate to strong relationship in the $\%DD_{DRP}$ across all participants for left breast fields and strong relationship in the $\%DD_{DRP}$ across all participants for right breast fields. In considering the average correlation coefficient of each group, it was found that right breast fields had more agreement in $\%DD_{DRP}$ than left breast fields.

Figures 5.7a and 5.7b show the variations in the EPIgray $\%DD_{DRP}$ from TPS following positional correction on EPIgray of small and large breast fields.

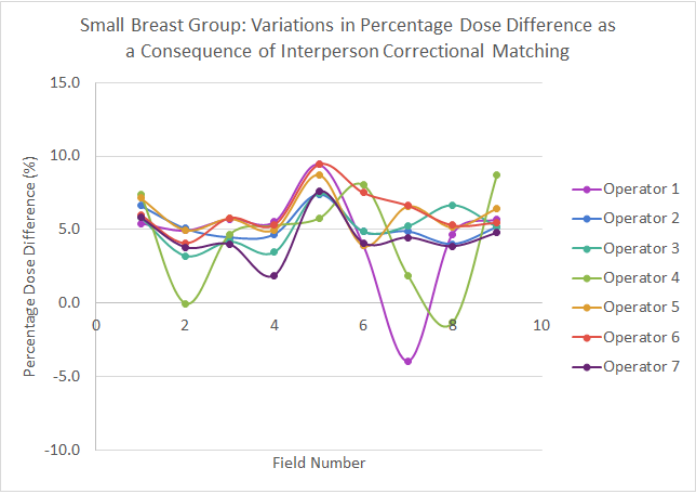

(a)

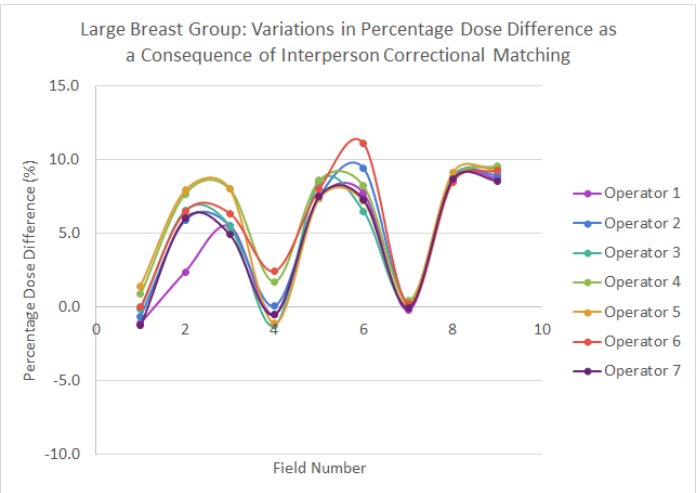

(b)

FIGURE 5.7: EPIgray $\%DD_{DRP}$ following correction analysis on EPIgray for (a) small and (b) large breast fields.

From Figures 5.7a and 5.7b it is visually evident that there is better agreement between the operators in terms of $\%DD_{DRP}$ for large breast fields than small breast fields. While certain large breast fields show similar levels of variations in the $\%DD_{DRP}$ as a consequence of positional correction, the variation was more pronounced with small breast fields than large breast fields. Correlation analysis revealed strong correlation in the $\%DD_{DRP}$ across all participants for both breast size fields. However in considering the average correlation coefficient of each group, it was found that large breast fields had more agreement in $\%DD_{DRP}$ than small breast fields.

5.6.3 Discussion

The volunteers for this investigation were physicists with varying levels of EPIgray experience. Positional correction conducted by these participants has revealed no significant differences in terms of magnitude of shifts required between fields of different breast sizes and lateralities. Participant feedback regarding positional correction on EPIgray has revealed consensus amongst the participants that compromise is required when perfect positional alignment between the EPID image contours and TPS contours is unattainable. Operators were not given specific instructions as to which regions they should compromise when matching. Therefore the compromises the operators chose were entirely at their discretion. Additionally results of this section indicate that there are no major discrepancies associated with the inter-operator matching for breast groups when performing positional correction on EPIgray. This finding provides evidence that the inter-operator matching error is minimal. Participants revealed that compromises were made when performing contour matching with particular consideration given to the position of the DRP. All participants, regardless of their experience with EPIgray compromised mismatch between the TPS and EPID image contours in regions away from the DRP. All participants paid particular attention at the level of the DRP when matching the contours and compromises were made at other lesser important regions. Consequently operators have identified that there was typically poor matching near the arm and axilla regions. These results have indicated that the inter-operator variability associated with positional correction on EPIgray is negligible granted that the matcher has sufficient experience with 3DCRT breast treatment plans in order to determine which matching compromises are clinically appropriate.

In considering the $\%DD_{DRP}$ between fields of different breast lateralities, it was found that left breast fields showed more of variation than right breast fields. This finding could be explained by the increase in the heterogeneities seen in left breast fields. The right breast fields typically have air, lung and breast tissue in the reconstruction environment. For left breast fields in addition to air, lung and breast tissue, the presence of the heart is also seen in some fields. Accuracy of EPIgray dose reconstruction algorithm with increasing density heterogeneities in the field has been previously discussed. Therefore the range of $\%DD_{DRP}$ seen for left breast fields being larger than right breast fields of similar size is partially explained by the EPIgray dose reconstruction algorithm itself. Similarly, in considering the $\%DD_{DRP}$ between fields of different breast sizes it was found that small breast fields showed more of variation than large breast fields. This result was expected as minor shifts in the small breast fields would result in a more drastic change in the environment over which the dose reconstruction is performed.

5.7 Proposed EPIgray Uncertainty Tolerance

Sections 5.3 to 5.6 have presented the major factors causing deviations in the EPIgray reconstructed doses. These errors were combined in quadrature in accordance with the International Bureau of Weights and Measures (BIPM) recommendations to provide the overall uncertainty [70]. The total combined error is presented in table 5.11.

Table 5.11 reveals that the smallest achievable uncertainty associated with the EPIgray reconstructed doses would be $\pm 3.3\%$. The retrospective study has shown that fields exceeding $\pm 5.0\%$ following positional correction may still represent a dosimetrically accurate treatment but are considered a failed result according to EPIgray due to the set tolerance. Fields that are dosimetrically accurate but present as failing results occur as a result of two main reasons:

1. Inaccurate EPID image acquisition, and/or
2. The imposed $\pm 5.0\%$ does not cover the entire range of patients seen in the clinical setting.

TABLE 5.11: Estimated total magnitude of error associated with $\%DD_{DRP}$

Contributing Factor		Estimated Error Contribution
Treatment Plan Parameter	Panel Position	±0.2%
	Dose Delivered	±2.0%
	Dose rate	±0.1%
	Field Size	±1.0%
	Gantry Angle	±1.5%
	SSD	±0.2%
Acceptable Setup Errors	Gantry Angle	±0.2%
	SSD	±0.1%
	Patient Setup Error	±1.0%
	Field Size	±0.1%
Inherent EPIgray Errors	EPID Calibration	±1.5%
	Output Dosimetric Error	±0.5%
	ISL	±0.2%
	Type A Measurement Error	±0.2%
Operator Related Errors		±0.0%
Total Combined Error		±3.3%

Due to these reasons and the results of this study, it is recommended that the ±5.0% tolerance be retained. Increasing this tolerance may result in a larger number of falsely passing fields passing through unnoticed. Decreasing this tolerance is also not appropriate as currently, fields that exceed the current tolerance given no major errors have occurred are still considered dosimetrically accurate treatments.

Nevertheless, the current ±5.0% tolerance results in a significant number of false passes. In order to reduce this number, the introduction of a new intervention tolerance is proposed. Currently the intervention tolerance and the passing tolerance are both ±5.0%. In order to find the most appropriate investigation tolerance a receiver operator characteristic (ROC) curve analysis was performed. ROC analysis is generally used to determine the optimal sensitivity and specificity of a test and to quantify the efficiency of the test [71]–[73]. ROC analysis can therefore be used to find the optimal intervention tolerance for EPIgray in order to more optimally classify passing and failing fields. ROC analysis considers the true positive rate (TPR), given in equation 5.9 and false positive rate (FPR), given in equation 5.10.

$$TPR = \text{Sensitivity} = \frac{\text{Fields correctly classified as passes (TP)}}{\text{Fields correctly classified as passes (TP) + Fields incorrectly classified as fails (FF)}} \tag{5.9}$$

$$FPR = 1 - \text{Specificity} = 1 - \frac{\text{Fields incorrectly classified as passing (FP)}}{\text{Fields incorrectly classified as passing (FP) + Fields correctly classified as fails (TF)}} \tag{5.10}$$

The 255 fields of the retrospective study were used to calculate the TPR and FPR for EPIgray intervention tolerances ranging from ±0.5% to ±5.0% in 0.5% increments. The resulting TPR and FPR are shown in table 5.12. Table 5.12 also presents the Youden's index, which was calculated using equation 5.11.

TABLE 5.12: ROC Analysis of Proposed EPIgray Intervention Tolerances

Intervention Tol.	FPR (%)	TPR (%)	Youden's Index
±0.5%	7.1	8.8	0.0
±1.0%	10.7	19.8	0.1
±1.5%	17.2	31.4	0.1
±2.0%	21.4	41.0	0.2
±2.5%	28.6	53.3	0.2
±3.0%	29.6	60.0	0.3
±3.5%	42.9	79.0	0.4
±4.0%	57.1	81.9	0.2
±4.5%	63.1	87.7	0.3
±5.0%	75.0	91.6	0.2

$$\text{Youden's Index} = \text{Sensitivity} + \text{Specificity} - 1 \tag{5.11}$$

Youden's index provides a method for obtaining the optimal cut off value, in this example it is the optimal EPIgray intervention tolerance. The maximum Youden's index value corresponds

to the optimal EPIgray intervention tolerance [74], [75]. According to table 5.12, this tolerance is ±3.5%. Figure 5.8 graphically shows the data of table 5.12. The dotted line in Figure 5.8 indicates a one-to-one relationship between the FPR and TPR. That is, the true positive rate equals the false positive rate, where the true positive rate indicates that all passing fields are correctly identified however all failing fields are incorrectly considered passing fields. The maximum distance between the ROC curve and the dashed line indicates the most optimal sensitivity and specificity. This distance is found to be the greatest for a tolerance of ±3.5%. This observation is in agreement with the Youden index analysis which also indicated the tolerance of ±3.5% to be the most optimal tolerance for identification of the falsely passing fields.

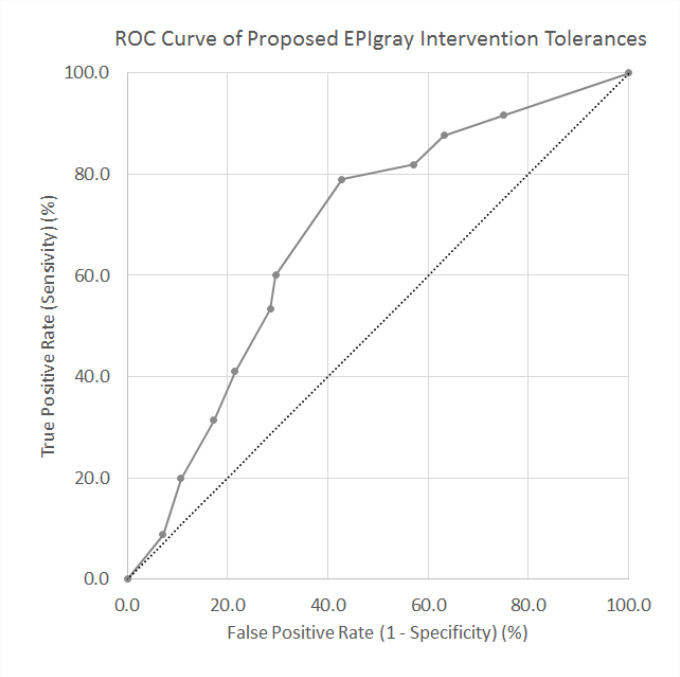

FIGURE 5.8: ROC curve of investigation tolerances

The area under the curve (AUC) was also analysed to assess accuracy of the ROC test. The AUC of the ROC curve was found to be 0.72. Greiner *et al.* have proposed the following categories to assess the accuracy of the AUC [71]:

- AUC = 0.5 indicates a non-informative test,
- $0.5 < \text{AUC} \leq 0.7$ indicates less accurate test,
- $0.7 < \text{AUC} \leq 0.9$ indicates moderately accurate test,
- $0.9 < \text{AUC} \leq 1.0$ indicates highly accurate test,
- AUC = 1.0 perfect test.

An AUC of 0.72 indicates a moderately accurate test, and therefore we can reliably use this tolerance as an intervention tolerance given that there are sufficient clinical resources. The combined error calculation indicated EPIgray to have an uncertainty of at least ±3.3%. The ROC analysis has indicated an optimal intervention tolerance of ±3.5%. These tolerances are sufficiently close to one another however, the ROC indicated tolerance would be considered more reliable as the combined error calculation is predicting the accuracy of EPIgray doses for the best case scenario. Therefore from these results, an intervention tolerance of ±3.5% is proposed. The feasibility of the new intervention tolerance was tested on the 255 fields of the retrospective study. The results of the investigation are shown in table 5.13.

TABLE 5.13: Passing and Failure Rates with Old and New Tolerances

Criteria	Intervention tol. ±5.0% Acceptable tol. ±5.0%	Intervention tol. ±3.5% Acceptable tol. ±5.0%
True Pass	208 (81.6%)	174 (68.2%)
True Fail	7 (2.7%)	16 (6.3%)
False Pass	21 (8.2%)	6 (2.4%)
False Fail	19 (7.5%)	59 (23.1%)

Results of table 5.11 reveal that with the proposed intervention tolerance, the number of truly passing and falsely passing fields decreased and the number of truly failing and falsely failing fields increased. These results are consistent with expectations. With a decrease in the intervention tolerance, the fields that have $\%DD_{DRP}$ between ±3.5% and ±5.0% before positional correction are now considered failing results. This reasoning provides an explanation for the decrease in the number of true passes and an increase in the number of false fails with the implementation of the new tolerances.

Table 5.13 shows the number of true fails to increase and the number of false passes to decrease with the implementation of the new tolerance. The falsely passing fields will have $\%DD_{DRP}$ between ±3.5% and ±5.0% before positional correction and have a $\%DD_{DRP}$ that exceeds ±5.0% following positional correction. One of the primary purposes of this study was to enable EPIgray tolerances to be more sensitive in order to identify falsely passing fields. Therefore the decrease in the intervention tolerance restricts those falsely passing fields with $\%DD_{DRP}$

between ±3.5% and ±5.0% before positional correction from passing. This consequently decreases the number of falsely passing fields and increases the number of truly failing fields. Evidence from this investigation shows that the decrease in the intervention tolerance resulted in increased EPIgray sensitivity for detection of falsely passing results.

In considering the most optimal tolerance for the clinic, the intervention rates of the tolerances should also be considered. With the implementation of the ±3.5% intervention tolerance, the intervention rate (manual investigation of all failing fields) increases to 10.2% and 29.4%. The implementation of the new tolerance results in the reduction of false passes from 8.2% to 2.4%. These results indicate that intervention is required for approximately 30% of the fields however the significant decrease in the number of false passes with the new tolerance justifies its implementation. The new intervention tolerance will enable effective identification of fields that have falsely passed and thereby increase the robustness of the EPIgray IVD system.

5.8 Conclusion

This chapter considered numerous errors contributing to the uncertainty associated with the EPIgray reconstructed doses. These factors included treatment-related parameters that are variable from patient to patient, on-treatment setup errors within an acceptable tolerance, inherent EPIgray errors and lastly operator-related errors associated with correctional matching on EPIgray.

The results of this investigation indicated that the current acceptable tolerance is appropriate as fields beyond the ±5.0% are still accepted as being dosimetrically accurate in certain situations. However this current tolerance has a significant number of falsely passing fields that go unnoticed. With this consideration a proposal of ±3.5% intervention tolerance was made. By employing a smaller intervention tolerance, the number of initially failing fields will increase the intervention rate however, the number of false passes are significantly reduced. The uncertainties investigation considered treatment parameters and setup errors specific to 3DCRT breast patients and therefore this recommendation applies to all 3DCRT breast treatments.

6 Project Conclusions

6.1 Conclusion

The use of EPIgray for IVD has numerous benefits. An EPID-based IVD system such as EPIgray provides confirmation that the treatment was delivered as expected with improved time efficiency than other currently used in-vivo dosimeters as additional setup is not required. There are however limitations in the accuracy of the EPIgray reconstructed doses as a result of the nature of radiotherapy treatments. The use of EPIgray for IVD of 3DCRT breast treatments was investigated in this study taking into consideration the inaccuracies associated with the treatment parameters as well as the innate uncertainties associated with EPIgray itself. In order to reliably use EPIgray, this study was designed to optimise the use of EPIgray for IVD of 3DCRT breast treatments.

This study addressed the aims discussed in Chapter 2 in three parts:

1. The retrospective study,
2. The phantom study,
3. Uncertainties associated with EPIgray reconstructed doses.

In order to achieve the first aim of identifying specific groups of patients at risk of having positional offsets on treatment using EPIgray, previously treated 3DCRT breast patients who have had EPID images acquired on treatment were categorised into groups according to breast size and laterality. These patients were retrospectively analysed within EPIgray as part of a retrospective study presented in Chapter 3. The results of this part of the study revealed that patient setup errors in the anterior-posterior direction and the proximal-distal directions were more common than superior-inferior direction across all breast groups. Positional correction within EPIgray revealed that right breast patients were more at risk of having errors associated

with positional setup when considering treatment laterality and large breast patients were at increased risk of having positional offset on treatment when considering breast size. The retrospective study also examined the effects of positional correction accounting for patient setup errors on the $\%DD_{DRP}$ provided by EPIgray. It was found that EPIgray showed no bias between breast laterality or size in its dose calculation. The retrospective study results provided clinical evidence that there is a linear one-to-one relationship between the TPS dose and the EPIgray reconstructed dose. Evidence in literature revealed that inaccuracies associated with EPIgray results increased in regions with highly varying tissues densities. The position of the DRP varies from patient to patient and consequently the proximity of the DRP (located in breast tissue) to the lower density lung tissue may affect the accuracy of the EPIgray reconstructed dose. The position of the DRP with reference to the distance from lung tissue was investigated to determine its suitability of use. The results of this investigation revealed that the position of the DRP over a range of patients had no significant impact on the accuracy of the EPIgray reconstructed dose. Aim three of Chapter 2 was to identify more optimal points in treatment verification analysis. However results have revealed that the current practice of using DRP dose for treatment verification is not impacted by the varying tissue densities in the reconstruction window. Despite this finding, the results of the retrospective study has found false passes are present across all breast groups. With the recent upgrade of EPIgray, DOSIsoft now recommends the use of $\%DD_{vol}$ in place of $\%DD_{DRP}$. The suitability of $\%DD_{vol}$ was investigated using patient data in retrospective analysis. Results of this investigation revealed a systematic offset between $\%DD_{vol}$ and $\%DD_{DRP}$. This part of the study provided evidence that the use of $\%DD_{DRP}$ in combination with $\%DD_{vol}$ may aid in the reduction of false passes.

The phantom study presented in Chapter 4 employed a breast-lung phantom specifically designed to isolate the setup error on treatment in terms of direction and the effects of these errors on the reconstructed dose were examined. Additionally, while the retrospective study found good agreement between TPS planned dose and EPIgray reconstructed dose, an independent validation that the reconstructed dose is indicative of the delivered dose was required. Therefore the breast-lung phantom was designed to incorporate two other established dosimeters for verification of EPIgray reconstructed dose with positional setup errors. The results of this section of the phantom study has revealed that EPIgray reconstructed doses were consistent with

the doses provided by the IC and film across all positional setup errors. However the EPIgray doses do present a systematic offset and higher uncertainty. Whilst the accuracy of EPIgray is offset from other dosimeters, this offset can be incorporated in the clinical tolerance. The agreement between $\%DD_{DRP}$ and $\%DD_{vol}$ with setup errors was investigated in the phantom. Results indicated that $\%DD_{vol}$ consistently provided a %DD that indicated a larger deviation from the TPS dose than that of $\%DD_{DRP}$. The retrospective study results in conjunction with the phantom study results indicated that a fractional clinical tolerance of $\pm$5.0% placed on the $\%DD_{vol}$ with an standard deviation of less than 0.1 Gy would aid in the reduction of false passes. In situations where the standard deviation is greater than 0.1 Gy or the $\pm$5.0% tolerance on $\%DD_{vol}$ has been exceeded, individual beam analysis should be performed using the DRP method following positional correction. The phantom study achieved aim four of Chapter 2 by verifying EPIgray's ability detect positional setup errors through discrepancies seen between the TPS dose and the delivered dose.

Lastly, uncertainty analysis was conducted to address the major sources of inaccuracy associated with the EPIgray reconstructed doses. Errors associated with variations in treatment plan parameters, setup on treatment, EPIgray uncertainties and operator judgement in positional corrections were considered. The contributing factors were summed in quadrature according to GUM methodology for uncorrelated errors to find a total combined error of $\pm$3.3% [70]. The results of the retrospective study indicated the $\pm$5.0% dosimetric tolerance to be appropriate for 3DCRT breast treatments however false passes were still evident. Consequently a new intervention tolerance was proposed and tested. ROC analysis has revealed $\pm$3.5% to be the optimal intervention tolerance for minimising the number of false passes whilst considering clinical resource availability. Findings of this part of the study indicated that the new intervention tolerance increases the intervention rate. However the new intervention tolerance significantly decreases the number of falsely passing fields. The uncertainty analysis and ROC analysis have indicated tolerances with minor differences. The uncertainty analysis has provided the tolerance of the best case scenario and therefore the ROC analysis provided intervention tolerance is recommended for clinical use. Whilst the second aim of the Chapter 2 of decreasing the $\pm$5.0% tolerance on the $\%DD_{DRP}$ was not directly achieved in that the dosimetric tolerance was not reduced, the purpose for which this aim was proposed for was met.

In conclusion, all the aims set at the commencement of this project were achieved. Right breast and large breast patients were found to be more at risk of having setup errors on treatment. The current intervention tolerance set for the $\%DD_{DRP}$ for 3DCRT breast patients was recommended to be reduced from $\pm 5.0\%$ to $\pm 3.5\%$. Further reduction of this tolerance for small and left breast fields is not recommended as this value was based on ROC and uncertainty analysis. While more optimal points were not investigated following the recognition of the primary relevance of the DRP, alternative dosimetric analysis within EPIgray was investigated using the $\%DD_{vol}$ method recommended by DOSIsoft. A new $\%DD_{vol}$ tolerance of $\pm 5.0\%$ is proposed with a standard deviation tolerance of ± 0.1 Gy. Lastly, a breast-lung phantom was used to verify the ability of EPIgray to detect the discrepancies between the TPS calculated dose and the delivered dose.

6.2 Future Work

The discrepancies in setup error directions between left and right breast fields were not expected and currently remains inconclusive. Potential causes of this discrepancy were discussed in Chapter 3. One of the potential causes discussed included variations in the arm positions of the patient. For future patients, confirmed consistency in arm positions will allow determination of whether this cause might be producing the discrepancies seen in the setup of patients of both lateralities.

Results of this project have also indicated that it would be useful to establish site specific EPIgray tolerances for other treatment sites treated using the 3DCRT technique. This project has revealed that false results are likely across a range of patients as a result of having a wide clinical tolerance of $\pm 5.0\%$ therefore it will be beneficial to perform a similar study for other treatment sites.

This project considered patients who were treated with a 6 MV photon beam. 6 MV photon beam is lowest energy photon beam available at Christchurch Hospital and is the most commonly used energy for 3DCRT breast treatments. Other photon energies available for treatment are 10 MV and 15 MV. However these energies are extremely uncommon. EPID information

from patients treated with higher energies were not available at the commencement of the retrospective study. Therefore the higher energies were not considered in this project. It is commonly known that the quality of an EPID image is diminished with increasing energy of the radiation beam and therefore the effects of radiation energy on the EPIgray reconstructed doses and accuracy would also be an interesting aspect to explore [76].

A EPIgray Correctional Analysis Instructions

A.1 Introduction

EPIgray allows two forms of panel position correction:

1. Panel offset correction figure A.1 – Allows alignment of the field edges from the TPS to the EPID image acquired on treatment.
2. Contour matching correction figure A.2 – Allows the alignment the planning CT breast contour from the TPS to the breast contour evident in the EPID image.

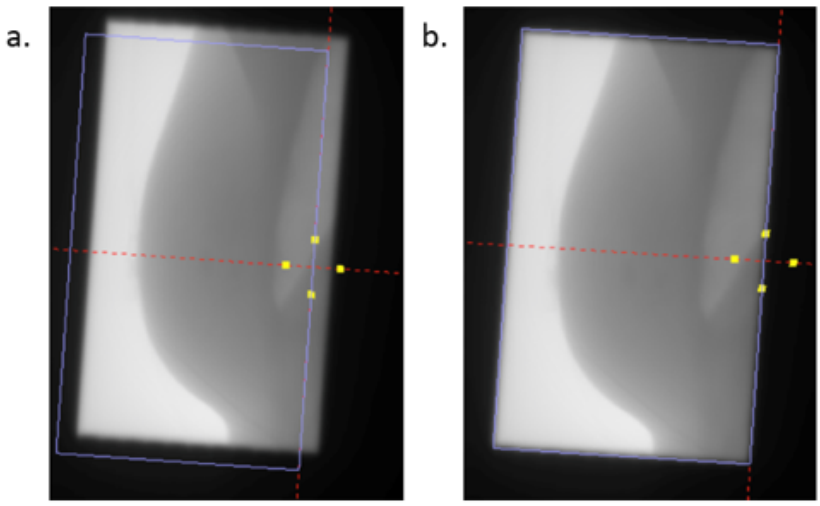

FIGURE A.1: a. Misalignment evident between field edges and EPID image. b. Field edges and EPID image aligned following panel offset correction

A.2 Purpose

Both correctional methods requires judgement of the analyser to find the best alignment. The purpose of this exercise is to determine the inter-person variability in aligning the field edges and planning CT breast contour to the EPID images acquired on treatment.

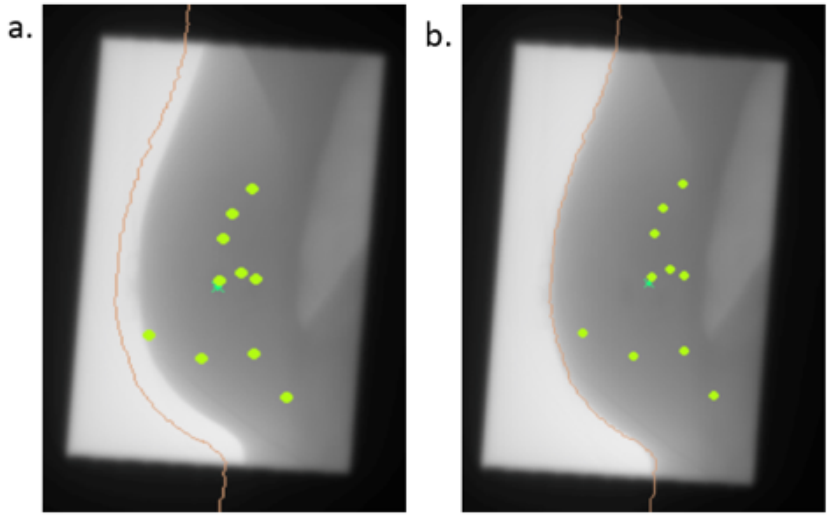

FIGURE A.2: a. Misalignment between planning CT breast contour and breast contour on EPID image. b. Alignment of patient breast contour and EPID image breast contour following contour matching correction.

A.3 Outline

Three existing 3DCRT breast patients (of different breast sizes) in our EPIgray database have been selected for this exercise. Please perform panel offset correction and contour matching correction and record the collimator axis position and the relative deviation before and after correction for all beams and fractions of the selected patients. Please also note in the comments section:

- Any difficulties faced during alignment using both correction methods,
- any reasons for choosing a panel position when perfect alignment was unattainable.
- If the initial panel position corresponds to good alignment in the panel offset correction method and/or the contour matching correction method and therefore no correction of the panel position was necessary.

A.4 Instructions

1. Open EPIgray by double clicking EPIgray Expert on the EPIgray computer desktop.
2. Find and select patient NHI under patient records → Under studies, right click Ballistic and select Start a dosimetric verification study. See figure A.3.
3. Enter user name and password.
4. Select EPIgray (target symbol) on the top left hand side of the EPIgray window.
5. Select the drop down arrow next to Follow-up: Ballistic to view beams grouped together from three fractions.

6. In the summary for each beam figure A.4, check that the initial relative deviation matches the corresponding value in table A.1 and record this value in the provided Excel Spreadsheet. If this value differs please let me know before performing any corrections.
7. Select a particular beam of a given fraction and press the centering symbol to begin matching (figure A.5).
    - The centering button will enable the field edges to be visible.
    - Record the collimator axis x and y positions in the Excel Spreadsheet. (Again check these initial collimator axis positions are identical to the values given in table 1 before proceeding).
    - Press the lock button to unlock the current collimator axis position to allow corrections to be made.
8. Matching could be performed manually by typing in the collimator axis co-ordinates in x and y directions OR by hovering over the crosshairs of the red dotted line and dragging the purple box.
9. First perform panel offset matching (in the top left hand window): matching field edges (purple box) to the EPID image. Note. You can adjust the window and level of the EPID image to aid alignment.
10. Once happy with alignment, press Apply. The collimator lock icon should now be in a closed state. Record the collimator axis x and y positions in the appropriate column only after applying the shift.
11. Select overall beam summary (of all 3 fractions) and record the relative deviation of the beam and the fraction you've just adjusted.
12. Return to the same fraction of the beam you were previously adjusting and perform the matching of the breast contour and the EPID image. Perform steps 10 – 11.
13. Perform these steps 6 – 12 for all beams and fractions for all three patients patients.
14. Once you have finished correction of each fraction of each beam for a given patient. Press the close icon on the top right hand side of the screen.
    - You will be asked if you want to save the changes made.
    - Select quit without saving.

TABLE A.1: Initial panel positions for each fraction of all beams for three patients of interest

Patient		Small Left Breast	Large Right Breast
Beam 1	#1	X: 204.80 Y: 208.03 %DD: 2.65	X: 204.80 Y: 208.01 %DD: 0.59
	#2	X: 204.80 Y: 208.03 %DD:-0.21	X: 204.80 Y: 208.01 %DD:0.05
	#3	X: 204.80 Y: 208.03 %DD: -0.6	X: 204.80 Y: 208.01 %DD: -2.37
Beam 2	#1	X: 204.80 Y: 208.03 %DD: -0.72	X: 204.80 Y: 206.58 %DD: -0.28
	#2	X: 204.80 Y: 208.03 %DD: 2.11	X:204.80 Y:206.58 %DD:-2.66
	#3	X: 204.80 Y: 208.03 %DD: -3.15	X: 204.80 Y: 206.58 %DD: -4.13
Beam 3	#1	X: 204.80 Y:206.56 %DD: 0.79	X: 204.80 Y: 206.58 %DD: 1.22
	#2	X: 204.80 Y: 206.56 %DD: -0.73	X: 204.80 Y: 206.58 %DD: -1.31
	#3	X: 204.80 Y:206.56 %DD: -0.79	X: 204.80 Y: 206.58 %DD: -2.36

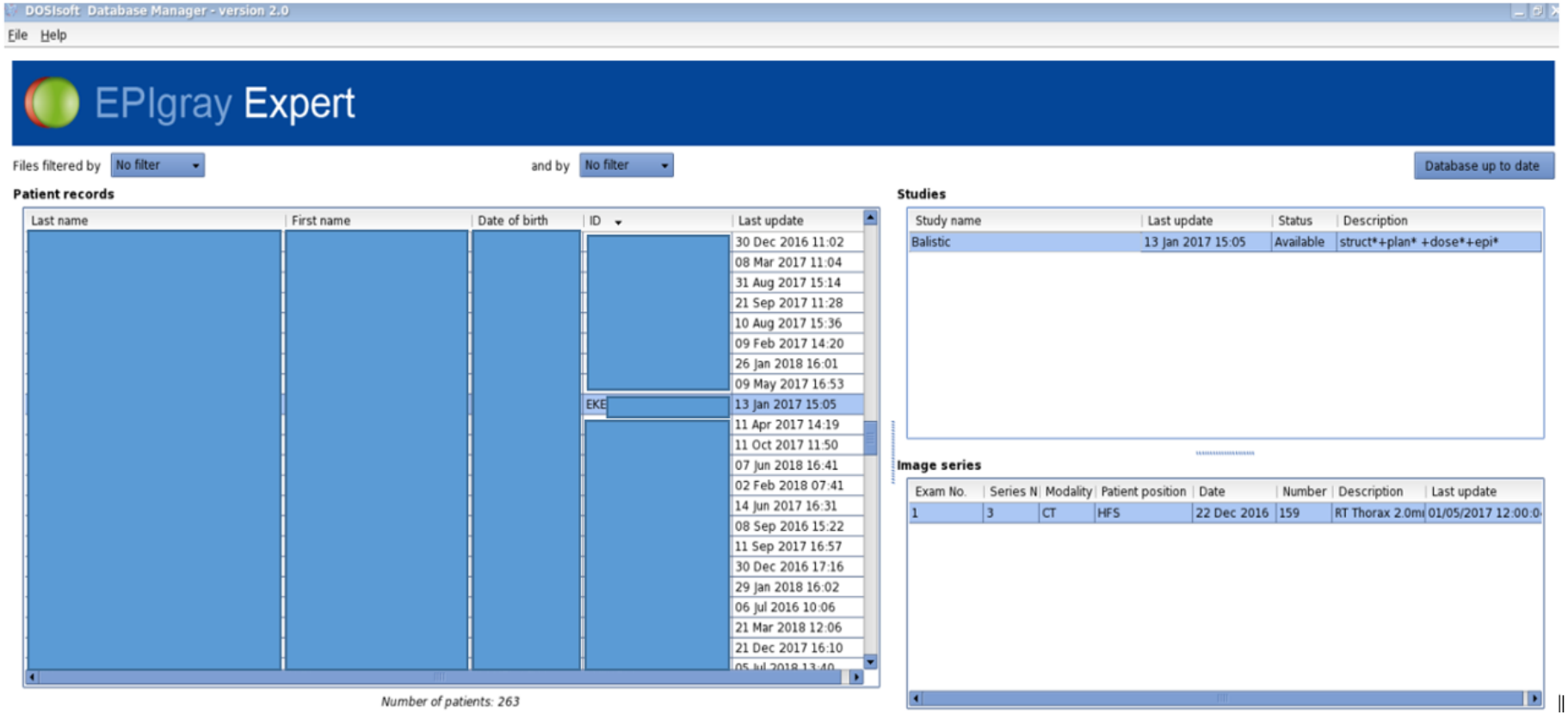

FIGURE A.3: Patient Selection Window

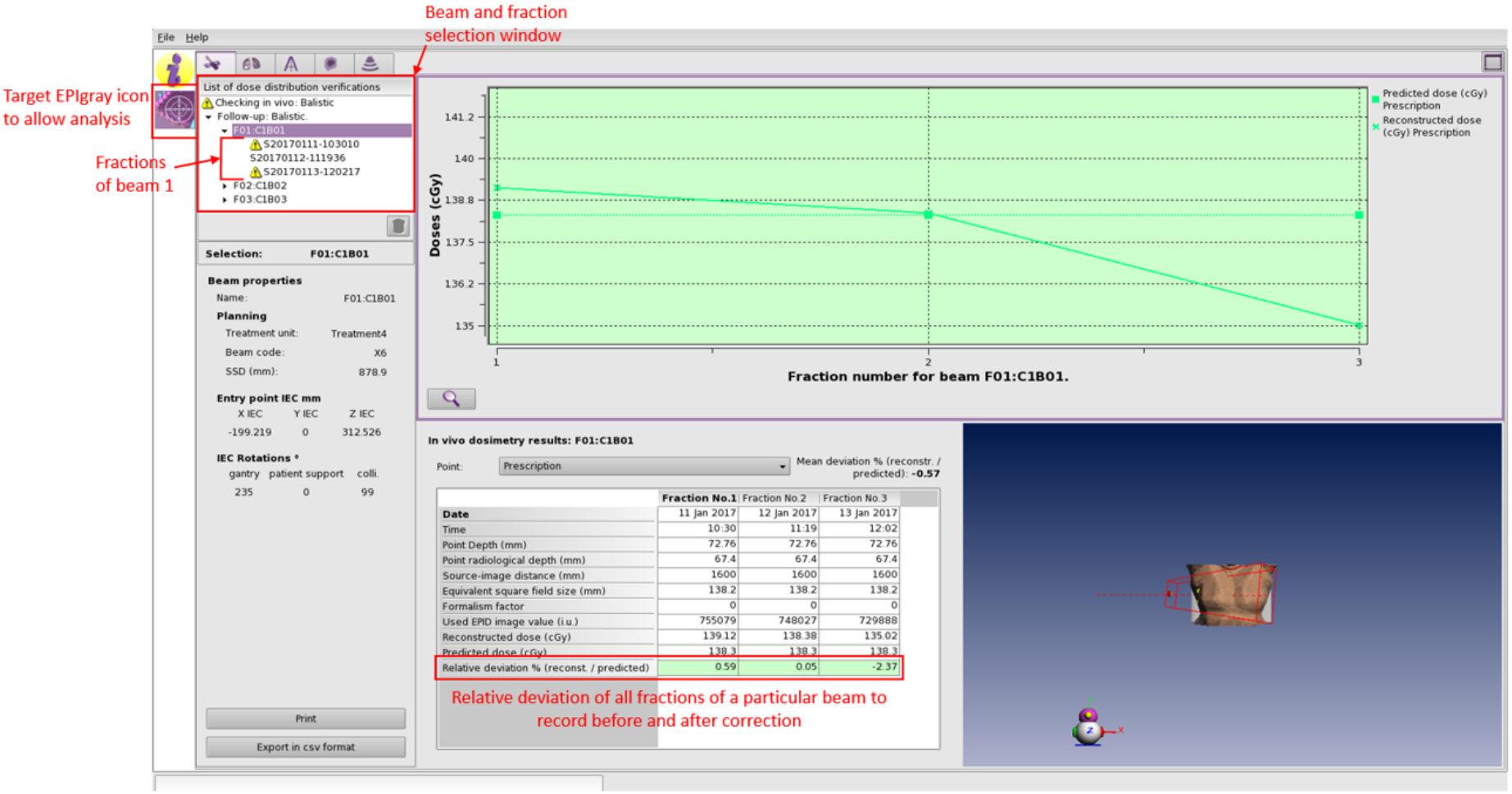

	Fraction No.1	Fraction No.2	Fraction No.3
Date	11 Jan 2017	12 Jan 2017	13 Jan 2017
Time	10:30	11:19	12:02
Point Depth (mm)	72.76	72.76	72.76
Point radiological depth (mm)	67.4	67.4	67.4
Source-image distance (mm)	1600	1600	1600
Equivalent square field size (mm)	138.2	138.2	138.2
Formalism factor	0	0	0
Used EPID image value (i.u.)	755079	748027	729888
Reconstructed dose (cGy)	139.12	138.38	135.02
Predicted dose (cGy)	138.3	138.3	138.3
Relative deviation % (reconst. / predicted)	0.59	0.05	-2.37

FIGURE A.4: Beam Summary Window

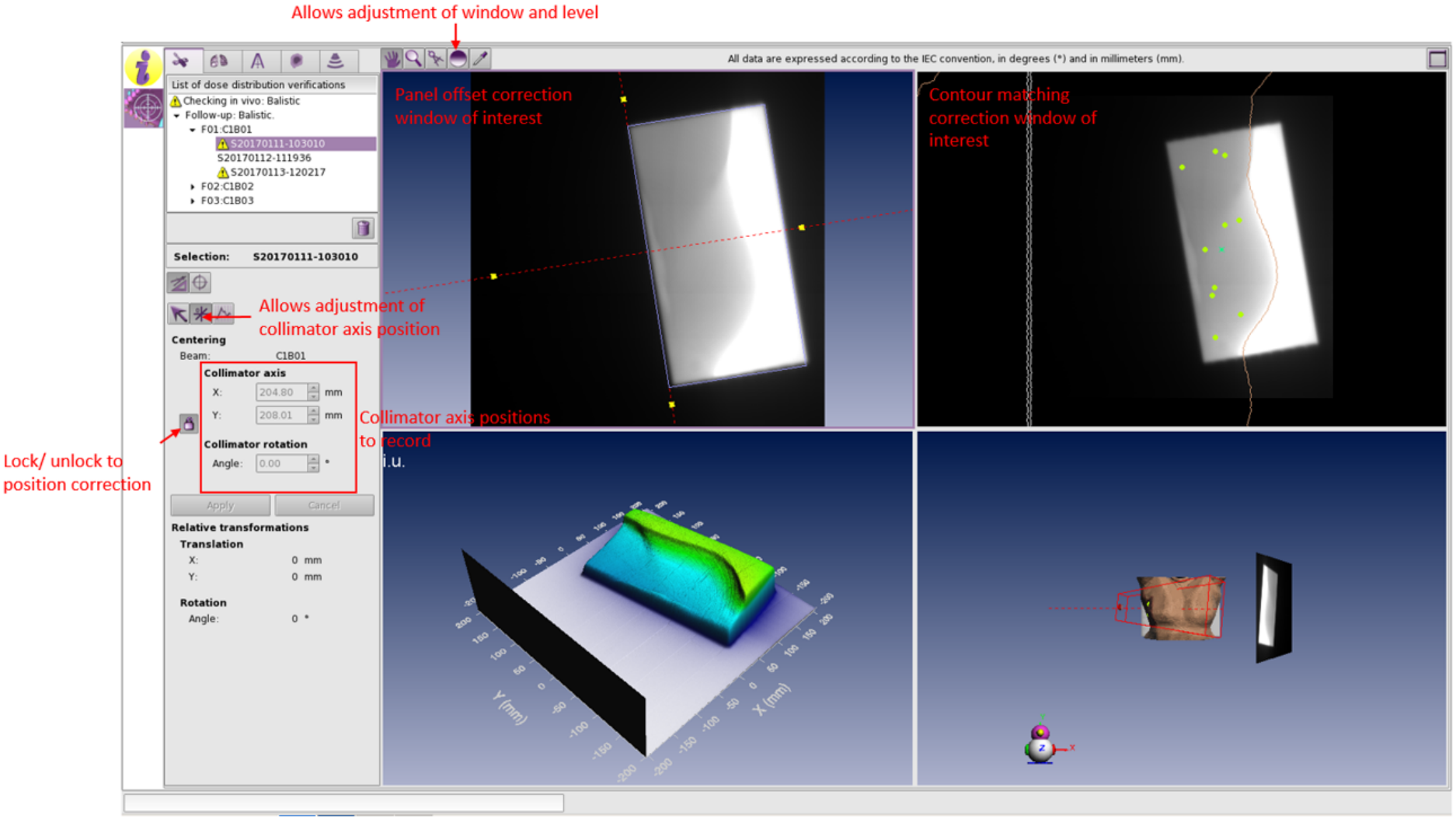

FIGURE A.5: Panel offset and contour matching correction window

Bibliography

[1] *World health organisation - health topics cancer*, http://www.who.int/topics/cancer/en/, Accessed: 2017-01-04.

[2] *Ministry of health - new cancer registrations*, https://www.health.govt.nz/nz-health-statistics/health-statistics-and-data-sets/cancer-new-registrations-and-deaths-series, 2016.

[3] *Worldwide cancer stats*, http://gco.iarc.fr/today/online-analysis-multi-bars?v=2018&mode=cancer&mode_population=countries&population=900&populations=554&key=total&sex=2&cancer=39&type=0&statistic=5&prevalence=0&population_group=0&ages_group.

[4] M. Toi, E. Winer, J. Benson, and S. Klimberg, *Personalized Treatmetn of Breast Cancer*. Springer, 2016.

[5] H. Gelband, P. Jha, R. Sankaranarayanan, and S. Horton, *Disease Control Priorities, Third Edition (Volume 3): Cancer*. Wolrd Bank Publications, 2015.

[6] T. P. Srokowski, S. Fang, Z. Duan, T. A. Buchholz, G. N. Horotbagyi, J. S. Goodwin, and S. H. Giordano, "Completion of adjuvant radiation therapy among women with breast cancer", *HHS Public Access*, vol. 113, 2008.

[7] S. C. Joshi, F. A. Khan, I. Pant, and A. N. Shukla, "Role of radiotherapy in early breast cancer: An overview", *Int J Health Sci (Qassim)*, vol. 2, pp. 259–264, 2007.

[8] E. J. Hall and A. J. Giaccia, *Radiobiology for the Radiologist*. Lippincott Williams & Wilkins, 2012.

[9] A. Sibtain, A. Morgan, and N. Macdougall, *Radiotherapy in Practice Physics for Clinical Oncology*. Oxford University Press, 2012.

[10] *Radiation therapy for breast cancer*, https://www.mayoclinic.org/tests-procedures/radiation-therapy-for-breast-cancer/about/pac-20384940, 2019.

[11] P. Hoskin, *Radiotherapy in Practice - External Beam Therapy Second Edition*. Oxford University Press, 2012.

[12] P. Mayles, A. Nahum, and J. Rosenwald, *Handbook of radiotherapy physics*. Taylor & Francis, 2007.

[13] M. Joiner and A. V. Kogel, *Basic Clinical Radiobiology Fourth Edition*. Macmillan Publishing Solutions, 2009.

[14] E. B. Podgorsak, *Radiation Oncology Physics: A Handbook for Teachers and Students*. IAEA, 2005.

[15] F. M. Khan, *The Physics of Radiotherapy*. Lippincott Williams & Wilkins, 2010.

[16] J. R. Williams and D. I. Thwaites, *Radiotherapy physics in practice*. Oxford University Press, 2000.

[17] E. C. Ford, R. Gaudette, and L. Myers, "Evaluation of safety in radiation oncology setting using failure mode and effects analysis", *Int J Radiat Oncol Biol Phys*, pp. 852–858, 2009.

[18] *On Target: Ensuring Geometric Accuracy in Radiotherapy*. The Royal College of Radiologists, 2008.

[19] T. Ganesh, "Incident reporting and learning in radiation oncology: Need of the hour", *J Med Phys*, pp. 203–205, 2018.

[20] IAEA, "Development of procedures for in vivo dosimetry in radiotherapy", *IAEA Human Health Report No. 8*, 2013.

[21] *Codes of safe practice for the use of irradiating apparatus in medical therapy*. Office of Radiation Safety - Ministry of Health, 1992.

[22] B. Mijnheer, S. Beddar, J. Izewska, and C. Reft, "In vivo dosimetry in external beam radiotherapy", *Med Phys*, 2013.

[23] W. V. Elmpt, L. McDermott, S. Nijsten, M. Wendling, P. Lambin, and B. Mijnheer, "A literature review of electronic portal imaging for radiotherapy dosimetry", *Radiother Oncol*, vol. 88, pp. 289–209, 2008.

[24] *Epid and cbct on radiation therapy*, https://www.slideshare.net/anjukv3/treatment-verification-systems-in-radiation-therapy, 2016.

[25] Elekta, "Iviewgt r3.02 - r3.4", *Elekta Oncology*, 1993.

[26] M. Beyzadeoglu, G. Ozyigit, and C. Ebruli, *Basic Radiation Oncology*. Springer, 2010.

[27] A. L. Boyer, L. Antonuk, A. Fenster, M. V. Herk, H. Meertens, P. Munro, L. E. Reinstein, and J. Wong, "A review of electronic portal imaging devices (epids)", *Med Phys*, vol. 19, pp. 1–16, 1992.

[28] L. E. Antonuk, "Electronic portal imaging devices: A review an historical perspective of contemporary technologies and research", *Phys Med Biol*, vol. 47, R31–65, 2002.

[29] M. C. Kirby and A. G. Glendinning, "Developments in electronic portal imaging systems", *Br J Radiol*, vol. 79, S50–65, 2006.

[30] G. Leunens, J. V. Dam, A Dutreix, and E. V. D. Schueren, "Quality assurance in radiotherapy by in vivo dosimetry. 1. entrance dose measurements, a reliable procedure", *Radiother Oncol*, vol. 17, pp. 141–151, 1990.

[31] E. Yorke, R. Alecu, L. Ding, D. Fontenla, A. Kalend, D. Kaurin, M. E. Masterson-McGary, G. Marinello, T. Matzen, A. Saini, J. Shi, T. C. Z. W. Simon, and X. R. Zhu, "Aapm report no. 87 diode in-vivo dosimetry for patients receiving external beam radiation therapy", *American association of physicist in medicine*, 2005.

[32] M Essers, J. H. Lanson, G. Leunens, T. Schnabel, and B. J. Mijnheer, "The accuracy of ct-based inhomogeneity corrections and in vivo dosimetry for the treatment of lung cancer", *Radiother Oncol*, vol. 37, pp. 199–208, 1995.

[33] K. L. Pasma, M. Kroonwijk, S. Quint, A. G. Visser, and B. J. Heijmen, "Transit dosimetry with an electronic portal imaging device (epid) for 115 prostate cancer patients", *Int J Rad Oncol Biol Phys*, vol. 45, pp. 1297–1303, 1999.

[34] S. M. Nijsten, B. J. Minjheer, A. L. Dekker, P. Lambin, and A. W. Minken, "Routine individualised patient dosimetry using electronic portal imaging devices", *Radiother Oncol*, vol. 83, pp. 65–75, 2007.

[35] J Chang, G. S. Mageras, C. S. Chui, C. C. Ling, and W. Lutz, "Relative profile and dose verification of intensity-modulated radiation therapy", *Int J Rad Oncol Biol Phys*, vol. 47, 2000.

[36] M. D'Andrea, G. Laccarino, S. Carpino, L. Strigari, and M. Benassi, "Primary photon fluence extraction from portal images acquired with an amorphous silicon flat panel detector: Experimental determination of a scatter filter", *J Exp Clin Cancer Res*, vol. 26, pp. 125–132, 2007.

[37] A. Piermattei, A. Fidanzio, G. Stimato, L. Azario, L. Grimaldi, G D'Onofrio, S. Cilia, M. Balducci, M. A. Gambacorta, N. D. Napoli, and N. Cellini, "In vivo dosimetry by an asi-based epid", *Med Phys*, vol. 33, pp. 4414–4422, 2006.

[38] A. Piermattei, A. Fidanzio, L. Azario, L. Grimaldi, G. D'Onofio, S. Cilia, G. Stimato, D. Gaudino, S. Ramella, R. D'Angelillo, F. Cellini, L. Trodell, A. Russo, L. Iadanza, S. Zucca, V. Fusco, N. D. Napoli, M. A. Gambacorta, M. Balducci, N. Cellini, F. Deodato, G. Macchia, and A. G. Morganti, "Application of a practical method for the isocenter point in vivo dosimetry by a transit signal", *Phys Med Biol*, vol. 52, pp. 5101–5117, 2007.

[39] K. Ricketts, C. Navarro, K. Lane, C. Blowfield, G. Cotten, D. Tomala, C. Lord, J. Jones, and A. A, "Clinical experience and evaluation of patient treatment verification with a transit dosimeter", *Int J Radiation Oncol Biol Phys*, vol. 95, pp. 1514–1521, 2016.

[40] S. Celi, E. Costa, C. Wessels, A. Mazal, A. Fourquet, and P. Francois, "Epid based in vivo dosimetry clinical experience and results", *J appl Clin Med Phys*, vol. 17, pp. 262–276, 2016.

[41] P. Francois, P. Boissard, L. Berger, and A. Mazal, "In vivo dose verification from back projection of a transit dose measurement on the central axis of photon beams", *Phys Med*, vol. 27, pp. 1–10, 2011.

[42] "Automatic volume generation for the maximum dose area deposition verificataion", *EPIgray by DOSIsoft*, 2018.

[43] "Prescribing, recording, and reporting photon beam therapy", *ICRU Report 50*, 2010.

[44] *Radiation therapy for breast cancer*, `https://www.mayoclinic.org/tests-procedures/radiation-therapy-for-breast-cancer/about/pac-20384940`, 2018.

[45] J. F. Ratcliffe, "The effect of the t distribution of non-normality in the sampled population.", *Appl. Stat.*, vol. 17, pp. 42–48, 1968.

[46] S. S. Sawilowsky and R. C. Blair, "A more realistic look at the robustness and type ii error properties of the t test to departures from population normality", *Psychol. Bull.*, pp. 352–360, 1992.

[47] S. S. Sawilowsky and S. B. Hillman, "Power of the independent samples t test under a prevalent psychometric measure distribution", *J. Consult. Clin. Psychol*, pp. 240–243, 1993.

[48] T. Lumley, P. Diehr, S. Emerson, and L. Chen, "The importance of the normality assumption in large public health data sets", *Annu. Rev. Public Health*, pp. 151–169, 2002.

[49] Student, "The probable error of a mean", *Biometrika*, vol. 6, pp. 1–25, 1 1908.

[50] R. G. D. Steel and J. H. Torrie, *Principles and Procedures of Statistics with Special Reference to the Biological Sciences*. McGraw Hill, 1960.

[51] S. A Glantz and B. K. Slinker, *Primer of Applied Regression and Analysis of Variance*. McGraw Hill, 1990.

[52] N. R. Draper and H. Smith, *Applied Regression Analysis*. Wiley-Interscience, 1998.

[53] ICRU, "Tissue substitutes in radiation dosimetry and measurement", *International Commission on Radiation Units and Measurements*, 1989.

[54] K. Venables, E. Winfield, A. Deighton, E. Aird, and P. Hoskin, "The start trial - measurement in semi-anatomical breast and cell wall phantoms", *Phys Med Biol*, vol. 46, pp. 1937–1948, 2001.

[55] J. B. Davis and V. Miltchev, "Tangential breast irradiation: A multi-centric intercomparison of dose using a mailed phantom and thermoluminescent dosimetry.", *Radiother Oncol*, vol. 52, pp. 65–68, 1999.

[56] K. T. Kalef-Ezra J A Karantanas A H, "Electron density of tissues and breast cancer radiotherapy - a quantitive ct study", *Int. J. Radiat. Oncol. Biol. Phys.*, vol. 41, pp. 1209–1214, 1998.

[57] D. F. Lewis and M. F. Chan, "On gafchromic ebt-xd film and the lateral response artifact", *Med. Phys.*, pp. 643–649, 2016.

[58] D. Lewis and M. F. Chan, "Correcting lateral response artifacts from flatbed scanners for radiochromic film dosimetry", *Med. Phys.*, pp. 416–429, 2015.

[59] D. Lewis and S. Devic, "Correcting scan-to-scan response variability for radiochromic film1 based dosimetry system", *Med. Phys.*, pp. 6592–6701, 2015.

[60] D. Lewis, A. Micke, X. Yu, and M. F. Chang, "An efficient protocol for radiochromic film dosimetry with flatbed ccd scanners combining calibration and measurement in single scan", *Med. Phys.*, pp. 6339–6350, 2012.

[61] A. Micke, D. Lewis, and X. Yu, "Multichannel film dosimetry with non-uniformity correction", *Med. Phys.*, pp. 2523–2534, 2011.

[62] Elekta, *Elekta Precision Radiation Therapy: Precise Table*. Elekta, 2008.

[63] P. Andreo, D. T. Burns, K. Hohlfeld, M. S. Huq, T. Kanai, V. S. F. Laitano, and S. Vynckier, *Absorbed Dose Determination in External Beam Radiotherapy: An International Code of Practice for Dosimetry based on Standards of Absorbed Dose to Water*. 2006, pp. 61–74.

[64] K. Ricketts, C. Navarro, K. Lane, M. Moran, C. Blowfield, U. Kaur, G. Cotten, D. Tomala, C. Lord, J. Jones, and A. Adeyemi, "Implementation and evaluation of transit dosimetry system for treatment verification", *Physica Medica*, vol. 95, 2016.

[65] P. Winkler, A. Hefner, and D. George, "Dose-response characteristics of an amorphous silicon epid", *Med. Phys.*, 2005.

[66] "3d conformal ebrt treatment plan checks", p. 6, 2018.

[67] J. Maggs, *TR5.4.8 Treatment Protocol - PH1 and PH2 Breast with or without nodes including Field in Field Treatment*. 2019.

[68] "Oncology dosimetry checks", pp. 1–4, 2018.

[69] *How to interpret a correlation coefficient r*, https://www.dummies.com/education/math/statistics/how-to-interpret-a-correlation-coefficient-r/, 2019.

[70] "Evaluation of measurement data — guide to the expression of uncertainty in measurement", *JCGM*, 2008.

[71] M. Greiner, D. Pfeiffer, and R. Smith, "Principles and practical application of the receiver operating characteristic analysis for diagnostic tests", *Prev. Vet. Med*, vol. 45, pp. 24–40, 2000.

[72] J. Hanley and B. McNeil, "The meaning and use of the area under a receiver operating characteristic curve", *Radiology*, vol. 143, pp. 29–36, 1982.

[73] K. Hajian-Tilaki, "Receiver operating characteristic (roc) curve analysis for medical diagnostic test evaluation", *Caspian. J. Intern. Med*, vol. 4, pp. 627–635, 2013.

[74] N. Perkins and E. Schistermann, "The inconsistency of optimal cutpoints obtained using two criteria based on receiver operating characteristic curve", *Am. J. Epidemiol.*, vol. 163, pp. 670–675, 2005.

[75] W. J. Youden, "Index for rating diagostic tests", *Cancer*, vol. 3, pp. 32–35, 1 1950.

[76] M. D. Wong, X. Wu, and H. Liu, "Image quality and dose efficiency of high energy phase sensitive x-ray imaging: Phantom studies", *J Xray Sci Technol.*, vol. 22, pp. 321–334, 3 2008.